Dissertation zur Erlangung des Doktorgrades der Fakultät für Chemie und Pharmazie der Ludwig-Maximilians-Universität München

Novel roles of miRNA-27a and miRNA-200c in breast cancer treatment and metastasis

Bojan Ljepoja
aus
Trostberg, Deutschland
2019

Erklärung

Diese Dissertation wurde im Sinne von § 7 der Promotionsordnung vom 28. November 2011 von Herrn Prof. Dr. Ernst Wagner betreut.

Eidesstattliche Versicherung

Diese Dissertation wurde eigenständig und ohne unerlaubte Hilfe erarbeitet.

München, 16.05.2019

Bojan Ljepoja

Dissertation eingereicht am: 16.05.2019

1. Gutachter: Prof. Dr. Ernst Wagner

2. Gutachter: Prof. Dr. Stefan Zahler

Mündliche Prüfung am: 11.07.2019

“

I shall endeavour still further to prosecute this inquiry,
an inquiry I trust not merely speculative,
but of sufficient moment to inspire the pleasing hope
of its becoming essentially beneficial to mankind.

Edward Jenner (1749-1823)

Table of contents

1. Introduction

1.1. Biogenesis and function of miRNAs

More than 25 years ago, first observations of the small RNA lin-4 were made in *C. elegans*. Much to the surprise of the researchers around Lee RC in the Ambros group, the RNA was not coding for any protein. Furthermore, the authors even found that lin-4 performed transcriptional regulation on another gene, lin-14 by suppressing its expression via complementary antisense RNA interaction[1]. While those findings were received with high interest in the early 1990's, the magnitude and importance for today's biology were not clear at that time. It was not until the early 2000's that those small, non-coding RNAs were regarded as their own class of regulatory RNAs and due to their size of around 22 nucleotides were termed microRNAs (miRNAs)[2]. Today, it is generally understood that miRNAs are involved in multiple cellular processes in plants as well as animals [3,4].

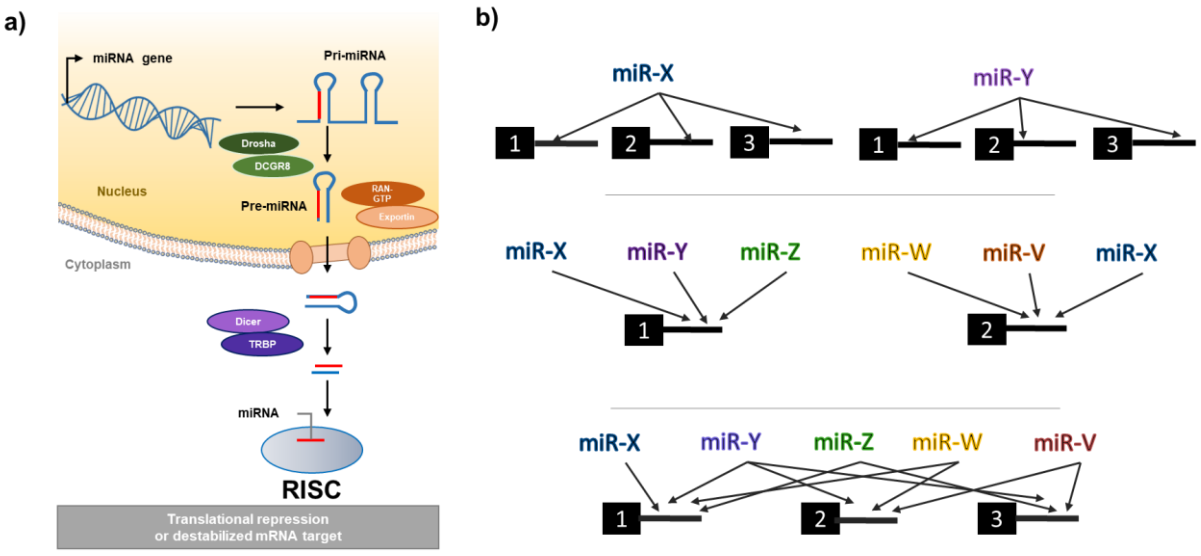

Figure 1 – Biogenesis and function of miRNAs

a) Adapted from Lodish et al. and Gebert et al. [4,5], miRNAs undergo extensive processing, shortening the length of the primary transcript from step to step. b) Adapted from Peter et al.[6], the complex multi-layered network of miRNA based translational regulation

In short, the biogenesis of miRNAs is based on the nuclear transcription of miRNA genes by RNA polymerase II, resulting in the primary transcripts, pri-miRNAs. This RNA segments are often polycistronic units and can contain multiple miRNA hairpin structures. A protein complex, consisting of the RNAse III endonuclease Drosha, as

well as the microprocessor complex subunit DGCR8, is able to recognize the hairpin-motifs and generates 60-70 nt stem-loop structures, the pre-miRNA.

After those stem-loops are transported to the cytosol, facilitated by Ran-GTP and Exportin, further processing is applied: The protein complex, consisting of Dicer, a RNAse III endonuclease, and the RNA-binding co-factor TRBP, cleaves the pre-miRNA. The resulting RNA of 22 nt length is the mature miRNA, a duplex consisting of the miRNA and its complementary strand, often referred to as miRNA* ("star-strand"). The miRNA*, or sometimes also called "passenger strand", undergoes RNA degradation, as the thermodynamically favored single stranded miRNA is loaded into the RISC (Figure 1a) [4,5].

With the Argonaut proteins (Ago), the miRNA-RISC recognizes target mRNAs based on sequence complementarity of the "seed region", located in the 3' UTR of the mRNA. Thus, miRNA regulation of protein expression is based on anti-sense matching of only about eight bases, nucleotides two to seven of the miRNA's 5' end, to the mRNA seed region. While a perfect match of bases is common in plants[3], it is highly uncommon in animals. The partial matching of only about seven or even six bases can cause translational repression, following different thermodynamic rules of anti-sense binding, like e.g. "Wobble hypothesis" [7].

Altogether, miRNAs have added a new level of complexity to translational regulation of protein expression: While one miRNA can target multiple mRNAs, one single mRNA can also be the target of many different miRNAs [6] (Figure 1b).

Since the first studies of Lee et al., more than 80,000 publications with the search term "miRNA" were registered in NCBIs database Pubmed.gov (https://www.ncbi.nlm.nih.gov) until early 2019, showing the vast increase of interest and therefore knowledge in this field.

1.2. miRNAs in breast cancer

Breast cancer is one of the leading causes of cancer deaths worldwide [8]. According to the American cancer association, in 2018 more than 260,000 women were estimated to be newly diagnosed with breast cancer, and almost 41,000 deaths will have occurred [9]. MiRNAs play a major role in the development and persistence of breast cancer [10,11]. While breast cancers are a group of highly heterogeneous tumors, often classified by their status of hormone receptors [12,13], miRNAs seem to play an

ubiquitous role, either as tumor suppressor or promotor, so called oncomiRs [14]. While tumor suppressing miRNAs are often shown to inhibit processes like epithelial to mesenchymal transition, uncontrolled proliferation or de-toxifying processes, oncomiRs are regarded as the contrary and often amplify proliferation, metastasis and enable avoidance of apoptosis [15].

The following chapters of this thesis will focus on two prominent miRNAs, miRNA-27a (miR-27a) and miRNA-200c (miR-200c) both with contrary roles on the first sight.

MiRNA-200c and the miR-200c family, are some of the most investigated miRNAs today and seem to be among the most effective miRNAs suppressing tumor growth and metastasis. In *chapter 3* the loss of miR-200c, induced by a genomic knock-out (KO) in epithelial breast cancer cells, was described by analysis of the proteome. Novel potential targets were identified, and the cellular phenotype of the KO cell line was characterized. In *chapter 4*, the focus was placed on migratory targets found in the previous proteome analysis and are further investigated, by utilizing novel cell line constructs and 1D migration assays.

The first part of this work, however, focuses on miRNA-27a (miR-27a). While this miRNA is often regarded as a potent oncomiR, in our study in *chapter 2* we found a positive correlation of high miR-27a expression and the beneficial survival in a subgroup of patients with luminal A breast cancer undergoing anti-estrogen therapies, as well as a potential molecular mechanism for this observation.

1.2.1. MiRNA-27a – an oncomir with ambivalence in breast cancer

MiR-27a is investigated in multiple indications and disease states. It has been shown that this miRNA can exhibit strong influence in metabolic settings [16], especially cholesterol homeostasis and arteriosclerosis [17], as well as in neurodegenerative disorders [18] and differentiation of benign cells, like myoblasts [19]. Of interest, miR-27a was also shown to regulate endothelial differentiation in breast cancer stem-like cells [20], and also correlate to the metastatic burden of the patients, i.e. miR-27a was increased in more aggressively spreading tumors [21]. Based on this and similar findings in oncological settings, miR-27a can be regarded as a tumor promoting oncomiR, due to its ability to increase cancer progression and as well as resistance to chemotherapeutic agents [22-24].

In "*2. MiRNA-27a Sensitizes Breast Cancer Cells To Treatment With Selective Estrogen Receptor Modulators*" we suggest that expression of miR-27a could also be utilized as biomarker of functional estrogen receptor expression in luminal A breast cancer. Thus, identifying miR-27a a potential predictor for the response of anti-estrogen therapies in patients, not in objection to its role as oncomiR [25].

1.2.2. Tumor suppressing effects of miRNA-200c in breast cancer

The miR-200 family consists of five members: miR-200a, miR-200b, miR-200c, miR-141 and miR-429. While the whole family shares common sequence elements as well as functions, described in more detail in chapter 3.2, the most investigated representative of this family is miR-200c.

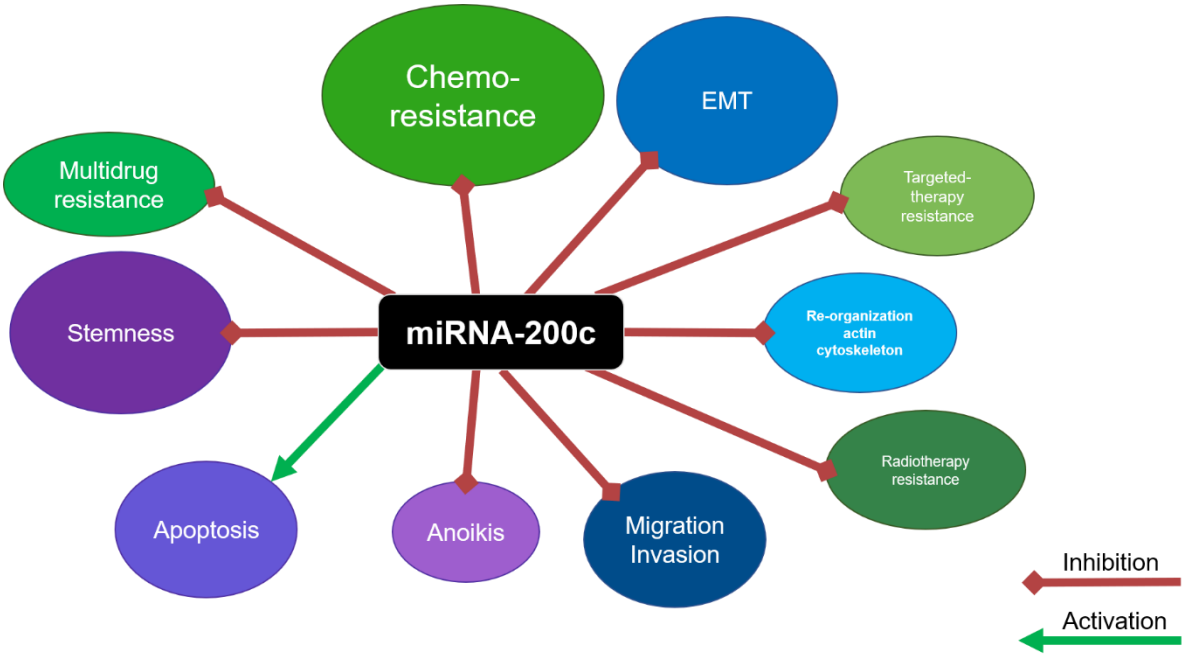

Figure 2 – miRNA-200c as "watchdog of cancer progression"
Adapted from Mutlu et al. [26]

In general, miR-200c is regarded as an effective tumor suppressor and sometimes even discussed as "watchdog of cancer progression" [26], due to its many inhibiting effects in cancer progression. Previous work in our group, conducted by Kopp et al., investigated the effect of miR-200c upregulation in sensitizing breast cancer cells to anthracyclines. It was shown that the increased efficacy of the doxorubicin treatment was facilitated by the decreased expression of TRKB and BMI1 [27]. In another study, the inhibition of the oncogene KRAS by miR-200c expression, showed a direct anti-

proliferative effect on triple negative MDA-MB-231 breast cancer cells [28]. While all those findings were made by utilizing miRNA-precursor or mimic based overexpression, novel developments in gene editing opened new experimental perspectives. Therewith, we generated a TALENs based genomic knock-out [29,30] in the miR-200c high expressing MCF7 breast cancer cells. This long-term stable approach allowed for a broad screen of changes in the proteome, resulting in many putative, but previously unrelated targets, which could be influenced by miR-200c, as discussed in 3.4.

The generated knock-out cell line, as well as modified MDA-MB-231 cells, were utilized to further investigate the possible effects of miR-200c on epithelial to mesenchymal transition or closely related processes. Novel targets from 3.3.4 were analyzed for their role in migration and cellular organization, as described in more detail in chapter 4.

1.3. Aim of the thesis

In this thesis, the effect of two different miRNAs, miR-200c and miR-27a, in breast cancer was to be evaluated. Both miRNAs have known roles in disease, development of tissues and have previously been found to have multiple effects in cancer.

With the focus on breast cancer, the profile of both miRNAs was to be evaluated and novel functions investigated. For a comprehensive approach, different stably modified breast cancer cell line models had to be generated, either as knock-out constructs. Causing depletion of the miRNA, or as inducible overexpression constructs, gaining full time- and dose control on the expression of miRNAs.

With these novel perspectives on the function of both miRNAs, their potential use as either biomarker or even therapeutic was to be discussed.

2. MiRNA-27a Sensitizes Breast Cancer Cells To Treatment With Selective Estrogen Receptor Modulators

The following sections are directly adapted from the original publication, which was finally published as Ljepoja et al., Breast. 2019 Feb;43:31-38.
Sections may have been moved for consistency

MiRNA-27a Sensitizes Breast Cancer Cells To Treatment With Selective Estrogen Receptor Modulators

Bojan Ljepoja[1], Jonathan García-Roman[1], Ann-Katrin Sommer[1], Ernst Wagner[1], Andreas Roidl[1]*, Breast. 2019 Feb;43:31-38
[1]Pharmaceutical Biotechnology, Department of Pharmacy, Ludwig-Maximilians-Universität München, Munich, Germany

Contributions:

BL performed the experiments and wrote the manuscript. JGR performed the analysis of transcription factor and ERE-binding sites. AS generated the TAM6 cells. EW provided conceptual advice. AR conceived the study and wrote the manuscript. All authors commented on the manuscript and conclusions of this work.

2.1. Abstract

Background: MicroRNA-27a (miR-27a) is a small non-coding RNA, shown to play a role in multiple cancers, including the regulation of ERα expression in breast cancer. Most ERα positive tumors are treated with Selective Estrogen Receptor Modulators (SERMs) and thus the role of miR-27a expression in response to SERM treatment is of interest.

Methods: Tamoxifen resistant cells were generated by molecular evolution with six cycles of tamoxifen treatment. MCF7 and T47D luminal A breast cancer cell lines were either treated with miR-27a mimics, or ER-signaling was modulated ectopically. The changes were analyzed with RT-qPCR, western blot and transcriptional activity ERE-reporter assays. Moreover, response to SERM treatments (tamoxifen, endoxifen and toremifen) was investigated by viability and apoptosis measurements. An *in silico* analysis of survival data from the METABRIC study was performed in order to assess the prognostic value of miR-27a for response to SERM treatment.

Results: Tamoxifen-resistant cells showed decreased expression of ERα and miR-27a. The overexpression of miR-27a increased the levels of ERα, while modulation of ERα decreased miR-27a expression. High miR-27a expression increased the sensitivity of MCF7 and T47D cells to SERM treatments and re-sensitized the cells to tamoxifen. Patient survival of luminal A breast cancer patients that underwent endocrine therapies was better in groups with high miR-27a expression.

Conclusion: MiR-27a sensitized luminal A breast cancer cells to SERM treatments based on a positive feedback loop with ERα. An increased overall-survival of ER-positive breast cancer patients that underwent endocrine treatments and displayed high miR-27a levels was found.

2.2. Introduction

Breast cancer is one of the leading causes of cancer deaths worldwide[8]. The group of breast cancers is highly heterogeneous in its prevalence, short- as well as long-term mortality. Therefore, the tumors are characterized and clustered according to different characteristics. The most common approach is based on determination of receptor expression, like the estrogen- and progesterone receptor (ER and PR) or HER2. While luminal A breast cancer, with positive expression of ER and PR, are the most prevalent tumors, they are also considered least harmful, as they tend to be less aggressive and in general well treatable with endocrine therapies, like estrogen receptor modulators (SERMs)[12,13].

Nevertheless, the ATLAS trial showed that therapies with anti-endocrine agents, e.g. the SERM tamoxifen (TAM), should be considered for a full treatment period of at least 5 years, ideally even 10 years and longer for best effects [31]. Still, previous reports suggest that as much as 40% of all ER-positive breast cancers treated with adjuvant tamoxifen undergo relapse, with eventually fatal outcomes [32]. It is unclear whether this poor response is based on initial (*ab initio*) resistance to the therapies or due to acquired (*de novo*) resistance.

Moreover, different side effects of SERMs, like increased risk for cervical carcinoma or osteoporosis, becloud their positive effects. In order to attenuate long-term adverse effects of SERM treatments, the ESMO guidelines suggest a switch of treatment to a newer class of drugs, i.e. selective estrogen receptor down regulators (SERDs) like fulvestrant. SERDs are often considered in long term second line treatments (after 5 years or more). Also transitions to aromatase-inhibitors like anastrozol are made [33]. While some of these approaches may circumvent adverse effects and resistance, the survival of luminal A breast cancer patients is declining over time, indicating that the current treatment approaches for luminal A tumors cannot be considered optimal for all luminal A tumors, in regard of their long-term outcome [31].

Thus, there is a practical need for further diversification of breast cancer in general and especially for ER-positive tumors. Additional sub-classifications of breast cancer tumors were suggested, e.g. the screening for GATA3 mutations [34-36]. While multiple protein-markers are already considered during the treatment of triple negative breast cancer (TNBC)[37], the main reference point for endocrine treatments is ER expression[38]. Additional surrogate markers could be used to identify high risk populations, which would profit from switches from standard therapies to suitable

chemotherapies already from the onset of the treatment, as is already part of the ESMO guidelines for patients with high tumor burden [13].

MicroRNAs (miRNA) are small non-coding RNAs which are important in transcriptional and translational regulation of cellular processes, making them promising prognostic markers. As the detection in tissue, as well as in blood samples, is getting easier, alterations in expression levels could be used to assess aggressiveness of tumors and in certain cases even predict treatment response [39]. A miRNA of special interest is miR-27a, which was shown to play a role in multiple metabolic processes and different cancer types. In general, miR-27a is considered tumor promoting, i.e. increasing cancer progression and resistance to chemotherapeutic agents, as observed in different cancer types including breast cancer cells [22-24]. Therefore miR-27a is considered a potent oncomiR, whose high expression is unfavorable for patients' survival in many settings, like osteosarcoma and gastric cancer [40,41]. Previous studies suggest that miR-27a is regulating the ERα expression indirectly via ZBTB10 and the sp-protein family[42], hence the role of miR-27a in ER-positive breast cancers is of interest.

Our findings, while not objecting miR-27a's tumor promoting effects, suggests that high expression of miR-27a may serve as an indicator of functional ER-expression in luminal A breast cancer and could therefore act as a positive marker for SERM response *in vitro*, resulting in a survival benefit as observed *in vivo*.

2.3. Results

2.3.1. Induction of tamoxifen resistance leads to repression of ERα and miRNA-27a expression

In order to induce resistance to tamoxifen, MCF7 cells were treated with tamoxifen for six cycles each followed by recovery phases, as described previously[43].

The resulting resistant MCF7 cells, labeled TAM6, showed an increasing IC50 of approximately 1.5-fold (Figure 3 a). As loss of ERα expression is common in acquired resistance to tamoxifen, an analysis of ERα expression changes was performed. The resistant TAM6 cells showed significantly decreased levels of ESR1 mRNA (Figure 3b) as well as decreased ERα protein expression (Figure 3c). The transcriptional activity of ERα was assessed via an ERE (estrogen-receptor-response element) luciferase

reporter assay which indicated a significant loss of relative signaling of about 40% in the TAM6 cells ($p \leq 0.05$) compared to wildtype MCF7 (Figure 3d). Interestingly, the resistant TAM6 cells showed also a decreased expression of miR-27a (Figure 3e).

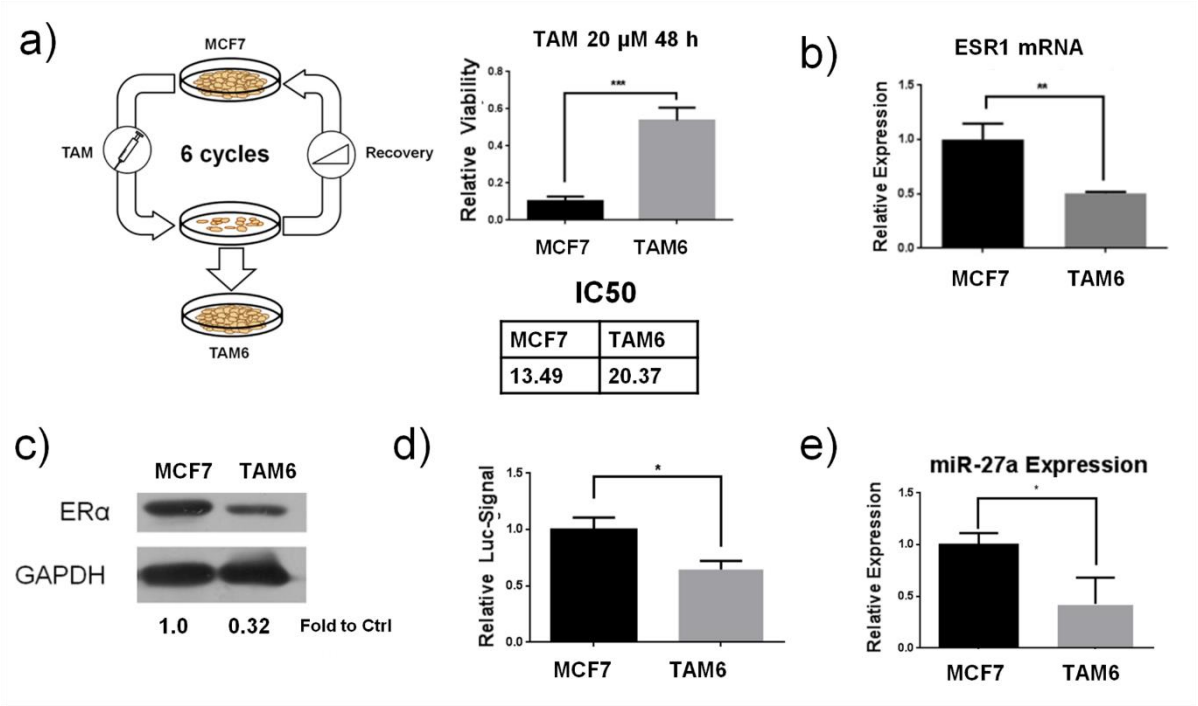

Figure 3 - Induction of tamoxifen resistance leads to repression of ERα and miR-27a expression

a) A Molecular Evolution Assay of 6 cycles tamoxifen (TAM) treatment resulted in resistant MCF7 cells, the TAM6 cells, with increased resistance to 20µM TAM ($p < 0.001$) as well as an increased IC50 value. b) ESR1 mRNA levels are significantly decreased by approximately 50% in the resistant cells, as shown by RT-qPCR ($p < 0.05$), c) as well as western-blot for protein levels, GAPDH was used as housekeeper. d) The relative luciferase signal of the ERE-reporter is significantly decreased in the resistant cells ($p < 0.05$). e) Expression of miR-27a is decreased to 50% in the the resistant TAM6 cells compared to MCF7 wildtype ($p < 0.05$).

2.3.2. The interplay of miRNA-27a and ERα in a positive feedback loop

To investigate whether miR-27a's is able to regulate the expression of ERα, basal miRNA expression was analyzed in two Luminal A breast cancer cell lines, T47D and MCF7. Both cell lines showed expression of miR-27a. In MCF7 the miR-27a levels were six times higher than in T47D cells (Figure 4a). Nevertheless, ectopic overexpression of miR-27a showed a further increase of ERα mRNA (ESR1) in MCF7 and T47D of 20% to 50%, respectively (Figure 4b), and a 1.3 and 2-fold increase in protein levels (Figure 4c). The ERE-reporter assay revealed a 40-50% increase in luciferase signal, indicating increased transcriptional activity of ERα (Figure 4d). These findings were supported by an immunofluorescence staining (Figure 4e), which showed that upon stimulation with estradiol the ERα localization into the nucleus is stronger after miR-27a overexpression compared to controls.

Of note, also the reintroduction of miR-27a into the low-expressing tamoxifen resistant TAM6 cells reactivated ERα expression and signaling as shown by a significantly increased ERE-luc signal of more than 50% compared to controls ($p \leq 0.05$, Figure 4f).

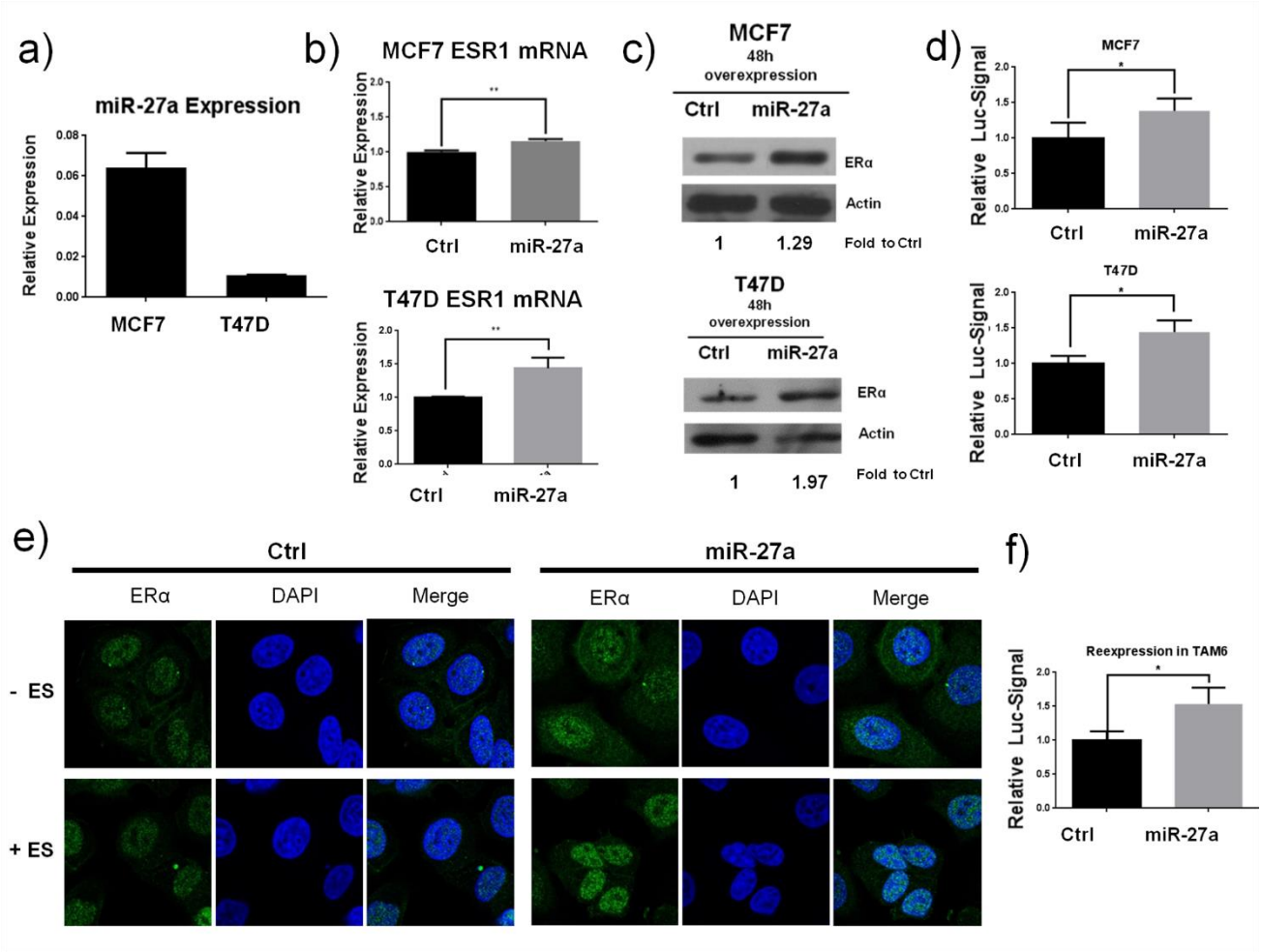

Figure 4 - The effect of miR-27a on ER-alpha signaling in luminal A breast cancer

a) Expression of miR-27a in the two luminal A breast cancer cell lines, MCF7 and T47D. b) Overexpression of miR-27a significantly increased expression of ESR1 mRNA in MCF7 and T47D ($p < 0.01$), b) ERα protein, as well as c) luciferase signal of the ERE-reporter compared to scrambled control ($p < 0.05$). e) Immunofluorescence staining of ERα and DAPI showed increased localization of ERα to the nucleus in miR-27a overexpressing cells which were stimulated with estradiol (ES). f) Re-expression of miR-27a in TAM6 cells significantly increased the relative luciferase signal of the ERE-reporter compared to scrambled control ($p < 0.05$).

To investigate a possible regulation of miR-27a expression by ERα activity, MCF7 cells were depleted of estrogen stimulation in estradiol- and phenol red free media or stimulated with estradiol for 48 h. The miR-27a expression was analyzed and as shown in Figure 5a, after the depletion of estrogen stimulation, the miR-27a expression was significantly decreased ($p \leq 0.001$) compared to control. Additionally, stimulation with estradiol showed a slight but not significant increase of miR-27a in MCF7 cells.

To further investigate the correlation, a stable MCF7 cell line with inducible expression of a short hairpin inhibitor of ERα mRNA, MCF7 shER, was generated. Upon induction with doxycycline for 48 h, the cells showed decreasing ERα protein of one third compared to uninduced control (Figure 5b). Long-term depletion of ERα by induction of the shER for 29 days compared to a scrambled hairpin control, showed a stable effect of 20% reduction of ESR1 mRNA (Figure 5c). Importantly, the ERα knock-down resulted also in a highly significant decrease in miR-27a expression of 30% (Figure 5d). These findings indicate a mutual influence of miR-27a and ERα expression in a positive feedback loop. Thus, a genomic analysis of the miR-27a locus was performed, investigating possible regulation mechanisms based on ERα transcriptional effects. Two different modes of transcriptional regulation were considered: Direct regulation of ERα via binding to known ERE structures located upstream of the miR-27a locus, or indirect influence by predicted binding of other transcription factors, which are known to be regulated by ERα. Figure 5e shows the possible bindings and interactions in the promotor (-500/-1 bp) and the enhancer region (-30,000/-1 bp) of miR-27a: Two putative ERE sites were found, one in the proximal promotor with a match of 11/13 bases to the consensus sequence, and one in the distant enhancer with 12/13 matching bases. Additionally, a site for JUN in the promotor, as well as the co-transcription factors of ERα AP-2αA and C/EBPβ in the enhancer, were predicted with high stringency[44,45]. This analysis indicated a high probability of transcriptional regulation of miR-27a by ERα, consolidating the hypothesis of an important function of both miR-27a and ERα in the development of resistance to tamoxifen treatment.

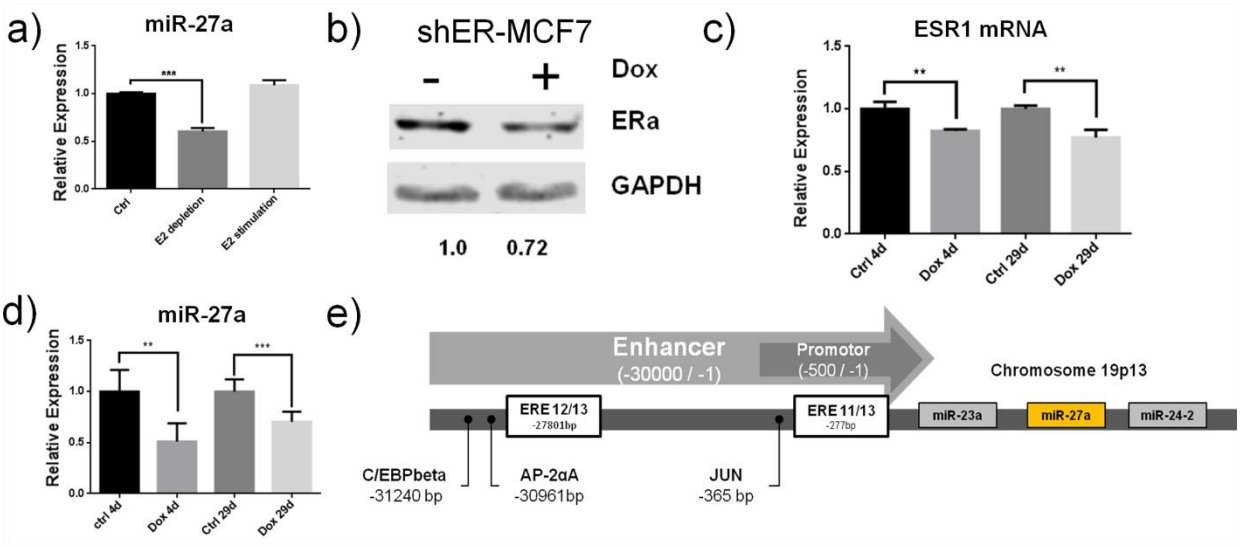

Figure 5 - The effect of ERα signaling on miR-27a expression

a) MCF7 cells that were depleted of estrogen-stimulation, showed significantly decreased expression of miR-27a ($p < 0.001$). b) Induction of shER-expressing MCF7 cells with 5µg/ml doxycycline for 48h decreased protein levels of ERα 30%. c) Long-term induction of shER for 4 and 29 days, significantly decreased ESR1 mRNA ($p < 0.01$), as well as d) the expression of miR-27a. e) Schematic overview of the promotor and enhancer region of the miR-27a locus. An analysis of possible transcription-factor interactions revealed three interaction partners of ERα, possibly controlling miR-27a transcription.

2.3.3. Overexpression of miRNA-27a induces sensitivity towards SERM treatment *in vitro*

While formation of resistance to tamoxifen is correlated to loss of miR-27a, the reverse setting of miR-27a overexpression in luminal A cell lines was of interest. In order to analyze the sensitivity towards the treatment, MCF7 and T47D were transfected with miR-27a mimics and subsequently treated with different SERMs: Tamoxifen, its active metabolite endoxifen as well as toremifene. As shown in Figure 6a-c, miR-27a sensitized MCF7 cells to all tested SERM treatments. To investigate whether the changes in viability induced by tamoxifen, as determined by ATP-content, were not only based on changes in metabolic activity, an annexin V assay was performed to determine ratios of induced cell death. Viability is regarded as the percentage of cells with negative annexin as well as propidium iodide stainings. In line with the ATP-measurements, MCF7 with an overexpression of miR-27a showed increased sensitivity towards tamoxifen treatment (Figure 6d)

Replication of this experiment with another luminal A cell line, T47D, showed similar results for tamoxifen, endoxifen and toremifen compared to controls (Figure 6e-g). Also

the rescue of miR-27a expression in the tamoxifen resistant and miR-27a-low TAM6 cells re-sensitized the cells towards tamoxifen treatment, as seen by a significant decrease in viability after the treatments, compared to control (Figure 6h). Further validation with the annexin V assay showed that these effects are based on apoptosis and cell death, rather than diminished metabolism (Figure 6i).

Together, these data showed a sensitizing effect of miR-27a to SERM treatments in both tested luminal A cell lines, as well as a re-sensitizing effect in tamoxifen resistant cells.

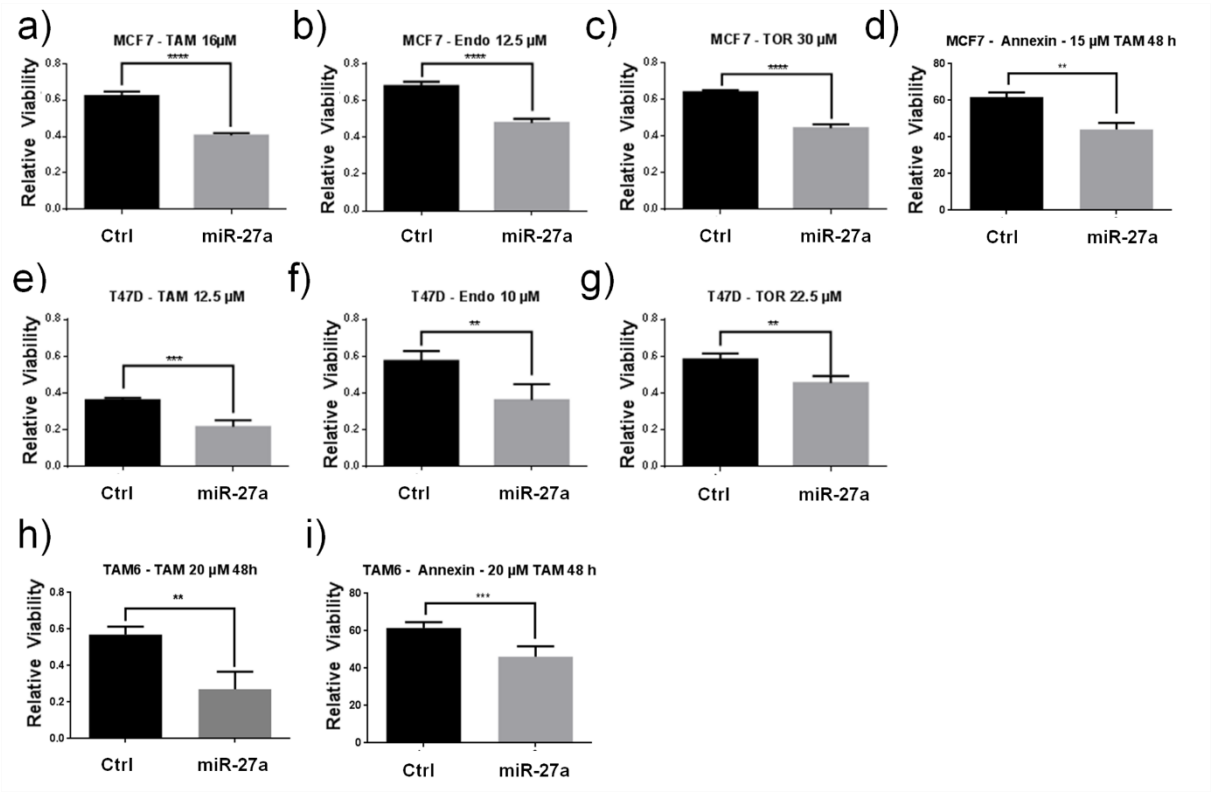

Figure 6 - Effect of miR-27a overexpression on resistance to SERMs

MCF7 cells with miR-27a overexpression showed significantly increased sensitivity towards treatments with the different SERMs as shown as viability measurement by ATP content, compared to scrambled control (Ctrl): a) 16µM tamoxifen (TAM), b) 12.5µM endoxifen (Endo) and c) 30µM toremifen. d) An annexin V-FITC assay of TAM treated MCF7 cells showed a decreased number of viable cells after miR-27a overexpression. T47D cells with overexpression of miR-27a with e) 12.5µM TAM, f) 10µM Endo, g) 22.5µM TOR showed significantly decreased viability, compared to scramble control. h) The resistant TAM6 cells were significantly re-sensitized to TAM treatment by overexpression of miR-27a shown as viability by ATP content, i) as also by Annexin measurements. All experiments were compared and normalized to a scrambled control transfection (** $p < 0.01$, *** $p < 0.001$, ****$p < 0.0001$)

2.3.4. MiRNA-27a is a putative prognostic marker for endocrine therapies in metastatic ER+ breast cancer

As validation of the *in vitro* results, the impact of miR-27a expression on the survival of patients with ER-positive tumors which underwent endocrine treatment was evaluated. An analysis of patient data derived from the METABRIC cohort was performed utilizing the tool “miR power” (http://www.kmplot.com) by Lanczky et al. [46]. In this analysis, patients were grouped according to their ER expression, as determined by immunohistochemistry and their status of node invasion. Patient groups with ER-positive tumors were narrowed down to the cohort which underwent endocrine treatment exclusively, while no further limitations were set in groups with ER-negative tumors in regard of the therapy.

As shown in Figure 7, patients with ER-positive tumors and high miR-27a expression had beneficial overall survival (OS) of about 20 months and a lower risk of events, compared to the low expressing group (N=726, HR 0.87 (0.6-1.08), p=0.15; not significant). The corresponding Kaplan-Meier curves show the biggest difference between the two groups during 100-150 months of follow up, corresponding to the usual follow-up care for breast cancer patients. In contrast, ER-negative breast cancer patients with high miR-27a expression were at approximately one third higher risk and had a 1.5 years lower median OS than the low expressing cohort (N=266, HR 1.33 (0.84-2.09), p=0.22). Further differentiation of the ER-positive group to a subgroup which is determined as luminal A, the relative risk additionally decreased to 0.61 (0.39-0.94) with p=0.025 (see supplemental Figure S3).

By further differentiation of the dataset, patients with more aggressive luminal A cancer were investigated. Those groups were constricted to subgroups with positive lymph node status, indicating a higher metastatic ability of the tumor and higher tumor burden of the patients. In this setting, the data showed highly significant difference in the ER-positive group towards a beneficial effect of high miR-27a in the OS. Patients with low miR-27a expression had an approximately 50 months shorter survival, therefore decreasing the risk in the high miR-27a to 0.65 (0.47-0.9; p=0.0083). Likewise, the comparison in ER-negative patients showed the reverse picture: High miR-27a expression lead to a significant decrease in OS of about 50 months with a two-fold increased relative risk (HR 2.02, (1.09-0.023), p=0.023). Here, in the luminal A subgroup (see supplemental Figure S3) high miR-27a lead to significantly increased OS of about 40 months and 0.51 (0.31-0.85) relative risk (p=0.0083). Similar results

were seen in another cohort of luminal A patients with early breast cancer, which underwent tamoxifen treatment, as analyzed with the MIRUMIR tool [47] (supplementary Figure S4).

These findings showed that miR-27a expression was high in aggressive tumors and was detrimental for patients with ER-negative breast cancer, but in the setting of ER-positive tumors that were treated with endocrine therapies high miR-27a levels were an indication for a good response to the treatment and increased survival rates.

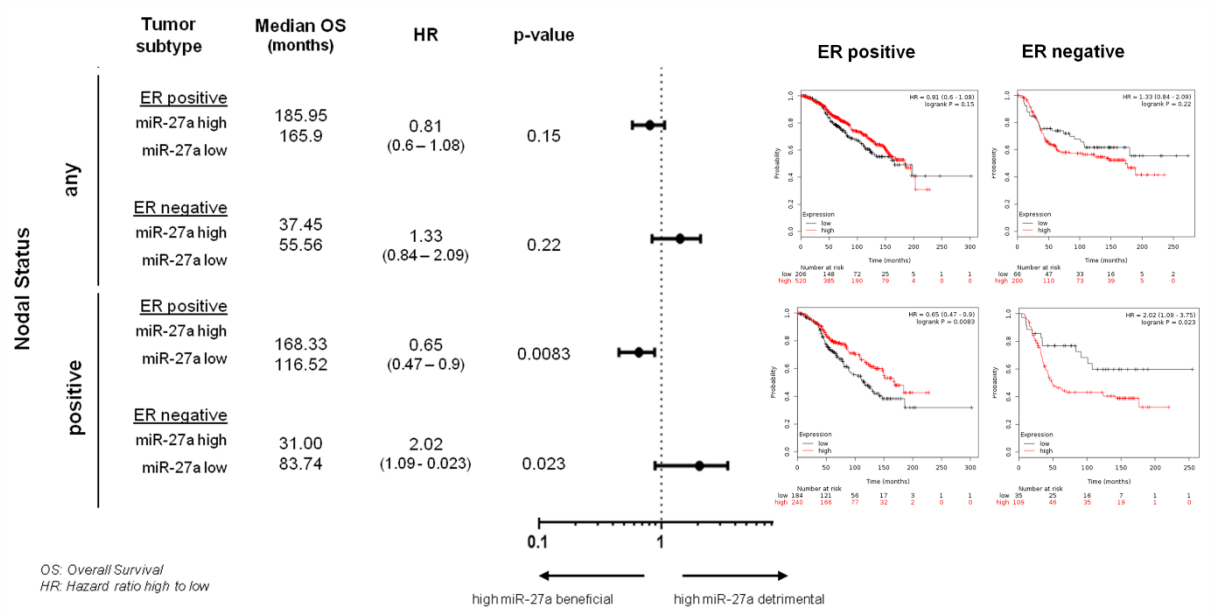

Figure 7 - Clinical data shows potential of miR-27a as prognostic marker for endocrine therapies ER+ and ER+ metastatic breast cancer

2.4. Discussion

While luminal A breast cancer is regarded as the one subtype with best prognosis and well established treatment options, current epidemiologic data suggest a need for better follow-up care of the disease, as evidently mortality of these patients is increasing after 5 years[31]. Different approaches are made to counteract bad long-term outcomes. Often SERM treatments are prolonged for a time of up to 10 years and longer or switched for different treatments with drugs of other therapeutic classes, usually aromatase inhibitors [31,48]. Many of these approaches are associated to the same adverse effects as SERM treatment, i.e. cardiovascular disease and the substantially increased risk of secondary cancers like endometrial carcinoma [49]. Hence, physicians are inclined to often discontinue therapies early to balance these risks. Still, the number of relapsing patients with therapy resistant tumors is high and therefore there is an urgent need for personalized treatment options to maximize efficacy of therapies while decreasing the adverse effects. MiRNAs are a class of potential markers, which show fine-tuned expression patterns in tissues, as well as offer the possibility to analyze their expression directly from blood samples as circulating miRNAs[39].

MiR-27 plays an ambivalent role in cancer. On the one hand, it is known to increase proliferation and metastasis in patients[22], in some cases even assumed to regulate chemoresistance [50]. This aspect makes it an interesting marker for numerous cancer types, like colon and esophageal cancer and also certain types of breast cancer, in order to adjust treatments and therapy regimes accordingly [22,23,50]. In the analysis of the METABRIC datasets, two cohorts of patients with ER-negative tumors, which consequently did not receive endocrine treatments, showed significantly worse outcomes for patients with high miR-27a expression. This result is in line with the discussed role of miR-27a as oncomir, inducing negative effects on patient survival.

On the other hand, the *in silico* analysis of both the METABRIC and MIRUMIR datasets revealed that miR-27a expression is a predictor of beneficial breast cancer patient survival, in a defined subgroup of ER-positive tumors treated with endocrine agents.

Multiple explanations can be considered for this ambivalence. First, due to the positive bidirectional feedback loop between miR-27a and ERα, the miR-27a expression may function as a surrogate marker for the ERα expression. MiR-27a was described to upregulate ERα expression, as observed in the current study and was previously reported, based on miR-27a inhibition of ZBTB10 and resulting increase of the

expression of the sp-protein family[42]. In this case, higher levels of ERα, based on increased miR-27a expression, could increase the susceptibility for SERMs and therefore improve the eradication of the tumor. While an increase of drug targets is often discussed as resistance mechanism, different studies suggest that SERM antitumor effects are based not only on inhibition of the estrogen signaling, but additionally on induction of maspin or of oxidative stress, which result of interaction with the receptor [51,52]. Therefore, an increased number of SERM targets could correlate with the induced damage in the tumor.

Additionally, our data showed that stimulation with or the deprivation of estradiol, as well as a direct knock-down of ERα, showed identically directed impact on miR-27a expression, as was also reported in a genomic expression study previously [53]. The *in silico* analysis of the promotor and enhancer region revealed multiple potential sites of transcriptional regulation of miR-27a via ERα, e.g. by direct translational effects based on EREs or upregulated transcription factor activity downstream of the ER-signaling pathway, like JUN.

Thus, high miR-27a levels may act as surrogate read-out for a high ERα translational activity in the tumor, likely with crucial cancer promoting effects due to ERα's role in cell cycle and proliferation[54]. This could explain the higher impact on cancer cell survival resulting from ERα inhibition.

Both of these discussed mechanisms do not contradict miR-27a's role as oncomiR, as increase of ER-activity leads to higher proliferation and metabolic activity in the cells[54]. In fact, the *in vitro* viability data suggest that treatments with tamoxifen and toremifen are significantly more effective in eradicating these potentially more aggressive tumors, underlined by the finding that the beneficial prognostic effect of miR-27a is highest for ER-positive tumors which spread to lymph nodes.

Besides acting as predictor for an enhanced response to SERM treatments, the observed loss of miR-27a may also function as indicator of resistance to the therapy, as observed in the TAM6 cells. Treatment with TAM for six rounds in the course of multiple weeks, caused the formation of a considerable resistance, accompanied by the loss of miR-27a, as was also demonstrated by Ye et al [55], showing increased miR-27a expression after generation of TAM resistant cells.

Many mechanisms are discussed for resistance development to tamoxifen. One obvious effect which may account for up to 17-28% of acquired resistance[56], may be the loss of ERα, rendering the cancer cells independent of estrogen, based on CpG

island methylation of the ER-promotor[57]. As no analysis of methylation patterns was performed on the TAM6 cells, it is possible that partial methylation of the ESR1 promotor occurred and therefore affected changes in ERα and miR-27a expression.
In addition, the occurrence of mutations of the ER-gene were reported, which are not influencing the ERα expression, but were observed to have no estrogen mediated translational activity while appearing as ER-positive in immunohistological stainings [58]. In this case, miR-27a may be a valuable indicator of functional ERα expression, as ER-positive tumors with low miR-27a expression might inherit a less functional ERα translational activity and thus decreased response to SERMs.
Taken together, miR-27a expression correlates with functional ERα expression and may therefore act as surrogate read-out for a frequent resistance mechanism.
MiRNA screening can play an important part in improving patient outcomes by enabling tailored treatments and personalized medicines for cancer. A screening of different miRNAs, including miR-27a in blood plasma of breast cancer patients was performed previously [59]. In the study of Jurkovicova et al. miR-27a was shown to be one of the modified miRNAs in the analysis of plasma samples from the patients. The data indicates that miR-27a expression may be used as marker for invasive breast cancers or carcinomas *in situ*. Further studies need to be conducted to prove whether miR-27a expression is a prognostic marker for therapeutic response also in blood plasma.
Taken together, our data suggests and encourages further studies of miR-27a as marker for SERM response in the clinics. Patients with ER-positive tumors with high miR-27a expression currently already receive suitable treatment with adjuvant tamoxifen, if treated according to the guidelines[13]. However, patients in the same setting with miR-27a low tumors may display resistance to the treatment, either initially or due to acquired resistance in the long-term. These patients would benefit most of an analysis of miR-27a levels.

Acknowledgments

The authors thank the German Research Foundation (DFG) for financial support (SFB 1032 project B4). JGR thanks the Mexican government for receiving a scholarship (CONACyT number 207973). AS thanks Hanns-Seidel Stiftung for receiving a scholarship.
The authors thank Florian Lengauer and Nicoletta Bruno for preliminary experiments.
The authors declare no competing financial interests.

2.5. Material and methods

Reagents

Puromycin dihydrochloride (cat. P8833), Tamoxifen (cat. T5648), Endoxifen (cat. E8284), Toremifen (cat. T7204) and Estradiol (E1024) were obtained from Sigma-Aldrich.

Cell culture

MCF7 were acquired from cell line service (Eppelheim, Germany), grown at 37 °C and 5 % CO_2 in high glucose DMEM (Sigma) supplemented with 10 % fetal calf serum (FCS / Gibco). TAM6 as resistant clone were generated from parental MCF7 by six rounds of treatment with tamoxifen as described before[43] and cultured like MCF7. T47D were acquired from ATCC, grown at 37 °C and 5% CO_2 in RPMI-media (Sigma). All cells were routinely tested and confirmed as mycoplasm free.

Overexpression of miR-27a

Overexpression experiments were performed by transfection of a miR-27a mimic (miRIDIAN Human hsa-miR-27a 3p, Dharmacon) and miRIDIAN Mimic Negative Control #1 (Dharmacon) with K2 transfection reagent (Biontex, Germany) according to the manufacturer's protocol. Cells were seeded in 6-well plates to 80% confluence depending on the experiment kept in 6-well or seeded 24 h after transfection for following experiments.

miRNA quantitative RT-PCR

Approximately 600,000 cells were harvested and total RNA isolated from cells using Total RNA Kit, peqGOLD (VWR). cDNA synthesis was carried out by a microRNA specific reverse transcription and detection with the qScript microRNA cDNA Synthesis Kit and PerfeCta SYBR Green SuperMix (Quanta Biosciences) with RT-PCR detection on a LightCycler 480 (Roche). The expression of miR-27a was normalized to miR-191, using the $2^{-\Delta CT}$ or $2^{-\Delta\Delta CT}$ method. The primers used for analysis were for miR-27a: GCCGTTCACAGTGGCTAAG and for miR-191: GCGCAACGGAATCCCAAAAG

mRNA quantitative RT-PCR

RNA was extracted utilizing the Total RNA Kit, peqGOLD (VWR) as by manufacturer's instructions. Translation to cDNA was performed utilizing the qScript cDNA synthesis kit (Quanta Bioscience) as by manufacturer's protocol.

Analysis of expression was performed with the Lightcycler 480 (Roche) and the Universal Probe Library (Roche) with following probe and primer (forward/reverse) combinations:

ESR1 Fwd:ATCCACCTGATGGCCAAG Rev:GCTCCATGCCTTTGTTACTCA; Probe #17

GAPDH Fwd: TCCACTGGCGTCTTCACC Rev:GGCAGAGATGATGACCCTTTT; Probe #45

The expression of ESR1 was normalized to GAPDH, using the 2-ΔCT or 2-ΔΔCT method.

ER-signaling via ERE-luc reporter

3X ERE TATA luc was a gift from Donald McDonnell (Addgene plasmid # 11354). Transfection was performed in 6-well with cells grown to 80% confluence with K2 transfection reagent (Biontex, Germany) according to the manufacturer's instructions. After 24 h cells were seeded in 96-well plates and luc-measurements were performed as described previously[28].

Generation and stimulation of TRIPZ-shER MCF7

MCF7 cells were transducted with a 2nd generation lentiviral system generated with the plasmids pCMV-dR8.2 dvpr and pCMV-VSV-G, which were a gift from Bob Weinberg (Addgene plasmid # 8454 and #8455) and a doxycycline-inducible TRIPZ-shER construct, which was a gift from Yunus Luqmani, Kuwait. For control, cells were transducted with a scramble hairpin, the TRIPZ-shCtrl construct (ThermoFisher).

Western blot analysis and immunofluorescence

Cells were cultured in a 6 well plate for 48h after transfection / stimulation, lysis, gel and blotting were performed as described previously[27], with the following primary antibodies: Estrogen Receptor-α (sc-543), Actin (sc-1616, Santa Cruz) and GAPDH (14C10, Cell Signaling). Immunofluorescence stainings were performed as described previously[60], -ES cells were cultured for the time of the experiment in phenol-red-free media with 10% charcoal stripped FCS (F6765 , Sigma), +ES cells were stimulated with 3,6 µM estradiol for 1h before fixation.

Analysis of transcription factors in promoter regions of found genes

For the analysis of the promoter region of the miR-27a locus, the sequence was retrieved from the RefSeq-Database (https://www.ncbi.nlm.nih.gov/refseq/ as of January 2018) in order to identify the +1 position. Assuming the +1 position as starting site of transcription, 500 nucleotides upstream were defined as the proximal promoter. The enhancer region was defined as the genomic sequence 30,000 base pairs upstream of the +1[44]. Then, for analysis of possible promoter sequences, ALGGEN[61] software was used, the analysis was performed with the highest stringency. Analysis of ERE-sites were performed by manual alignments of the consensus sequence and known variances that were previously discussed[62].

Treatment with SERMs and relative viability assays

Stock solutions of TAM, ENDO and TOR were prepared in DMSO with a concentration of 20mM. Dilutions were prepared freshly in according media, controls contained appropriate amounts of DMSO. Treatments were performed 48 h after stimulation / transfection for 48 h. Relative viability as ATP-content was assessed by Celltiter-Glo (Promega) according to manufacturer's instructions.

Annexin V assay

The cells were cultured and treated as described above. Samples were harvested, and analyzed with the Annexin V-FiTC Apoptosis Detection Kit Plus (BioVision) according to the manufacturer's protocol. Measurement was performed using CyAn ADP Flowcytometer (Dako Cytomation / Beckmann) and FlowJo 7.6.5. (TreeStar).

In silico analysis of patient data

Patient survival data, treatment information and expression of ERα / miR-27a was acquired from the database of kmplot software (http://www.kmplot.com[46]). Analysis for miR-27a was based on data from the METABRIC study (syn1688369)[35].

Statistical analysis

Results are expressed as the mean ± SD of at least three replicas, if not stated otherwise. All experiments were conducted three times independently, one representative example is depicted. Software GraphPad Prism v6 and SigmaPlot 11 were utilized for the analysis of the data.

Data availability

The data that support the findings of this study are available from the corresponding author upon reasonable request.

Conflict of Interest statement

The authors declare that they have no conflict of interest.

Author contributions statement

BL performed the experiments and wrote the manuscript. JGR performed the analysis of transcription factor and ERE-binding sites. AS generated the TAM6 cells. EW provided conceptual advice. AR conceived the study and wrote the manuscript. All authors commented on the manuscript and conclusions of this work.

3. A proteomic analysis of an in vitro knock-out of miRNA-200c

The following sections are directly adapted from the original publication, which was finally published as Ljepoja et al., Sci Rep. 2018 May 2;8(1):6927.

A proteomic analysis of an *in vitro* knock-out of miR-200c

Bojan Ljepoja[1#¶], Jonathan García-Roman[1#¶], Ann-Katrin Sommer[1], Thomas Fröhlich[2], Georg J. Arnold[2], Ernst Wagner[1], Andreas Roidl[1]* Sci Rep. 2018 May 2;8(1):6927

[1]Pharmaceutical Biotechnology, Department of Pharmacy, Ludwig-Maximilians-Universität München, Munich, Germany

[2]Laboratory for Functional Genome Analysis (LAFUGA), Gene Center, Ludwig-Maximilians-Universität München, Munich, Germany

Contributions

BL analyzed and presented the proteomic data, performed the biological and qPCR experiments and wrote the manuscript. JGR generated the cell lines, performed qPCR and migration experiments, analyzed transcription factors and wrote the manuscript. AS performed sample preparations for proteomics and provided support in presenting the data. TF conducted the LC-MS experiments and helped with data analysis. EW and GJA provided conceptual advice. AR conceived the study and wrote the manuscript. All authors commented on the manuscript and conclusions of this work.

3.1. Abstract

Loss of miR-200c is correlated to advanced cancer-subtypes due to increased EMT and decreased treatment efficacy by chemotherapeutics. As miRNAs regulate a multitude of targets, the analysis of differentially expressed proteins upon a genomic knock-out (KO) is of interest. In this study, we generated a TALENs KO of miR-200c in MCF7 breast cancer cells, excluded its compensation by family-members and evaluated the impact on the proteome by analyzing three individual KO-clones. We identified 26 key proteins and a variety of enrichments in metabolic and cytoskeletal pathways. In six of these targets (AGR2, FLNA/B, ALDH7A1, SCIN, GSTM3) the differential expression was additionally detected at mRNA level. Together, these alterations in protein abundance accounted for the observed biological phenotypes, i.e. increased migration and chemoresistance and altered metabolism, found in the miR-200c-KO clones. These findings provide novel insights into miR-200c and pave the way for further studies

3.2. Introduction

MicroRNAs (miRNAs) are short non-coding RNAs which are known to regulate protein expression at the translational level via base pairing to mRNA or by induction of mRNA decay[26,63]. Since their discovery, miRNAs have had a tremendous impact on our understanding of physiology and pathophysiology, leading to ever increasing efforts to discover miRNA genes, their function and targets[1,64]. MiRNAs are important for a broad spectrum of biological processes, such as embryonic development, immune differentiation, metabolism and cardiac function[65-68]. On the other hand, their aberrant expression is involved in a vast number of diseases, such as diabetes and cancer[65,69,70]. Therefore, miRNAs are promising tools as biomarkers or therapeutic agents[71].

An important group of miRNAs in the context of cancer research is the miR-200 family, consisting of miR-200a, miR-200b, miR-200c, miR-141 and miR-429. Many family members are known to play a role in a large variety of biological processes like Epithelial to Mesenchymal Transition (EMT), cell invasion, proliferation, metastasis, apoptosis, autophagy, and therapy resistance in several cancer types[26,72-76]. MiR-200c is the most prominent member in tumorigenesis, as its role in several hallmarks of cancer, such as EMT, chemoresistance, migration and stemness[26,77], was already described. Although the involvement of miR-200c in these processes was demonstrated, many underlying mechanisms and players remain unknown[26], especially in controversially discussed processes like chemoresistance or proliferation[26-28,78,79].

In our previous work, we were able to show the involvement of miR-200c in sensitizing breast cancer cells to doxorubicin, via regulating BMI1 and TRKB[27] as well as the direct interaction of miR-200c with the mRNA of the prominent oncogene KRAS[28].

The vast majority of the studies analyzing the biology of miR-200c utilizes short-term inhibition approaches making use of LNAs or antagomirs, but omitting the impact of miR-200c depletion in the long-term[27,80,81]. The latter reflects the loss of miR-200c expression in a tumor, as is frequently observed in the clinics[82,83]. Thus, analyzing the knock-out (KO) of miR-200c leads to novel insights into miR-200c's role in advanced breast cancer.

With current genome editing tools like TALENs (Transcription Activator-Like Effector Nucleases) and CRISPR-Cas9 (Clustered Regularly Interspaced Short Palindromic Repeats)[30,84] a revolution in many fields of gene research was initiated. While both

tools have different properties and demand different strategies, they also equally harbor high potential for research of non-coding genes, like miRNAs. TALEN are fusion proteins that induce a double strand break in the DNA, but have to be designed as pair, specifically targeting the desired genomic site. The nuclease-activity will cause a double strand break (DSB) which can be repaired on the hand by error prone Non-Homologous End Joining (NHEJR), in most cases leading to an indel formation and thus to the knock-out of the gene. On the other hand Homologous Recombination (HR) results in successful repair of the DSB[30,85].

CRISPR-Cas9 is based on the nuclease-activity of Cas9, but the targeting is initiated by short-guiding RNAs (sgRNA) and is limited to genomic sites with a protospacer adjacent motif (PAM). CRISPR approaches usually lead to a double strand break and only one sgRNA needs to be designed[29,84,86].

In this study, we utilized TALENs for a genetic KO of miR-200c, due to its flexibility to target any genomic sequence. This approach allowed us to develop a long-term *in vitro* model of miR-200c depletion (KO) in MCF7 breast cancer cells. With a subsequent proteomic analysis, we were able to gain novel insights to changes in the proteome, i.e. differentially expressed proteins, resulting from the absence of only 22 non-coding basepairs of the miR-200c.

3.3. Results

3.3.1. A miRNA-200c knock-out - strategy and validation

To generate the miR-200c KO, we chose to genetically disrupt the drosha processing site. Generally two options for genomic editing were available – CRISPR/Cas9 and TALENs. While a PAM-sequence was present in the drosha processing site, suitable sgRNAs were designed with the CRISPR-design tool[87] but resulted in 60-75 off-targets, amongst them 6-9 in coding regions. Utilizing a Cas9-Nickase would result in lower off-targets, but it was not possible to design a pair inducing a site-specific mutation within the limited number of base-pairs of the drosha-site. Therefore, we chose a pair of TALENs to disrupt miR-200c 3p gene expression by targeting the flanking regions of the drosha processing site as described previously[88]. Eventually we sought to induce a double strand break in the vicinity of the drosha processing site (Figure 8a). MCF7 cells were chosen as model for an epithelial breast cancer cell line with high miR-200c expression[27]. A single cell dilution was performed, and clones were selected to sequence indel formation at the genomic locus of the miR-200c drosha site. Three of the monoclonal cell lines, namely M1, M2 and M3 showed deletions in both alleles of the miR-200c gene which were located in vicinity of the drosha processing site (i.e. homozygous KO of miR-200c). One clone (MCtrl) showed a heterozygous mutation (Figure 8b).

A qPCR-measurement of miR-200c expression of M1, M2 and M3, confirmed the knock-out of the miR-200c gene (Figure 8c). The heterozygous mutations in MCtrl had no significant effect on the miR-200c expression, as levels were comparable to MCF7 wild-type ($p>0.05$). Therefore, besides wild-type MCF7, MCtrl was considered as additional control for further analysis.

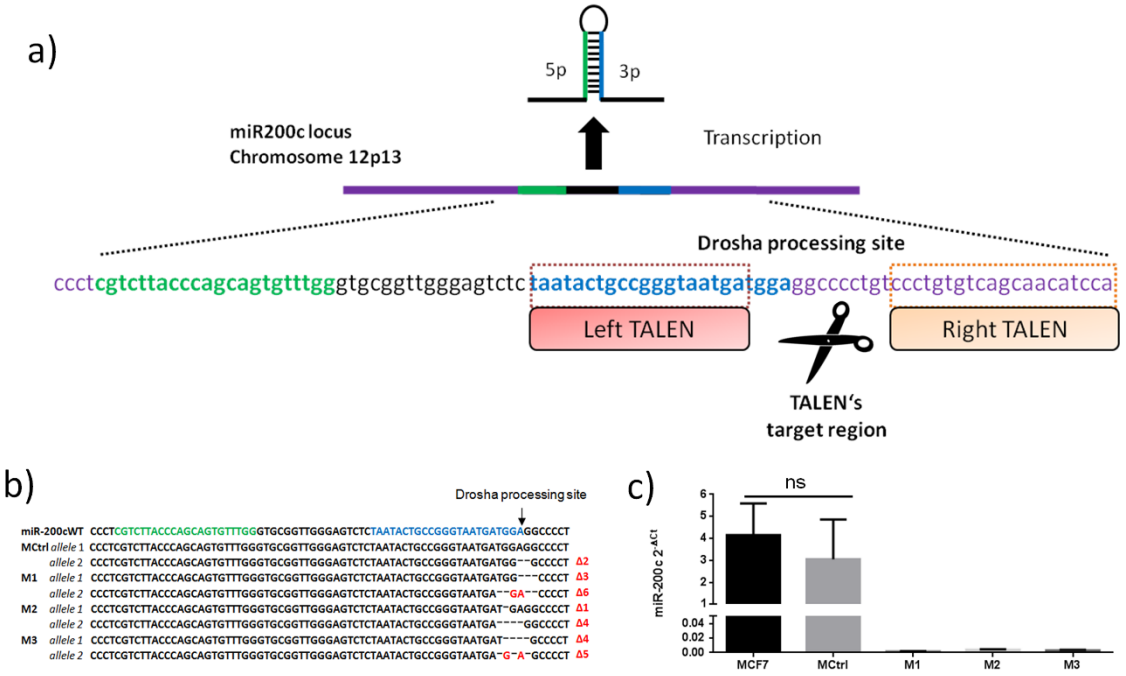

Figure 8 - miR-200c genetic TALEN target sequences and knock-out confirmation.

a) The miR-200c gene is located at chromosome 12p13, TALENs were designed to target miR-200c 3p drosha processing site. b) Genomic DNA was extracted from MCtrl and M1, M2 and M3 clones, afterwards the miR-200c gene was amplified by PCR to perform sequencing of the miR-200c loci; MCtrl shows a heterozygous mutation while M1, M2 and M3 show various indels in proximity of the miR-200c 3p drosha processing site on both alleles. c) MCF7, MCtrl, M1, M2 and M3 miR-200c expression levels were analyzed by quantitative RT-PCR. Expression of miRNAs is shown as mean of three independent experiments ± SD .ns: no statistical difference, p>0.05, one-way ANOVA post hoc Bonferroni.

3.3.2. Unchanged expression of miR-200 family members

To investigate possible compensation effects of the knock out, we analyzed the expression levels of the other miR-200c family members. The genomic loci are comprised of two genomic clusters, one located at chromosome 1p36 including miR-200a, miR-200b and miR-429, and chromosome 12p13 containing miR-200c and miR-141[26]. MiR-200c shares the same seed region with miRs 200b and 429 (Figure 9a). Subsequently, a qPCR analysis of the expression of all family members was performed.

This data showed that miR-200c is the family member with highest expression in MCF7. Further analysis revealed that no family member was compensating for the loss of miR-200c by an increase of expression and no general upregulation of all family members was observed (p>0.05) compared to the control group (MCF7 and MCtrl). Of note, also the expression levels of miR-141 remained similar, i.e. not influenced by the KO of miR-200c, despite the localization in the same polycistronic unit (Figure 9b).

The knock-out of a miRNA is fundamentally different to its short term inhibition, giving the cells more time to compensate the loss of miR-200c. Therefore, late compensatory mechanisms were ruled out by re-evaluation of the expression of miR-200c family members at a late cell passage number. Compared to earlier passages, the data showed no remarkable changes in the different clones over time (p=0.896**,** Figure 9c). The slight increase of miR-141 is not significant.

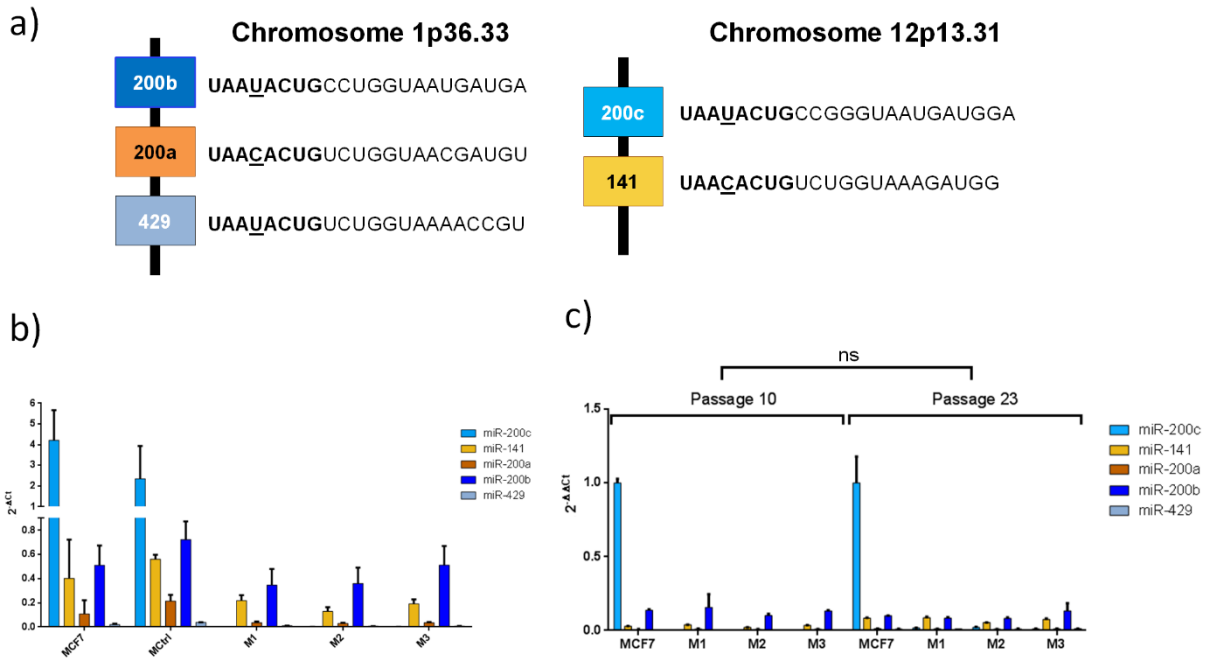

Figure 9 - Expression of miR-200 family members among the KO clones.

a) The miR-200 family is distributed on two chromosomes; miR-200b, miR-200a and miR-429 are located on chromosome 1p36.33 and miR-200c and miR-141 are located on chromosome 12p13.31. miRs with the same seed region are colored in tones of orange or blue respectively. b) MCF7, MCtrl, M1, M2 and M3 were analyzed for miR-200c, miR-141, miR-200a, miR-200b and miR-429 relative expression levels by quantitative RT-PCR. c) Cells from passage 10 and passage 23 were compared regarding their miR-200c, miR-141, miR-200a, miR-200b and miR-429 relative expression levels via quantitative RT-PCR. Expression of miRNAs is shown as mean ± SD of three independent replicas. ns means no statistical difference, p>0.05, three way ANOVA post hoc Bonferroni.

3.3.3. Proteomic analysis of three individual KO clones results in 26 novel targets

To evaluate the effect of the miR-200c KO on a wide range of proteins, a proteomic approach was chosen (
Figure 10a):
All clones (M1, M2, M3, MCtrl), as well as wild-type MCF7 cells were harvested in three replicas (A/B/C), and subsequently, proteomic data analysis was performed, resulting in a set of 1736 identified proteins. For the following analysis, we chose to narrow the set down to proteins that were identified in every single measurement.
This filtering resulted in a subset of 675 proteins. On this subset, a principal component analysis (PCA) was performed to investigate the similarity of the clones and replicas.
Figure 10b shows a general trend of grouping of the replicas (with exception of MCtrl C) as well as a closer relation between the KO-clones M1, M2 and M3 and the controls MCF7 and MCtrl, respectively. A similar behavior is seen in a cluster analysis, as shown in the Supplement S 1. For statistical evaluation of differentially expressed proteins a Volcano plot analysis was performed (
Figure 10c), comparing the expression of the KO-clones M1, M2 and M3 (KO) to the controls MCF7 and MCtrl (Ctrl). This analysis revealed nine proteins with significant changes in regulation as shown in Table 1.
To investigate effects on single-clone level, a further T-test with the same parameters was performed, comparing each KO-Clone (M1, M2 or M3) to the grouped controls (e.g. M1 vs. MCtrl and MCF7). The analysis revealed 17 significant hits, as shown in Figure S2 and summarized in Table 2. Here, M2 is pointed out as most diverse from the controls with 14 proteins being differentially expressed, while the two other clones show only statistical difference in one or six proteins for M1 and M3, respectively (Supplement S 2).
Next, to further analyze targets which may have had changes in expression in response to the miR-200c KO but have not been detected in the previous analysis, we searched for proteins that were not detected in the KO-group, but were found in the control-group (found at least 3 times in Ctrl, not at all in the KO). These proteins were termed “OFF”. Vice versa, “ON” proteins display no expression in the control-group but are expressed in the KO-group (at least 5 times in KO, but not in Ctrl). Table 3 lists the three targets gaining expression after knock-out (ON) and the two proteins losing expression (OFF).

The 26 targets shown in Table 1, 2 and 3 were grouped according to their main function as stated by the Uniprot-Database[89]. As shown in
Figure 10d, more than half of the proteins are found in migratory processes and metabolism (45% and 17% respectively), while other functions are detoxification (10%) and apoptosis (11%), with remaining 17% of proteins, with no known function.

Table 1 - Targets with significant difference between both groups – M1 and M2 and M3 vs MCF7 and MCtrl

Protein	Gene	p-Value	fold change	Expression	Function
Anterior gradient protein 2 homolog	AGR2	$6.36x10^{-3}$	0.59	down	Migration
Filamin-A	FLNA	$4.32x10^{-5}$	1.31	up	Migration
Filamin-B	FLNB	$1.20x10^{-5}$	1.41	up	Migration
Glutathione S-transferase Mu 3	GSTM3	$1.43x10^{-5}$	3.54	up	De-Tox
Pyridoxal kinase	PDXK	$2.27\ x10^{-3}$	0.53	down	Metabolism
4F2 cell-surface antigen heavy chain	SLC3A2	$1.25\ x10^{-4}$	2.00	up	Apoptosis
Spectrin alpha chain, non-erythrocytic 1	SPTAN1	$3.26\ x10^{-4}$	0.73	down	Migration
Tropomyosin alpha-1 chain	TPM1	$3.74\ x10^{-3}$	1.93	up	Migration
UDP-glucose 6-dehydrogenase	UGDH	$7.10\ x10^{-3}$	0.39	down	Migration

Table 2 - Targets with significant difference between control and at least one clone: M1 or M2 or M3 vs. MCF7 and MCtrl

Protein names	Gene	p-Value	fold increase	Expression	Function
Anterior gradient protein 2 homolog	AGR2	M2 vs Ctrl 2.82×10^{-4}	M2 vs Ctrl 0.397	down	Migration
Alpha-aminoadipic semialdehyde	ALDH7A1	M2 vs Ctrl 4.69×10^{-4}	M2 vs Ctrl 1.96	up	De-tox
Carbonic anhydrase 2	CA2	M2 vs Ctrl 4.07×10^{-3}	M2 vs Ctrl 0.361	down	Unknown
Src substrate cortactin	CTTN;EMS1	M2 vs Ctrl 4.67×10^{-4}	M2 vs Ctrl 0.743	down	Migration
Aspartate aminotransferase	GOT2	M3 vs Ctrl 1.38×10^{-4}	M3 vs Ctrl 0.556	down	Metabolism
Glutathione S-transferase Mu 3	GSTM3	M1 vs Ctrl 6.03×10^{-5} M2 vs Ctrl 1.50×10^{-7} M3 vs Ctrl 1.21×10^{-5}	M1 vs Ctrl 2.48 M2 vs Ctrl 6.17 M3 vs Ctrl 2.91	up	De-tox
Heat shock protein HSP 90-alpha	HSP90AA1	M2 vs Ctrl 4.64×10^{-4}	M2 vs Ctrl 1.39	up	Metabolism
D-3-phosphoglycerate dehydrogenase	PHGDH	M2 vs Ctrl 6.57×10^{-3}	M2 vs Ctrl 1.89	up	Metabolism
Kynureninase	KYNU	M2 vs Ctrl $1. \times 10^{-3}$	M2 vs Ctrl 1.61	up	Metabolism
DNA replication licensing factor MCM4	MCM4	M2 vs Ctrl 2.12×10^{-4}	M2 vs Ctrl 0.761	down	De-tox
Ras-related protein Rab-14	RAB14	M2 vs Ctrl 1.23×10^{-5}	M2 vs Ctrl 0.595	down	Migration
SH3 domain-binding glutamic acid-rich-like protein	SH3BGRL	M3 vs Ctrl 4.01×10^{-5}	M3 vs Ctrl 1.85	up	Migration
4F2 cell-surface antigen heavy chain	SLC3A2	M2 vs Ctrl 7.09×10^{-6} M3 vs Ctrl 6.42×10^{-4}	M2 vs Ctrl 2.91 M3 vs Ctrl 1.71	up	Apoptosis
Triosephosphate isomerase	TPI1	M3 vs Ct 7.95×10^{-5}	M3 vs Ctrl 0.69	down	Metabolism
Tropomyosin alpha-1 chain	TPM1	M2 vs Ctrl 4.76×10^{-3}	M2 vs Ctrl 2.71	up	Migration
UDP-glucose 6-dehydrogenase	UGDH	M2 vs Ctrl 3.67×10^{-6} M3 vs Ctrl 3.28 x10-3	M2 vs Ctrl 0.155 M3 vs Ctrl 0.533	down	Migration
Tryptophan-tRNA ligase	WARS	M2 vs Ctrl 1.20×10^{-3}	M2 vs Ctrl 1.58	up	De-tox

Table 3 - Targets detected in just one of the groups: M1 and M2 and M3 OR MCF7 and MCtrl

Protein	Gene	Expression	Function
N-acetylserotonin O-methyltransferase-like protein	ASMTL	ON	Unknown
Serine/threonine-protein phosphatase PP1-gamma catalytic subunit	PPP1CC	OFF	Unknown
Apoptosis-associated speck-like protein containing a CARD	PYCARD	OFF	Apoptosis
Regulator of microtubule dynamics protein 1	RMDN1	ON	Migration
Adseverin	SCIN	ON	Migration

Figure 10 - Proteomic analysis of three different KO clones (next page)

a) Schematic overview of the experimental procedure to generate three different clones. Each clone was measured in independent replicas b) Principal component analysis of the measurements, KOs are shown in red, Ctrls in blue c) Volcano plot analysis of grouped controls: (MCF7 WT A/B/C and MCtrl A/B/C) vs. (M1 A/B/C and M2 A/B/C and M3 A/B/C), N=675 with 250 randomizations, FDR 0.05 and S0 of 0.1 d) Percentage of main functional pathways of targets in Tables 1, 2 and 3, as derived from the Uniprot-Database e) Analysis for possible seed-interaction of miR-200c with the targets of Tables 1,2 and 3 and further analysis of not-directly regulated targets for binding of transcription factors with predicted miR-200c regulation, see also Supplemental Table S 3: f) Validation of mRNA expression with grouped statistical analysis (M1 and M2 and M3 vs MCF7 WT and MCtrl, N= 9 (KO) / 6 (Ctrl)) for the anterior gradient protein 2 homolog, aldehyde dehydrogenase 7 family member A1, filamin A and B, glutathione S-transferase M3 and adseverin, *$p \leq 0.05$ ***$p \leq 0.001$ **** $p \leq 0.0001$

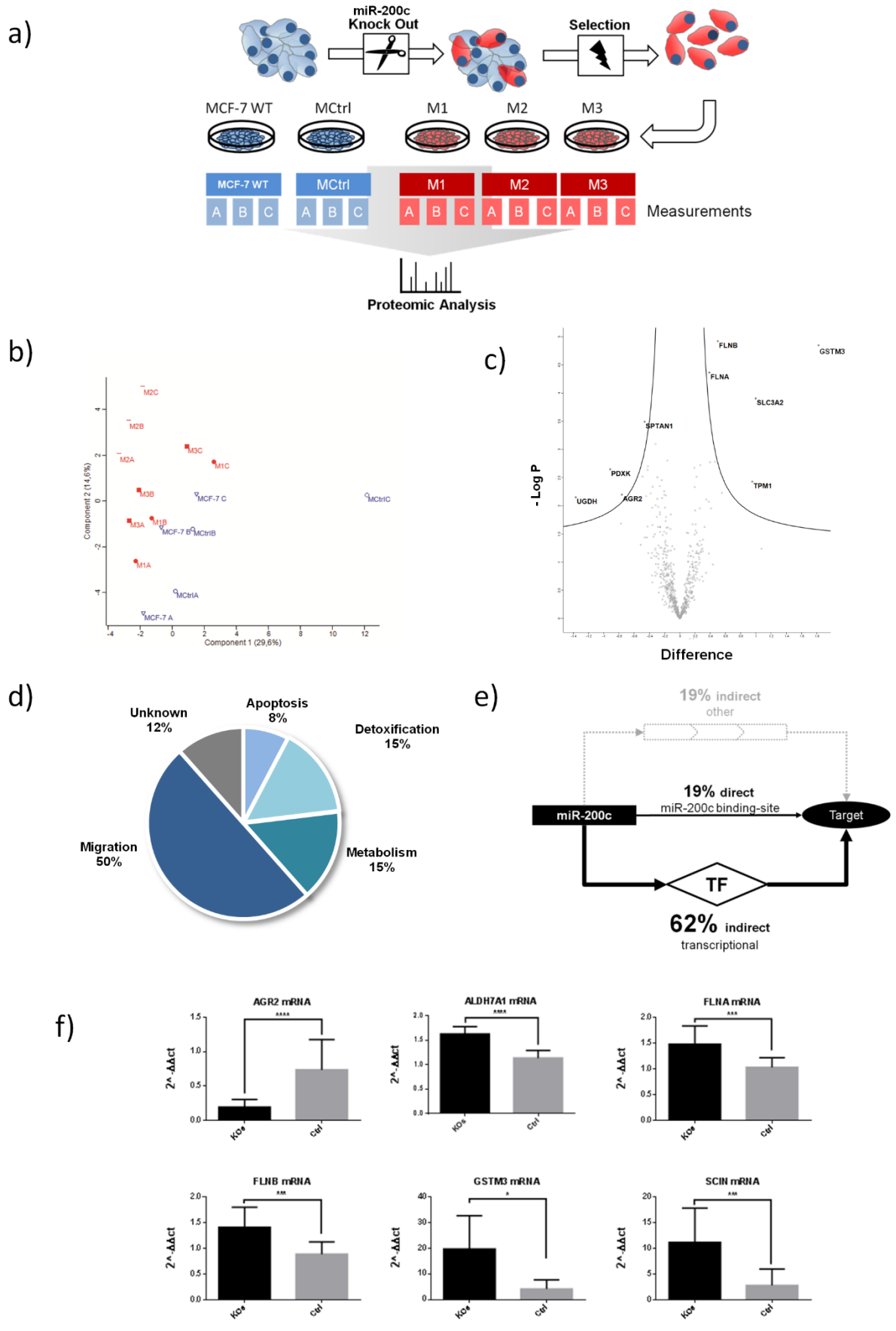
a)
miR-200c
Knock Out
Selection
MCF-7 WT
MCtrl
M1
M2
M3
A B C
Measurements
Proteomic Analysis
b)
Component 1 (29,6%)
Component 2 (14,6%)
c)
- Log P
Difference
FLNB
GSTM3
FLNA
SLC3A2
SPTAN1
PDXK
TPM1
UGDH
AGR2
d)
Unknown
12%
Apoptosis
8%
Detoxification
15%
Migration
50%
Metabolism
15%
e)
19% indirect
other
19% direct
miR-200c binding-site
miR-200c
Target
TF
62% indirect
transcriptional
f)
AGR2 mRNA
ALDH7A1 mRNA
FLNA mRNA
FLNB mRNA
GSTM3 mRNA
SCIN mRNA
2^-ΔΔct
KOs
Ctrl

3.3.4. Analysis of targets for miRNA-200c regulation

To evaluate whether the targets are directly regulated by miR-200c, the genes were analyzed for binding sites with the TargetScan database. One fifth of the proteins harbor a potential targeting site (8mer or 7mer-m8/A1 seed-region match) in their 3'UTR. For the remaining 21 genes, a possible promotor binding site of miR-200c regulated transcription factors was investigated. This analysis revealed that 62 % of the genes without binding site may be indirectly regulated by miR-200c: The promotor region of these genes contains at least one putative binding site for a transcription factor which is potentially regulated by miR-200c (
Figure 10e and Supplemental Table S 3).

Further, we measured whether the differential protein-levels resulted from changes of the mRNA levels. Therefore, we compared mRNA levels of the single clones to their proteomic data each each (see Supplement S 3). For six targets alterations n protein abundance were reflected at the mRNA level (
Figure 10f).

AGR2, the anterior gradient protein 2 homolog, was found to be statistically significant differentially expressed in the proteomic analysis in Table1. The mRNA expression correlates with the protein expression from the proteomic approach and the grouped analysis, i.e. M1 and M2 and M3 vs MCF7 WT and MCtrl, showed an almost four-fold increase with a highly significant difference between KO and Ctrls respectively ($p \leq 0.0001$). Furthermore, aldehyde dehydrogenase 7 family member A1, ALDH7A1's protein expression changed significantly in a part of the clones, but on mRNA it shows highly significant ($p \leq 0.0001$) increased expression of 43%. Additionally, Filamins FLNA and FLNB were found to be significantly changed on protein level (Table 1). Again, on mRNA level both filamins show a significant ($p=0.0004$ / $p=0.0003$) increase of 44% and 59% in FLNA and FLNB respectively. Glutathione S-transferase Mu3 shows an increase in the mRNA expression compared to the controls ($p=0.138$). SCIN, adseverin protein from the "ON" target list (Table 3), also showed a four-fold increase in the KO compared to the controls ($p=0.0004$). Taken together in these six cases, the mRNA-measurements are indicating a regulation of these targets on mRNA level.

3.3.5. The KO of miRNA-200c results in changes in cellular processes and pathways

For a broader analysis of changes in biological processes and pathways, the original dataset was filtered for proteins that appeared at least three times in at least one group (i.e. three times in KO or Ctrl), this resulted in a new subset of 1243 proteins. Missing values were replaced by the imputation algorithm of Perseus. After a two tailed t-test comparing KO to Ctrl, all proteins with $p \leq 0.05$ were analyzed with the DAVID functional gene annotation tool[90,91] with the GoTerm BP (Biological Processes) database (N=118, Figure 11a).

The majority of functional annotations was categorized to BP1 cellular process (92), metabolic processes (72) and cellular component biogenesis (26). A detailed view on the processes is showing the top most frequent sub-classifications according to the number of attributed genes in GoTerm BP FAT. Prominent processes involve intracellular transport, translation and oxidation reduction as well as macromolecular complex assembly and subunit organization. These findings indicate a broad influence of miR-200c on essential processes.

Moreover, a Gene-Set Enrichment Analysis of the whole dataset after imputation (N=1243) was performed against GO and KEGG databases. The global Enrichment Score (ES) histogram revealed that miR-200c knock-out resulted mainly in the inactivation of pathways, as shown by an accumulation of negative ES (Figure 11b). For depicting exemplary pathways, we chose KEGG pathway annotations. Enriched pathways (Supplemental Table S 1) contain mainly metabolic processes like oxidative phosphorylation citrate cycle and glycolysis, or cytoskeletal organsiation as shown in changes in focal adhesion (Figure 11c). Negative pathway enrichment was observed in adherens junctions and tight junctions, regulation of actin skeleton as well as other metabolic pathways like purine metabolism and decrease in the cell cycle (Figure 11d and Supplemental Table S 1). Heatmap analysis of the GSEA (Supplement S 4 and Supplement S 5) show a high occurrence of table 1 and 2 targets in all these pathways. Taken together, the GSEA findings indicate an increase in metabolic pathways, which also may increase de-toxification in the cells as well as numerous de-regulations in cell-cell contacts and cytoskeletal organization, which may lead to increased metastatic potential.

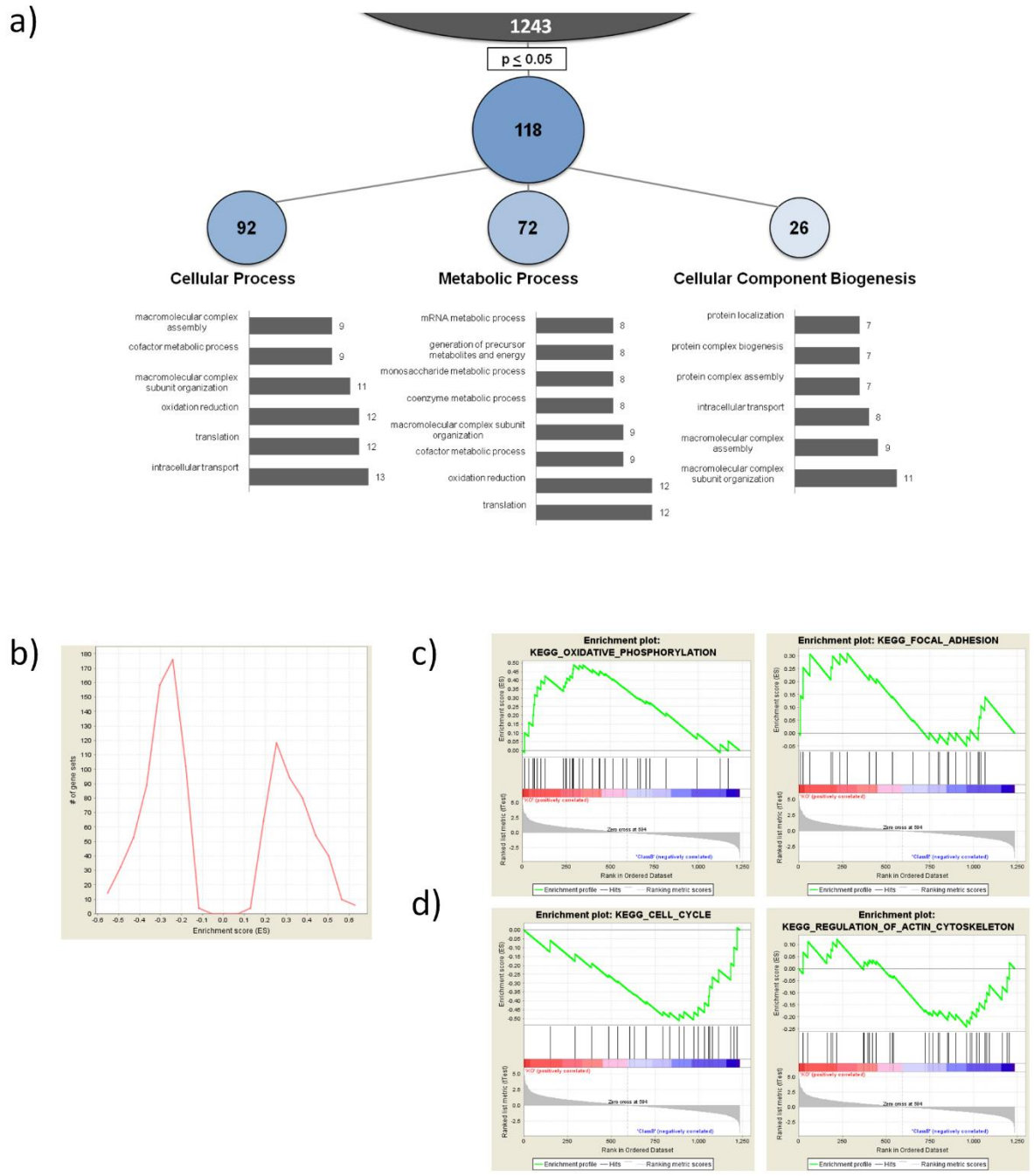

Figure 11 - Bioinformatic analysis of the proteomic dataset

a) Targets for DAVID 6.7 analysis with the GOterm BP database were chosen from whole dataset for every protein with $p \leq 0.05$ after student's t-test KO vs Ctrl b) Distribution of ES Scores in a GSEA of KO vs Ctrl with Gene Ontology (c5.all.v5.2) and KEGG (c2.cp.kegg.v5.2) reference database c) GSEA Enrichment-Plot analysis of the whole dataset shows two exemplary KEGG pathways. Oxidative phosphorylation and focal adhesion showing overexpression while d) cell cycle and regulation of actin cytoskeleton are being down regulated

3.3.6. Biological assays reveal the impact of miRNA-200c KO on EMT, chemoresistance and metabolism

To confirm the biological relevance of the data, different *in vitro* assays were performed utilizing the clonal cell lines (KOs and MCtrl). The metabolic activity was assessed by measuring NAPD(H)-turnover via MTT assay over the course of 72h. All clones showed a significantly higher turnover (***$p \leq 0.001$ for M1 and **$p \leq 0.01$ for M2 and M3), either due to increased metabolic activity or higher proliferation (Figure 12a). The effect of change of resistance to chemotherapeutics was analyzed by treating the cells with doxorubicin (DXR) analyzing relative viability via the Celltiter-Glo assay (Figure 12b). The strongest effect was observed in M2, which was almost 4-times higher than MCtrl. Still, also all other clones show a highly significantly increased viability and therefore higher resistance to chemotherapeutics ($p \leq 0.0001$).

Previously described de-regulations in cell-cell contacts and cytoskeleton were analyzed by investigation of colony-formation abilities as well as of the migratory potential. A significant increased colony area ($p \leq 0.05$) after seven days was observed in the KO cells (Figure 12c and supplemental figure S7). The live imaging experiment with single cell tracking (20h, N=30), as shown in Figure 12d, indicates that the KO cells show a tendency of migrating further and faster than Ctrl, with the differences between M2 and M3 to Ctrl being statistically significant ($p \leq 0.05$) and M1 to Ctrl highly significant ($p \leq 0.0001$) (additional information in Supplement S 6). While these results indicate EMT, well-known mechanisms, like activation of ZEB1/2 or Vimentin were not detected and E-cadherin levels were not changed (Supplement S 8).

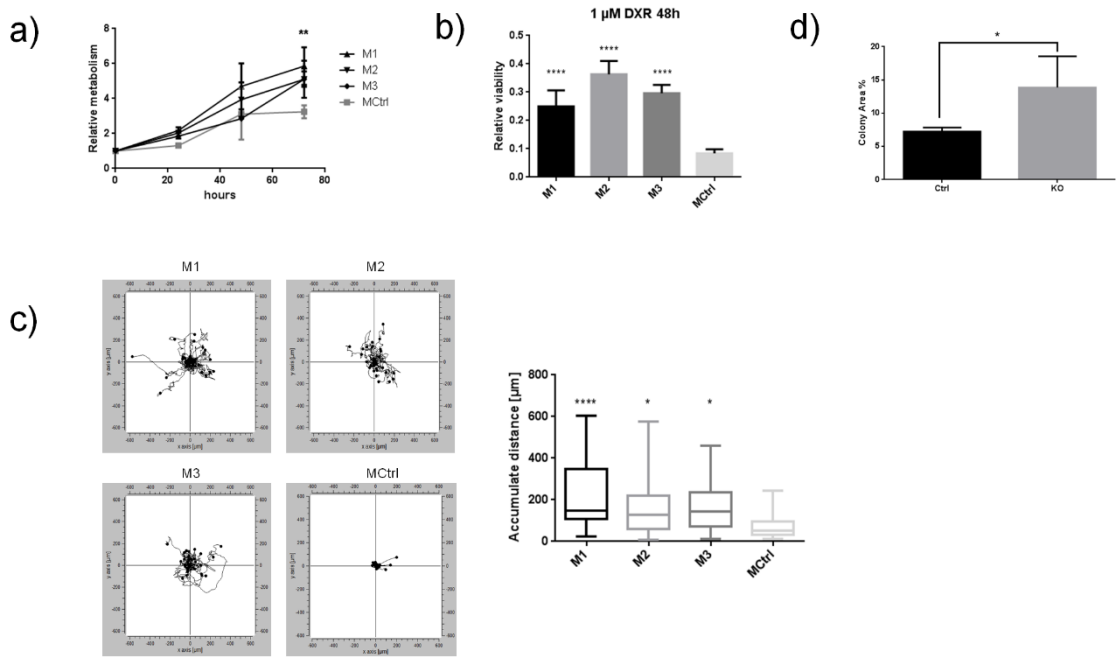

Figure 12 – Biological data to validate predicted phenotype

a) Analysis of relative increase of metabolic activity via MTT-Assay, normalized to each starting point , ***p<0.001 for M1 and **p<0.01 for M2 and M3 compared to MCtrl, N=4, two-way ANOVA with Dunnett's multiple comparison b) Treatment with 1 µM doxorubicine for 48h and analysis of viability as by CTG assay , N=6, ****p<0.0001 compared to Ctrl, two-way ANOVA with Bonferroni's multiple comparison) c) Analysis of colony forming abilities via the clonogenic assay shows a significantly higher colony area in the KOs after seven days of incubation, student's t-test, p<0.05, N=3/9, images in Supplement S 7d) Single cell tracking measurement for evaluation of migratory potential, displayed as accumulative distance after 20 h, N=30, ****p<0.0001, *p<0.05 compared to MCtrl, one-way ANOVA with Dunnett's multiple comparison after outlier test, velocity displayed in S6).

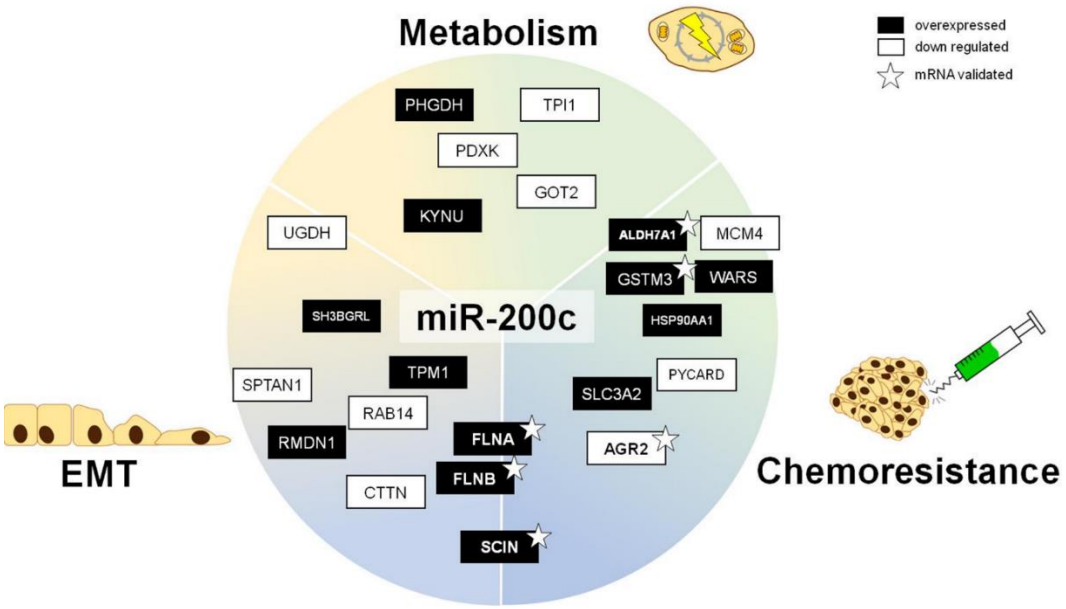

Figure 13 - Summary of important pathways and biological phenotypes, with targets from Tables 1-3 matched to the known functions

Taken together, our results show that miR-200c plays a crucial role in cancer progression, by modulating the protein expression leading to a change of fundamental physiological properties, i.e. increasing metabolism and proliferation, the induction of EMT and enabling cell migration as well as increasing chemoresistance (Figure 13).

3.4. Discussion

Recent publications on the role of miR-200c in cancer progression and metastasis[28,74] point towards a multilayered and complex interplay[92], also involving other numerous pathways like angiogenesis and therapy resistance[72,93]. These facts emphasize the need to utilize more comprehensive tools like genomics and proteomics, as key to generate novel insights. With the genomic knock-out, followed by proteome analysis, we chose two state-of-the-art techniques to investigate new modes of action of miR-200c.

While knock-outs of protein coding genes are quite common, the genetic disruption of non-coding regulatory RNAs is still rarely reported. CRISPR/Cas9 is probably the most frequently utilized genome-editing technology at this time, nevertheless this tool's main disadvantage lies in the tendency to off-target cleavage[29,84]. Also, the need of a PAM-sequence may impede certain knock-out strategies, especially when site-specific mutations are necessary. While different modifications were performed to enhance Cas9's specificity, like the conversion to the Cas9n nickase-mutant or rational design of the nuclease[87,94], TALENs offer high specificity from the beginning, as was also demonstrated by successful use in a first human patient[95]. Therefore, in our experiment we chose to utilize TALENs, allowing us to specifically target the miRNA's drosha processing site[30,88]. The genetic disruption in the drosha site minimizes the risk of inducing a mutation in the seed region, which could lead to the generation of a new, artificial miRNA with unpredictable off-targets. Kim et al. provided the pre-designed TALENs-plasmids, and previously showed that a mutations of the drosha processing site leads to a decrease in miR-expression. Further, the group was able to verify the KO-strategy for miR-200c by demonstrating effects of the miR-200c KO in the Her2-positive SK-BR-3 cell line, like an increase of the miRNA's seed-targets via a motif enrichment analysis and decreased proliferation[88].

In our work, we were able to generate mutations in both alleles of miR-200c in three independent clones, namely M1, M2 and M3, as well as one clone with a heterozygous mutation, i.e. MCtrl. As miR-200c family members share most of their sequence and were reported to have similar functions[72,73], and as the knock-out of a gene can induce compensation effects[96], it was necessary to analyze the expression of the family members after the knock-out of miR-200c. The measurements emphasize the general importance of miR-200c among its family members in this cell line, as the levels are about 20-fold higher than the average miR-200c-family members. No significant

transcriptional compensation of any other family member was observed. In MCtrl the compensation of the loss of one-allele could be based on a higher transcription rate of the polycistronic unit, which would result in higher levels of miR-141. However, the observed increase in miR-141 expression is not significantly higher and does not correlate with the increase needed for the compensation of the loss of one allele of miR-200c needed. These findings together suggest a different compensatory mechanism in MCtrl, like inhibited degradation or changes in the miRNA processing of miRNA-200c. Still, it is not clear whether the basal expression levels of miR-200b and miR-429, which share the same seed region as miR-200c, could suffice for the regulation of certain targets and pathways.

Only few miRNA-knock-outs, especially with TALENs, were described before[97 98], but the subsequent target analysis has been mainly based on genomic approaches. The protein expression profile analysis therefore may reveal important novel information about the regulation network of miRNA-200c. In the proteomic approach, three knock-out clones were analyzed and compared to both: the wild-type cells as well as MCtrl with a heterozygous mutation. The later was chosen, as the expression level of miR-200c was not significantly changed, and the clone went through the same procedures as the miR-200c KOs. Therefore, it served as an appropriate control, to rule out expression changes based solely on selection and introduction of TALENs proteins.

The PCA underlines the similarity of MCtrl to the wild type, prompting us to regard both as control groups. Moreover, a clustering analysis shows a close correlation between the replicas, as well as a tendency towards grouping the KO clones close together. This indicates that the knock-out of miR-200c does not lead to dramatic changes in the proteome, but to a surgical change in key elements and pathways, which are important for tumorigenesis.

For a comprehensive overview of changed expression patterns, we utilized two independent bioinformatic methods. While the DAVID analysis is based on p-value pre-filtered set of proteins, analyzing gene ontology annotations on a broad level, the GSEA-Tool generates results due to a list-walk enrichment scoring analysis. Both analyses showed similar results, while used for a different purpose. One aim was to investigate pathways that are attributed to miR-200c expression and are involved in previously described physiological processes in cancer, like change in metabolic processes, EMT[99,100] and resistance to chemotherapeutics[27]. The DAVID Analysis

enabled a global understanding of process-changes attributed to a small set of differentially regulated proteins, revealing changes in metabolism and cellular organization in general. With the GSEA, we were able to analyze certain crucial pathways in cancer in detail, revealing changes in cancer progression and metastasis. This is shown by enrichments in pathways increasing metabolic activity, loss of cell cycle regulation and actin cytoskeleton as well as cell-cell contacts. These findings, based on changes of protein expression were successfully correlated to phenotypes of the cells after the KO. After eradication of miR-200c expression, the cells showed increased migration, which could be attributed to changes in focal adhesion and cellular interaction. Also, increased NADP(H) turnover, as measurement of proliferation and metabolic activity is observed in the KO clones, which may also contribute to the increased resistance to doxorubicine treatment. The latter can also be caused by an increase of detoxification and the evasion of apoptosis.

While we do see changes in pathways and targets involved in cell motility and morphology as well as a changed phenotype towards more migratory cells, common EMT markers like vimentin were not found and E-cadherin expression was unchanged. Epithelial MCF7 cells express low levels of ZEB1/2, as was confirmed previously[101]. Our data suggests that the miR-200c KO as such does not lead to an activation of ZEB1/2 and eventually to a decrease of E-cadherin. This may be due to the poised chromatin structures[102] and not due to a persistent down-regulation via miR-200c. Our data suggests that miR-200c has additional effects on the cytoskeletal organization besides the ZEB1/2 axis, as was also proposed before [103].

In more detail, the analysis of 675 proteins showed significant differential expression in 21 proteins in total, nine of those to a high extend in all three biological replicas. None of the obtained targets shown in Tables 1-3 was published to be regulated by miR-200c before. Comparing a list of confirmed miR-200c targets[72] to our whole proteomics dataset, we found only 1 of 37 to be present, i.e. PRDX2. This protein displayed no significant differential expression in our analysis. The lack of prominent miR-200c targets in our tables may be based on different cell line models, as well as different analytical and experimental approaches used in the studies. Our proteomic approach as method does not allow gathering information of the whole proteome. Still, in this case the analysis of protein expression compared to a transcriptomic method may be beneficial, due to mainly translational changes which are expected after a miRNA KO. Nevertheless, on the basis of our data, it cannot be excluded that certain

family members may facilitate the regulation of certain proteins, without changing their own expression. Even low expression of miRNAs may be enough to regulate translation, especially for low abundant proteins which often cannot be detected appropriately in proteomics approaches.

The regulatory mechanisms of miR200c seems to be different in our model cell line MCF7. MCF7 cells show high expression of miR-200c and as miRNA-inhibition is not very common this cell line model is not frequently used in miR-200c research. Consequently, most published miR-200c targets were unraveled in other cellular systems. Additionally, the KO of an inhibitor leads to different results than the addition/overexpression of it, which was performed in the majority of the published studies. In a KO only physiologically direct targets and corresponding downstream effects become obvious while other inhibitory mechanisms (e.g. DNA methylation) are not affected in our settings and thus these potential miR-targets display no altered expression.

Moreover, we were analyzing a KO which is a longterm effect and might display different changes than those observed in transient overexpression or inhibition models. Transient experiments additionally may lack compensatory mechanisms.

While transient inhibition of miR-200c has revealed several functions in breast cancer, the long-term disruption of the gene may be more similar to the setting in a tumor. Of note, it was shown that miR-200c expression can be lost due to locus methylation, leading to more aggressive breast cancer phenotypes[104]. With our approach we were able to discover novel targets which are truly governed by miR-200c in MCF7 cells and might play crucial roles in normal cellular settings.

Based on the information from the GO-Database, these targets were allocated to their main biological function: Most of the proteins play a role in cellular processes involving the cytoskeleton, metabolism and detoxification. This supports previous studies of miR-200c's function in EMT, proliferation and chemoresistance[27,28,99,100], while additionally revealing yet unknown miR-200c downstream proteins.

Our findings were affirmed by validation of changes on mRNA level by RT-qPCR on a set of six novel miR-200c targets (namely FLNA, FLNB, AGR2, SCIN, GSTM3 and ALHD7A1), originating from different data-mining methods and pathways.

Filamins A and B (FLNA, FLNB. Further, filamins can cause cell migration and invasion, by mediation of HGF/c-MET signaling as shown in hepatocytes[105], as well as via the interplay with Cyclin D in highly metastatic human MDA-MB-231 cells[106], which

lack the expression of miR-200c[27]. Notably, also in a set of miR-200c low triple negative breast cancers (including MDA-MB-231) it was reported that filamin A[107] knock-down leads to increased chemosensitivity to docetaxel.

Different proteins may contribute to enrichments in metabolic and cellular processes, like the Anterior Gradient Protein 2 Homolog (AGR2). AGR2 has been shown to play a critical role in numerous cancers and other diseases[108], but especially in breast cancer, a high AGR2 expression shows negative effects on survival of tamoxifen treated patients[109]. After overexpression *in vitro,* increased proliferation and drug resistance to cisplatin was shown in A375 cell line[110] and even a apoptotic bystander effect of cancer cells on normal cells was shown[111]. These findings suggest an influence of AGR2 on drug resistance and breast cancer progression and as the miR-200c knock-out significantly increases its expression, miR-200c may be an important regulatory system for AGR2 expression. GSTM3, glutathione S-transferase Mu3 is a member of the glutathione transferase superfamily, which are known to play an important role in different processes of detoxification, likely also of chemotherapeutic drugs[112]. Recent publications show that inhibiting glutathione transferases may overcome resistance to platin-based DNA damaging drugs[113].

Furthermore, Adseverin, the Calcium-Dependent Actin Severing and Capping Protein (SCIN), has been shown to have effects on different cancers. While no observations in breast cancer were reported, previous data show that a silencing of SCIN leads to a decrease in proliferation of A549 and H1299 lung carcinoma cells[114]. SCIN was also described as a driver in metastasis and outcome marker in patients with gastric cancer[115], as well as its role in mediation of cisplatin resistance in bladder cancer cells[116]. All these findings correlate with effects observed in loss-of-miR-200c scenarios, which according to our data leads to an increase in SCIN.

Aldehyde dehydrogenases are a family of proteins oxidating aldehydes to carboxylic acids in NADP(H) dependent manner. Due to xenobiotics, reactive oxygen species (ROS) accumulate, finally leading to oxidative stress. Brocker et al. suggest ALDH7A1 may play an important role in the defense of the cell against oxidative stress and its cytotoxicity[117]. As the cytotoxic effect of doxorubicin and similar drugs is in parts accounted to reactive oxygen species (ROS) and oxidative stress[118,119], the loss of miR-200c may cause the increase of ALHD7A1, leading to an increase in resistance to these therapeutics.

In this study, we combined a miRNA knock-out with a proteome analysis to investigate long-term effects, analogues to the loss of miR-200c during tumor progression in patients. Thereby, we were able to confirm known mechanisms of miR-200c, as shown by enrichment and pathway analysis. Moreover, we unraveled a set of novel target candidates involved in those mechanisms and were able to confirm the predicted effects by biological assays. Our data further emphasizes the role of miR-200c in tumorigenesis and underscores its potential as biomarker as well as putative therapeutic agent for miRNA-based therapies.

3.5. Materials and methods

Reagents

Puromycin dihydrochloride and Doxorubicine hydrochloride were obtained from Sigma-Aldrich (cat. P8833, D1515).

Cell culture

MCF7 cells stably expressing eGFP were generated in our lab. The parental cells were acquired from cell line service (Eppelheim, Germany), grown at 37 °C and 5 % CO_2 in high glucose DMEM (Sigma) supplemented with 10 % fetal calf serum (FCS / Gibco), as well as the miR-200c KO clones M1, M2, M3 and MCtrl. All cells were routinely tested and confirmed as mycoplasm free.

miR-200c knock-out

Analysis for putative CRISPR-Targets was performed via the CRISPR-Design Tool from Feng Zhang's lab (http://crispr.mit.edu, last target review: 18th of January, 2017) [120].The TALENs pair was acquired from the TALENs Library of the Seoul National University (http://cge.ibs.re.kr/html/cge_en/)[88], the binding sequences for left and right TALENs are: CTAATACTGCCGGGTAATGA, TCCCTGTGTCAGCAACATCCA – respectively, the target sequence is TGGAGGCCCCTG. In order to develop a stable miR-200c KO in MCF7 cells, 600,000 cells per well were seeded in a 6 well plate and transfected on the following day with 3µg DNA (equimolar ratio of two TALENs and a reporter plasmid containing a puromycin resistance cassette and red fluorescence protein (RFP)) using K2 Transfection System (Biontex) according to the manufacturers

protocol. Two days post transfection, the cells were selected with 1 µg/ml of puromycin for two weeks, followed by single cell dilution to obtain monoclonal cultures.
DNA was extracted using Phenol-Chloroform (both Sigma), and analyzed by the T7-Surveyor assay (NEB). In mutation-positive clones, a sequencing of the miR-200c gene locus was performed. Three homozygous miR-200c KO clones were acquired, called M1, M2 and M3. The reporter-plasmid (SBI cat. MIR-KO-200cHR-1), comprises a puromycin and RFP reporter.

Sequencing

DNA was extracted from MCF7 miR-200c KO cells using the standard protocol (phenol-chloroform). Approximately 500ng of DNA were used to amplify the miR-200c gene using the following primers:
Forward *CTCGAGGCTCACCAGGAAGTGTCCCC*
Reverse *ACGCGTCCTTGTGCAACGCTCTCAGC*.
The PCR product was purified by a PCR purification Kit (Qiagen Cat. 28104) and finally 50 – 100 ng of purified PCR product was sequenced (GATC Biotech AG).

miRNA quantitative RT-PCR
Approximately 600,000 cells of each clone were harvested and total RNA isolated from cells using miRCURY RNA Isolation Kit (Exiqon). cDNA synthesis was carried out by a microRNA specific reverse transcription and detection with the qScript microRNA cDNA Synthesis Kit and PerfeCta SYBR Green SuperMix (Quanta Biosciences) with RT-PCR detection on a LightCycler 480 (Roche). The expression of miR-200 family members (miR-141, miR-200a, miR-200b, miR-200c) was normalized to miR-191[121], using the $2^{-\Delta CT}$ or $2^{-\Delta\Delta CT}$ method. The following list contains the primers used for analysis of miRNAs:
miR200c: *GCGTAATACTGCCGGGTAAT*;
miR-191: GCGCAACGGAATCCCAAAAG;
miR-141:*GCGTAACACTGTCTGGTAAAGA;*
miR-200a: GAGTAACACTGTCTGGTAACGA;
miR-200b:GCGTAATACTGCCTGGTAATGA;
miR-429: GAGTAATACTGTCTGGTAAAACC

Sample preparation for proteomic analysis

Protein was extracted from approximately $6x10^6$ cells using lysis buffer containing 8 M urea and 400 mM NH_4HCO_3. Briefly, cells were washed three times with cold PBS, treated with lysis buffer and harvested using cell scrapper. Lysates were concentrated with QIA-shredder mini spin column (Qiagen, Germany) following manufacturer's instruction. Protein quantifications were performed using BCA Protein Assay Kit (Thermo Fisher Scientific). 20 µg of protein were prepared for disulfide bond reduction by adding 45 mM of dithioerythritol (DTE), and incubated for 30 min at room temperature. Alkylation of cysteines was performed by adding 0.1M iodocetamide, followed by 30 min incubation at room temperature in the dark. Water was added to a concentration of 1M urea. 400 ng sequencing grade modified porcine trypsin (Promega, Madison, WI, USA) was added for overnight incubation at 37 ^oC. Afterwards, samples were purified using C18 spin columns (Pierce, Thermo Scientific, IL, USA) complying manufacturer's instruction. Resulting supernatants were combined and freeze-drying was performed. Peptide samples were stored at -20 °C prior to LC-MS/MS.

Proteomic LC-MS/MS analysis

Samples were diluted in 0.1 % formic acid. Nano-LC separation was done with a nano-liquid chromatography system (EASY-nLC 1000, Thermo Scientific, USA)). 2.5 µg of peptide samples were loaded onto a trap column (PepMap100 C18, 75 µm x 2 cm, 3 µm particles, Thermo Scientific) and separated at a flow rate of 200 nl/min by an analytical reversed phase column (PepMap RSLC C18, 75 µm x 50 cm, 2 µm particles, Thermo Scientific) using a 260 min gradient from 5 % B to 25 % B (solvent A: 0.1 % formic acid; solvent B: CH3CN/0.1 % formic acid) followed by a 60 min gradient from 25 % to 50 % B. Tandem mass spectrometry was performed with an Orbitrap XL mass spectrometer (Thermo Scientific, USA). MS and MS/MS spectra were acquired using cycles of one MS scan (mass range m/z 300-2000) and five subsequent data dependent CID MS/MS scans (dynamic exclusion activated; collision energy: 35%).

Analysis of proteomic data and bioinformatics processing

All data were processed with MaxQuant and analyzed in Perseus (version 1.5.3.2)[122-124] at an FDR of 1 % for the peptide and protein level. In Perseus, following operations were performed: Transformation (log2) and removal of possible contaminants and false positive identifications from the reversed database. For relative quantification, only those proteins were considered that showed valid LFQ-values in all three replicas in all samples. No imputation was performed.

In addition, proteins were considered “ON” when at least 5 valid values were found in M1, M2 and M3, and no value in the control. Proteins were considered “OFF” when at least 3 valid values were found in MCtrl and MCF7 and not at all in the KO group.

For pathway analysis, the whole data set was re-analyzed: After transformation and removal of contaminants and false positives, data was filtered for proteins found at least 3 times in one of the groups KO or Ctrl. The whole dataset was analyzed by the Gene Set Enrichment tool (GSEA, version 3.0 beta2)[91], following the originators’ instructions. For analysis with DAVID Bioinformatics 6.7[90], proteins were chosen which showed $p \leq 0.05$ in a two-tailed student’s t-test, comparing Ctrl to KO group.

Analysis of miR-200c binding in genes of target proteins

For the analysis of a potential miR-200c binding in the found genes, the Targetscan 7.1 database[125] was used.

Analysis of transcription factors in promoter regions of found genes

For the analysis of the promoter region, each gene’s sequence was retrieved from the RefSeq-Database (https://www.ncbi.nlm.nih.gov/refseq/ as of April 2017) in order to identify the +1 position. Assuming the +1 position as starting site of transcription, 500 nucleotides upstream were defined as the proximal promoter. Then, for analysis of proximal promoters, PhysBinder[61] software was used, the analysis was performed with the highest stringency. The resulting transcription factors were evaluated for miR-200c and family binding with Targetscan 7.1 [125].

qPCR validation of mRNA expression

RNA was extracted utilizing the Total RNA Kit, peqGOLD (VWR) as by manufacturer's instructions. Translation to cDNA was performed utilizing the qScript cDNA synthesis kit (Quanta Bioscience) as by manufacturer's protocol.

Analysis of expression was performed with the Lightcycler 480 (Roche) and the Universal Probe Library (Roche) with following probe and primer (forward/reverse) combinations:

AGR2, Probe 47, GGTGGGTGAGGAAATCCAG / GTAGGAGAGGGCCACAAGG

ALDH7A1, Probe 7, CACTCAGGTGGGAAAACAGG / AATGGCATTGTTTCCTCCAA

FLNA, Probe 32, TCGCTCTCAGGAACAGCA / TTAATTAAAGTCGCAGGCACCTA

FLNB, Probe 21, CGGACTTCGTGGTAGAATCC / TGAGAGGGGCCTTCAATG

GSTM3, Probe 85, CCAATGGCTGGATGTGAAAT / TCCAGGAGGTAGGGCAGAT

SCIN, Probe 19, TTTCAAAGGCGGTCTGAAAT / CAGGTCGTTCGTAAGAACATGA

Measurements of metabolic activity

All clones were seeded triplicates in a concentration of 5000 cells / well in four identical 96-well plates. The cells were treated with 10µl of 5 mg/ml MTT (Sigma Aldrich) at the timepoints 0h (about 2h after seeding) and 24h, 48h and 72h later respectively. The plates were incubated for 2h at 37°C and stored at -80°C over night. Afterwards100µl DMSO (Sigma Aldrich) were added and incubated for 37°C for 30mins, while shaking. Measurements were performed with the Spark 10M (TECAN).

Live cell imaging and 2D migration

Live Cell Imaging was performed using a Nikon Eclipse Ti Inverted Microscope (Nikon, Düsseldorf, Germany). Cells were kept under constant 37°C, 5% CO2 and 80% humidity by the heating and incubation system from Ibidi (Martinsried, Germany). Imaging was performed with the 10x phase contrast objective. For the 2D migration experiments 8-well slides (Ibidi, Martinsried, Germany) were coated with 50 µg/ml fibronectin for 1 h, afterwards cells were seeded in a density of $25x10^3$/well, and were allowed to attach to the coated surface for 2 h. Cell Displacement was imaged every 10 min over 20 h in all settings. For analysis of movement, single cells were tracked manually using ImageJ Manual Tracking Plugin. Acquired trajectories in 2D were

further analyzed for mean velocity using Ibidi Chemotaxis and migration tool, afterwards an outlier-analysis was performed by the Identify outliers tool of Prism GaphPad.

Clonogenic assay

1000 cells were seeded in a 6-well plate (TPP, Switzerland), and grown for 7 days, fixed and stained with paraformaldehyde (PFA) containing crystal violet (Sigma). Survival colony were analysed by ImageJ ColonyArea

Doxorubicine resistance

All clones were seeded in a concentration of 5000 cells per well in 96 well plates. 24h after seeding, cells were treated with 1 µM Doxorubicine for 48h (Sigma Aldrich, stock 10mM in DMSO). Analysis of viability was performed via Celltiter-Glo assay (Promega) and normalized to DMSO control.

Statistical analysis

Results are expressed as the mean ± SD of at least three biological replicas, if not stated otherwise. Software GraphPad Prism v6 and SigmaPlot 11 were utilized for the analysis of the data. For analysis of miR-200c expression (only one variable and more than two groups), the One Way Analysis of Variance test was used, followed by the two tailed Bonferroni´s multiple comparison test, with DF = 4. For analysis of all family members (two variables and more than two groups per variable), the Two Way Analysis of Variance test was used, followed by two tailed Bonferroni´s multiple comparison test with DF = 16. For analysis of family expression between early and late passage (three variables and more than two groups per variable) we used the Three Way Analysis of Variance test, followed by two tailed Bonferroni´s multiple comparison test, with DF = 12

Data availability

The data that support the findings of this study are available from the corresponding author upon reasonable request.

3.6. Supplemental information

S1

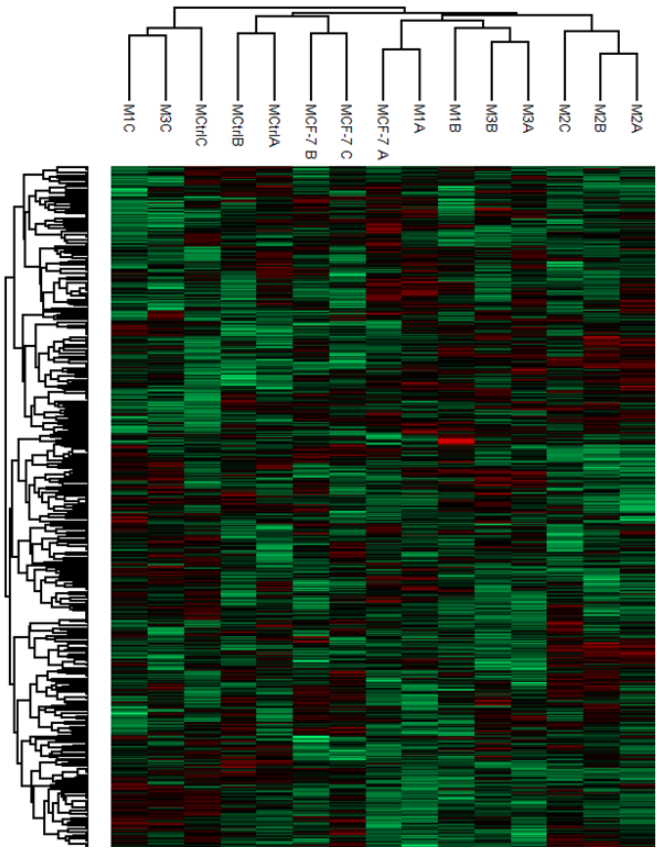

S2

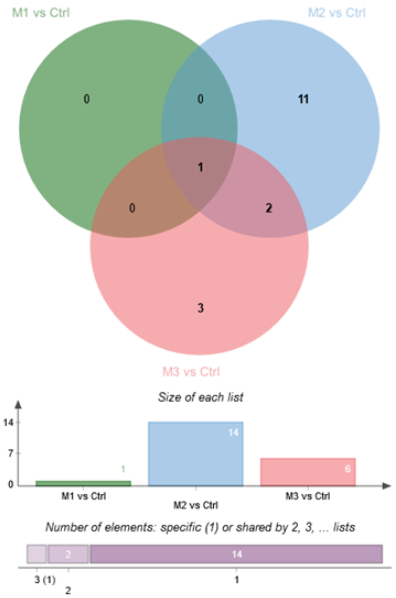

Supplement S 1

Clustering analysis of the measurements after vertical and horizontal z-score normalization

Supplement S 2

Venn-diagramm with results of the vulcano blot analysis of M1 or M2 or M3 vs (MCF7 and MCtrl) each N=675 with 250 randomizations, FDR 0.05 and S0 of 0.1 as shown in Table 2

S3

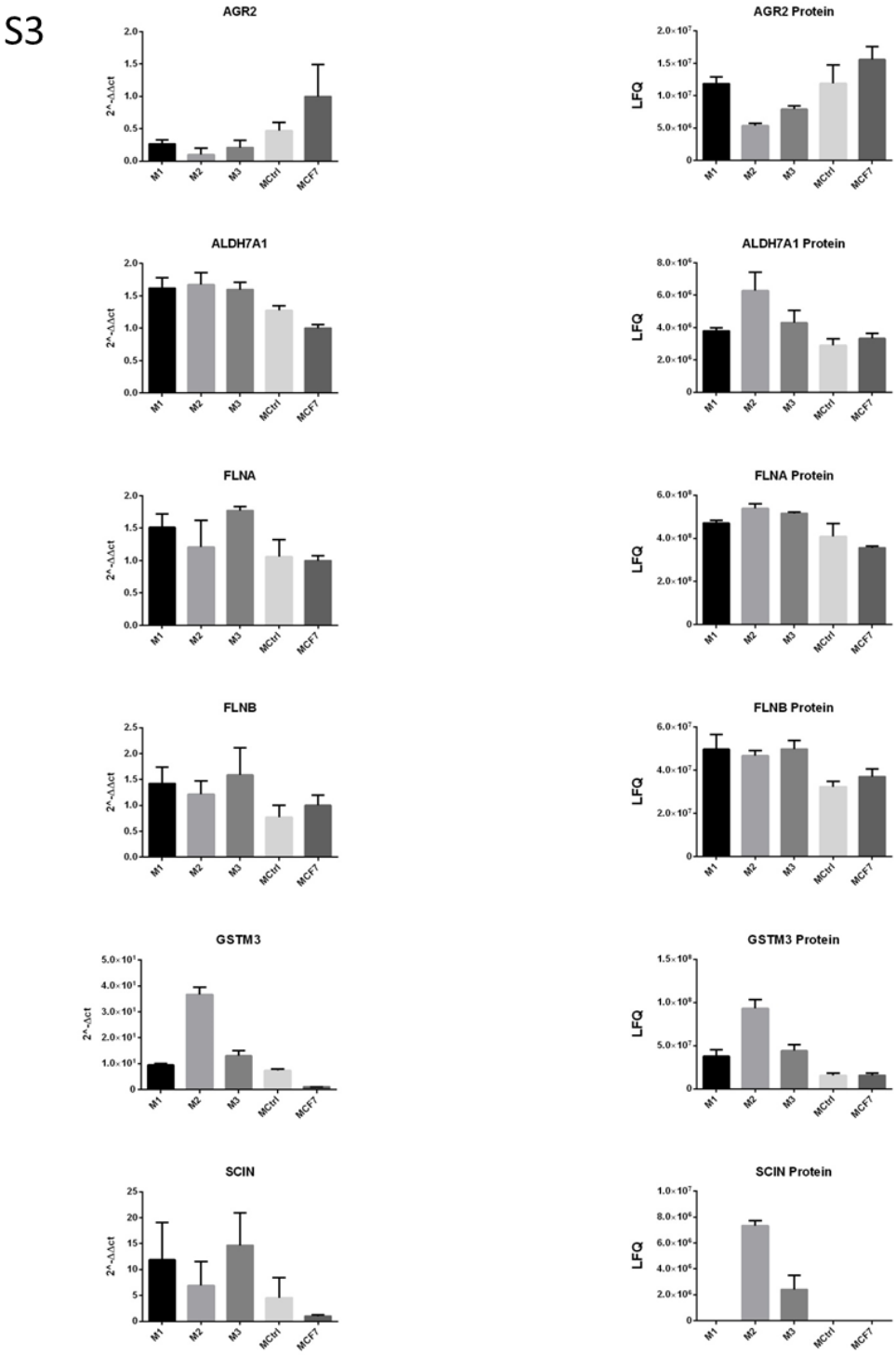

Supplement S 3

Detailed results of
Figure 10F, with mRNA measurements compared to the protein expression data for each clone

S4

KEGG OXIDATIVE PHOSPHORYLATION

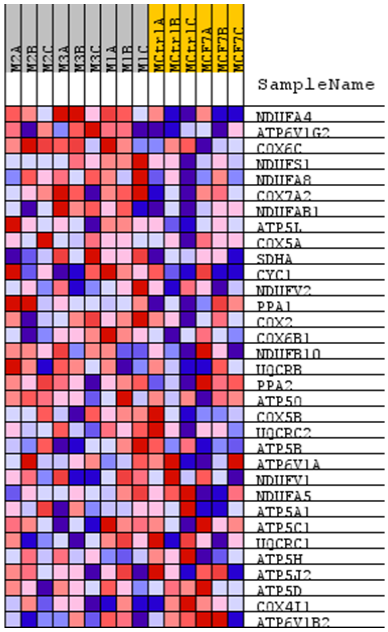

KEGG FOCAL ADHESION

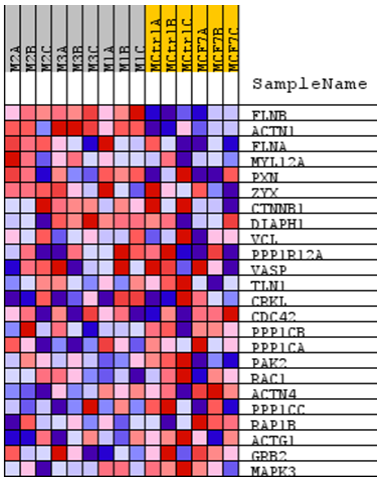

Supplement S 4

Heatmaps corresponding to the Enrichment blots in Figure 11c

S5

KEGG CELL CYCLE

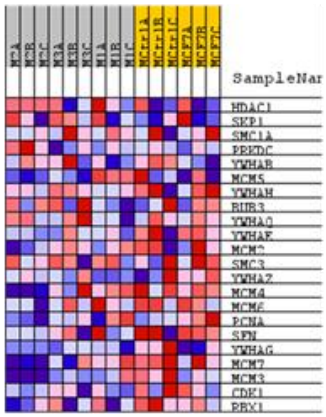

KEGG REGULATION OF ACTIN CYTOSKELETON

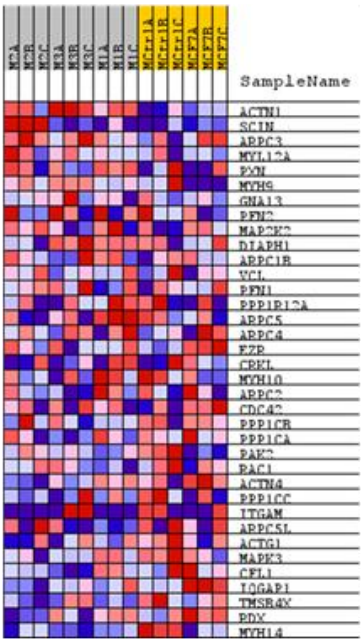

Supplement S 5

Heatmaps corresponding to the Enrichment blots in Figure 11d

S6

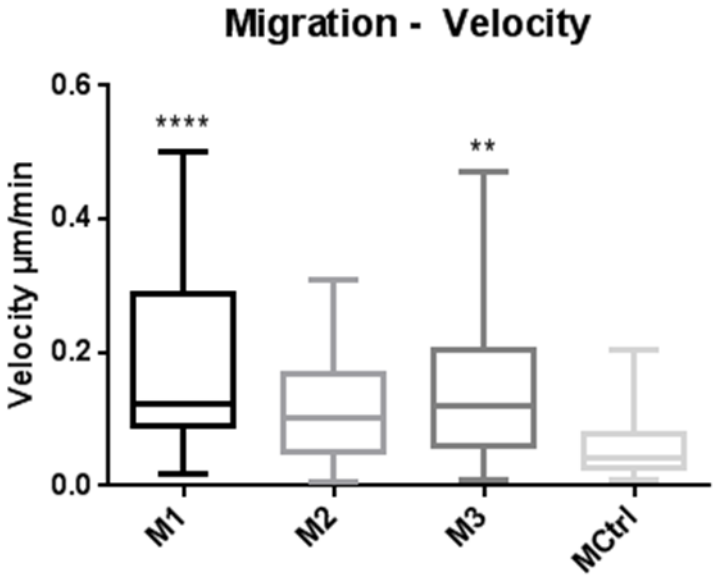

Supplement S 6

Evaluation of migration data in Figure 12b (N=30, *p≤0.05, one-way ANOVA with post-hoc Bonferroni's multiple comparison)

S7

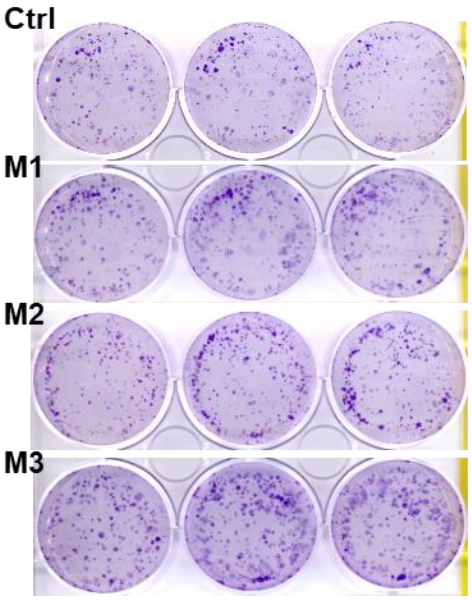

S8

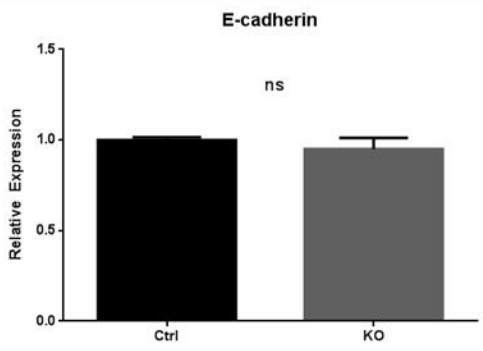

Supplement S 7

Clonogenic assay – imaging of colonies, as evaluated in the pooled analysis in Figure 12d

Supplement S 8

qPCR measurements of E-Cadherin mRNA levels in Ctrl vs KOs shows no significant difference

Supplemental Table S 1 15 / 32 gene sets are enriched in phenotype KO

NAME	SIZE	ES	NES	NOM p-val	FDR q-val	FWER p-val	RANK AT MAX	LEADING EDGE
KEGG_PARKINSONS_DISEASE	34	0.46907002	15.940.783	0.009861933	0.24380365	0.214	345	tags=50%, list=28%, signal=67%
KEGG_OXIDATIVE_PHOSPHORYLATION	33	0.48710477	15.471.032	0.018480493	0.17806831	0.293	345	tags=52%, list=28%, signal=70%
KEGG_ALZHEIMERS_DISEASE	35	0.420356	14.566.842	0.046	0.24040706	0.479	292	tags=40%, list=24%, signal=51%
KEGG_CITRATE_CYCLE_TCA_CYCLE	20	0.4615872	13.821.458	0.12048193	0.29699662	0.648	132	tags=30%, list=11%, signal=33%
KEGG_HUNTINGTONS_DISEASE	43	0.36943752	13.720.317	0.03508772	0.2523027	0.664	292	tags=42%, list=24%, signal=53%
KEGG_GLUTATHIONE_METABOLISM	15	0.44105875	13.544.401	0.08317215	0.23395455	0.703	78	tags=27%, list=6%, signal=28%
KEGG_MAPK_SIGNALING_PATHWAY	16	0.4151188	13.413.316	0.10453649	0.22068681	0.734	136	tags=25%, list=11%, signal=28%
KEGG_AMINOACYL_TRNA_BIOSYNTHESIS	20	0.44356683	13.299.485	0.15369262	0.20533033	0.744	263	tags=40%, list=21%, signal=50%
KEGG_CARDIAC_MUSCLE_CONTRACTION	17	0.46564567	12.798.785	0.18257262	0.23733874	0.82	292	tags=53%, list=24%, signal=68%
KEGG_ANTIGEN_PROCESSING_AND_PRESENTATION	15	0.42715377	12.191.079	0.24395162	0.285524	0.892	308	tags=47%, list=25%, signal=61%
KEGG_PYRUVATE_METABOLISM	15	0.49441242	11.757.169	0.28846154	0.31522772	0.919	122	tags=33%, list=10%, signal=37%
KEGG_GLYCOLYSIS_GLUCONEOGENESIS	23	0.39739954	11.214.875	0.33840305	0.35995352	0.95	200	tags=30%, list=16%, signal=36%
KEGG_FOCAL_ADHESION	24	0.30988422	10.625.255	0.36055776	0.41783723	0.972	277	tags=29%, list=22%, signal=37%
KEGG_LYSOSOME	17	0.24309203	0.69935	0.9089184	0.94843	1.0	162	tags=18%, list=13%, signal=20%
KEGG_LEUKOCYTE_TRANSENDOTHELIAL_MIGRATION	17	0.19984435	0.660395	0.934236	0.92140806	1.0	195	tags=18%, list=16%, signal=21%

Supplemental Table S 2 17 / 32 gene sets are upregulated in phenotype

NAME	SIZE	ES	NES	NOM p-val	FDR q-val	FWER p-val	RANK AT MAX	LEADING EDGE
KEGG_CELL_CYCLE	22	-0.51119137	-16.219.078	0.035643563	0.19916053	0.172	348	tags=55%, list=28%, signal=75%
KEGG_RIBOSOME	68	-0.31785846	-14.187.368	0.016746411	0.49701187	0.529	392	tags=41%, list=32%, signal=57%
KEGG_ENDOCYTOSIS	20	-0.40655762	-13.007.351	0.12331407	0.70801485	0.78	193	tags=30%, list=16%, signal=35%
KEGG_PURINE_METABOLISM	23	-0.36597934	-11.775.029	0.24390244	0.9449636	0.925	14	tags=13%, list=1%, signal=13%
KEGG_PROTEASOME	34	-0.30099234	-11.316.409	0.29045644	0.9364207	0.95	457	tags=53%, list=37%, signal=82%
KEGG_ADHERENS_JUNCTION	15	-0.35883263	-11.289.837	0.28879312	0.78668696	0.95	338	tags=53%, list=27%, signal=73%
KEGG_TIGHT_JUNCTION	20	-0.3472254	-10.904.311	0.3391473	0.7903667	0.964	294	tags=40%, list=24%, signal=52%
KEGG_OOCYTE_MEIOSIS	19	-0.3068673	-0.99786586	0.49278352	0.9669546	0.988	440	tags=58%, list=36%, signal=89%
KEGG_UBIQUITIN_MEDIATED_PROTEOLYSIS	16	-0.319742	-0.979242	0.4989059	0.909404	0.991	251	tags=31%, list=20%, signal=39%
KEGG_INSULIN_SIGNALING_PATHWAY	17	-0.29883376	-0.95862424	0.51827955	0.8756116	0.994	256	tags=35%, list=21%, signal=44%
KEGG_REGULATION_OF_ACTIN_CYTOSKELETON	36	-0.24238425	-0.9287425	0.6079295	0.8686062	0.998	275	tags=31%, list=22%, signal=38%
KEGG_PATHOGENIC_ESCHERICHIA_COLI_INFECTION	22	-0.28710213	-0.9233835	0.595092	0.8081302	0.998	514	tags=55%, list=42%, signal=92%
KEGG_NEUROTROPHIN_SIGNALING_PATHWAY	17	-0.29578927	-0.90542006	0.5875831	0.7824528	0.999	440	tags=59%, list=36%, signal=90%
KEGG_SPLICEOSOME	58	-0.22438549	-0.8703807	0.6956522	0.7967216	0.999	364	tags=38%, list=29%, signal=51%
KEGG_PATHWAYS_IN_CANCER	27	-0.22919808	-0.7894147	0.8729839	0.8798361	0.999	338	tags=41%, list=27%, signal=55%
KEGG_FC_GAMMA_R_MEDIATED_PHAGOCYTOSIS	16	-0.24920684	-0.7617598	0.872	0.8646141	1.0	218	tags=25%, list=18%, signal=30%
KEGG_SYSTEMIC_LUPUS_ERYTHEMATOSUS	16	-0.28722718	-0.7255098	0.8017058	0.8583328	1.0	362	tags=44%, list=29%, signal=61%

Supplemental Table S 3 Overview of predicted transcription-factor binding sites

Gene	Quality* of predicted miR-200c binding-site
ALDH7A1	7mer-m8
CA2	7mer-A1
GSTM3	7mer-m8
KYNU	8mer / 7mer-m8 / 7mer-A1
SCIN	8mer / 7mer-A1

* as described on https://www.targetscan.org

	TF with predicted miR-200c binding site														
TF → / Gene ↓	KLF4	ZFX	EGR1	NRF1	ELK4	ETS1	GABPA	ZEB1	FOSL2	JUN	SP1	STAT1	TFAP2A	GATA2	MYC
ASMTL	x	x		x											
CTTN	x	x	x		x	x	x		x		x		x		x
FLNA	x	x	x						x	x	x				
FLNB	x	x	x	x									x		
GOT2	x	x													
HSP90AA1	x			x											
PDXK	x	x	x	x		x		x							
PPP1CC	x	x	x		x	x								x	
PYCARD	x	x										x			
RAB14	x			x											
RMDN1	x	x	x												x
SLC3A2	x			x											
SPTAN1	x		x		x		x								
TPM1	x		x												
UGDH	x	x	x		x		x	x							
TPI1	x														
AGR2															
SH3BGRL															
PHGDH	NA														
MCM4	NA														
WARS	NA														

TF → / Gene ↓	Tfcp2l1	Esrrb	RELA	Sp2	XBP1	CTCFL	Sp4	ELF1	TFAP2C	RUNX3	MEF2C	CTCF	GTF3C2	RAD21	BRCA1
ASMTL	x	x		x	x	x									x
CTTN	x	x	x			x	x	x	x	x			x	x	x
FLNA	x	x	x	x	x	x	x		x	x		x	x		
FLNB	x	x	x	x	x	x	x	x	x		x	x			x
GOT2	x	x	x											x	
HSP90AA1	x	x		x	x			x	x						
PDXK	x	x		x	x		x		x	x			x	x	
PPP1CC	x	x	x	x	x	x	x	x							
PYCARD	x	x	x		x	x			x					x	
RAB14	x	x	x								x				
RMDN1	x	x	x	x	x	x	x	x		x		x			
SLC3A2	x	x	x	x			x								
SPTAN1	x	x		x	x	x	x	x							
TPM1	x	x	x			x				x	x				
UGDH	x	x	x	x	x	x	x	x							
TPI1															
AGR2	x	x	x							x	x				
SH3BGRL	x		x												
PHGDH	NA														
MCM4	NA														
WARS	NA														

TF → / Gene ↓	GATA1	MAFF	USF2	YY1	E2F1	ELK1	ESRRA	FOS	IRF3	JUNB	Mycn	REST	TAF1	TAF7	BHLBE40
ASMTL															
CTTN	x					x		x		x					x
FLNA							x	x	x	x					
FLNB															
GOT2	x														
HSP90AA1				x								x	x	x	
PDXK															
PPP1CC															
PYCARD															
RAB14		x													
RMDN1		x	x								x				x
SLC3A2	x			x											
SPTAN1															
TPM1															
UGDH			x			x									
TPI1															
AGR2															
SH3BGRL															
PHGDH	NA														
MCM4	NA														
WARS	NA														

TF: Transcription Factor, NA: Algorithm was not providing any binding site or the intergenic region was too short for valid prediction

4. Inducible miRNA-200c decreases motility of breast cancer cells and reduces filamin A

The following sections are directly adapted from the original manuscript.

Inducible microRNA-200c decreases motility of breast cancer cells and reduces filamin A

Bojan Ljepoja[1], Christoph Schreiber[2], Florian A. Gegenfurtner[3], Jonathan García-Roman[1], Stefan Zahler[3], Joachim O. Rädler[2], Ernst Wagner[1], Andreas Roidl[1]*

In Submission

[1]Pharmaceutical Biotechnology, Department of Pharmacy, Ludwig-Maximilians-Universität München, Munich, Germany
[2]Faculty of Physics and Center for NanoScience, Ludwig-Maximilians-Universität München, Munich, Germany
[3]Pharmaceutical Biology, Department of Pharmacy, Ludwig-Maximilians-Universität München, Munich, Germany

Contributions:

BL performed the experiments and wrote the paper. CS performed the 1D migration assays and wrote the paper. FAG performed the imaging experiments and wrote the paper. JGR generated the TRIPZ-constructs and performed the transcription factor analysis. SZ, JOR and EW provided conceptual advice. AR conceived the study and wrote the manuscript. All authors commented on the manuscript and conclusions of this work.

4.1. Abstract

Cancer progression and metastases are frequently related to changes of cell motility. Amongst others, the microRNA-200c (miR-200c) was shown to maintain the epithelial state of cells and to hamper migration. Here, we describe two miR-200c inducible breast cancer cell lines, derived from miR-200c knock-out MCF7 cells as well as from the miR-200c-negative MDA-MB-231 cells and report on the emerging phenotypic effects after miR-200s induction. miRNA-200c expression appears to cause. The induction of miR-200c expression seems to effect a rapid reduction of cell motility, as determined by 1D microlane migration assays. Sustained expression of miR200c leads to a changed morphology and reveals a novel mechanism by which miR-200c interferes with cytoskeletal components. We find that filamin A expression is attenuated by miRNA-200c induced downregulation of the transcription factors c-Jun and MRTF/SRF.This potentially novel pathway that is independent of the prominent ZEB axis could lead to a broader understanding of the role that miR200c plays in cancer metastasis.

4.2. Introduction

Metastasis, i.e. the nesting of tumor cells in adjacent tissues and even distant organs, is one of the most malicious aspects of cancer, causing nine out of ten cancer deaths [126]. While primary tumors often can be treated well, the uncontrollable spread of cancer cells remains a major challenge in most clinical settings. One prevalent example for risks of metastatic cancers are tumors of the breast, which show a clear association between metastasis and survival of patients [127,128]. While the primary breast carcinomas show rather good resectability due to their location, the cancer often has reached distant organs before the primary tumor was detected. Progress in understanding the disease has been made by identifying certain subtypes of breast tumor cells which inherit particularly high metastatic potentials [129]. However, current studies show a rise in incidence of metastatic breast cancer [130]. Therefore, still more and deeper insights into the key regulators of migratory and metastatic processes are needed.

Epithelial to mesenchymal transition (EMT) is often regarded as one of the most important steps in the initiation of migration and thus the onset of invasion and metastasis of tumors [131-133]. While EMT can be influenced by multiple cellular processes, RNA interference by microRNAs (miRNAs) was shown to be a direct and important regulatory mechanism [63].

In general, miRNAs are small, non-coding RNAs, influencing the translation of multiple fundamental cellular processes like metabolism, proliferation and cellular organization. Even small changes in miRNA expression patterns can have tremendous impact on the cell fate and can prompt towards various malignancies or even be the root cause of those [65,69,70]. One miRNA family with important implications in cancer is the miR-200 family, consisting of miR-200a, miR-200b, miR-141, miR-429 and miR-200c. While all members have demonstrated effects in the regulation of cancer processes, miR-200c is the family member which unifies well investigated associations in the most important cancer pathways, like the inhibition of chemoresistance[27,134,135], regulation of metabolic activity[28,67,72] and also in epithelial-to-mesenchymal transition (EMT) and thus potentially cancer cell metastasis [26,27,72,74,92,99].

MiR-200c's role in the regulation of EMT is based on its stabilizing effect on the expression of E-cadherin by preventing the inhibition of E-cadherin by ZEB1 and ZEB2 (Zinc finger E-box-binding homeobox members1 and 2). Previous studies have shown that the introduction or re-expression of miR-200c *in vitro* reverses the mesenchymal

phenotype of cancer cells, i.e. leading to EMT reversion, termed MET (mesenchymal to epithelial transition) [74,99].

Although EMT may be one of the main pathways of metastasis induced by the loss of miR-200c, the metastatic capabilities of tumor cells also rely on multiple other mechanisms. Interestingly, miR-200c was shown to influence other migratory pathways, for example by regulation of fibronectin secretion and moesin expression or by targeting the SRF-regulating proteins FHOD1 and PPM1F [26,100,103].

To further investigate the function of miR-200c as regulator of both, ZEB-dependent as well as independent mechanisms, we generated a genomic knock-out (KO) of miR-200c in MCF7 breast cancer cells in our previous work [136]. The resulting KO phenotype showed increased migration, even of the epithelial and usually low-migrating MCF7 cells. A pooled proteomic analysis revealed a number of common differentially regulated proteins, half of which are attributed to the regulation of migratory processes. From this set of proteins, novel players were chosen for further investigation. One protein of particular interest was Filamin A, a member of the filamins protein family that are known building blocks of the cytoskeleton and involved in many cellular and migratory processes [137]. Filamins, and especially filamin A, function as important actin filament crosslinkers, thereby facilitating actin-actin interactions, but also actin-connections to membrane bound proteins and intracellular signaling macromolecules [137,138] and previous studies described the role of filamin A in the regulation of cell migration [139]. However, a systematic study of miRNA-200 mediated expression of filamin A and concomitant changes in migration has not yet been carried out.

In this study, we generated two different inducible miR-200c breast cancer cell line models, derived from mesenchymal MDA-MB-231 cells or the miR-200c knock-out of the epithelial MCF7 cells, respectively. By doxycycline induction, we investigated the effect of increased miR-200c expression on morphological changes and motility. We used a micro-pattern based 1D migration assay, as described previously by Schreiber *et al*. [140] to get a multiparameter quantification of cell motility. We also found strong indications of a regulatory network of miR-200c and FLNA in both breast carcinoma models. This pathway, which is independent of the ZEB-expression of the cells, may point towards an important further function of miR-200c in impeding cancer metastasis.

4.3. Results

4.3.1. The migratory potential of MDA-MB-231 cells decreases after miRNA-200c induction

To investigate the effect of miRNA-200c induction on the metastatic potential of cells, we performed an in-depth analysis of single cell migration.

Therefore, the miR-200c non-expressing, highly migratory MDA-MB-231 cell line[28] was chosen for stable transduction with a TET-off construct containing either miR-200c or a scrambled control, resulting in the MDA-MB-231 TRIPZ-200c or MDA-MB-231 TRIPZ-Ctrl cells. Treatment with doxycycline for 48 h showed a reliable and easy controllable induction of miR-200c expression as well as of an RFP reporter tag (Figure 14a, b).

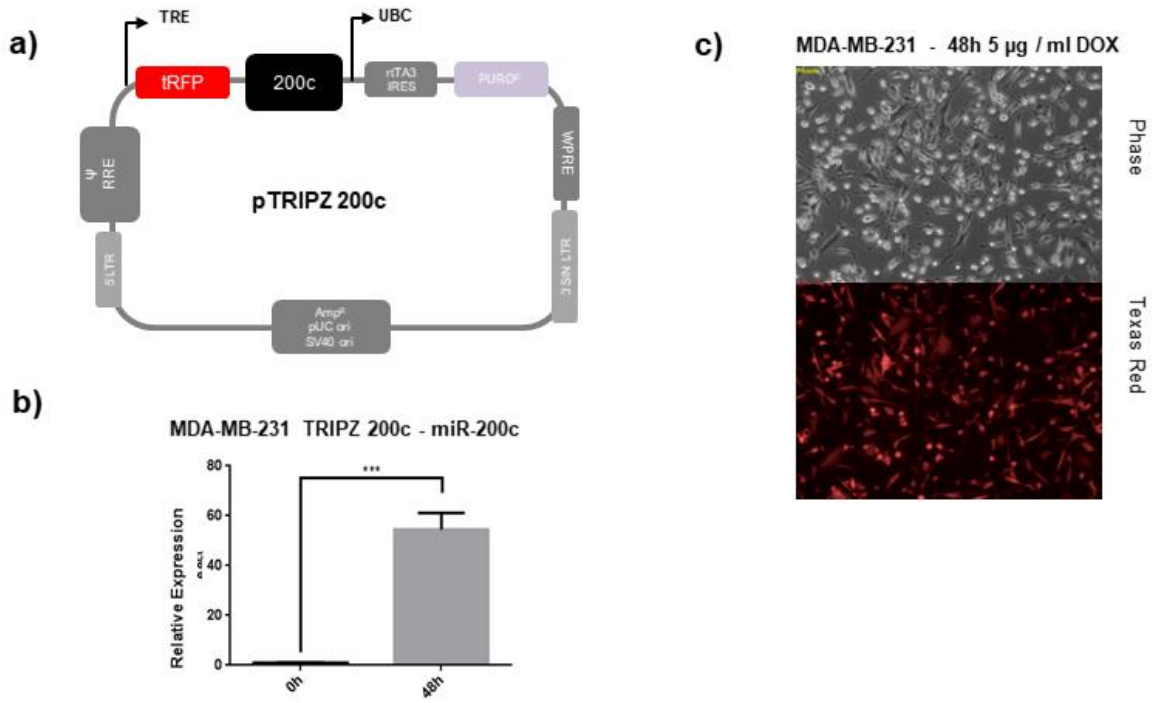

Figure 14 Inducible miR-200c construct with RFP reporter

(a) Description of the inducible pTRIPZ-200c construct (b) and verification of functional transduction in MDA-MB-231 cells by induction of the RFP reporter tag by 5 µg / ml doxycycline for 48 h. (c) Expression analysis by RT-qPCR of miRNA-200c after induction with 5µg / ml doxycycline after 48 h.

Using these cell lines we perform an multi-parameter analysis of motility by studying 1D migration on ring-shaped micro-lanes. Compared to other common migratory assays, the real time tracking of the 1D migration allows to analyze high numbers of

cells and to assess a migratory fingerprint, i.e. cell velocity, cell persistence, cell resting times, cell run times and the run fraction, at the single cell and population level.

For this purpose, cells were seeded on arrays of fibronectin-coated ring micropatterns and were observed using time-lapse microscopy (Figure 15 a, b). We found that the 1D cell motion is divided into distinct run states, where cells move persistently in one direction, and rest states with no or random wiggling motion[140] (Figure 15c). This two state analysis results in characteristic parameters quantifying cell motility (Figure 2d). By discriminating between run and rest states we make sure that the velocity is only evaluated when cells are actually migrating (v_{run}). Furthermore, we analyze the typical lifetime of run and rest states τ_{run} and τ_{rest}, which are exponentially distributed. This allows distinguishing between the stability of the run state, given by τ_{run} and the ability of cells to establish polarization indicated by τ_{rest}. For a comprehensive overview of the different motility parameters, spider-plots were generated (Figure 15e, f). As expected, the doxycycline induction in the MDA MB-231 TRIPZ-Ctrl cells showed no significant effects compared to the uninduced cells, while miR-200c induction distinctly changed the migratory behavior of the cells. The run velocity and the typical duration of a run state were significantly decreased whereas the typical duration of a rest state was increasing. The strongest effect was observable in the fraction of time that cells spent in the run state, P_{run}, which decreased by a factor of three. Thus, induction of miR-200c expression affects the polarization of cells leading to longer rest states and a decreased persistence of the run states. To show that the decrease of persistence of the cell motion was also visible without the division into run and rest states we evaluated the persistence path q, which is given by the effective maximum displacement of a cell divided by the actual length of the trajectory, as described in Maiuri *et al.* [141]. The described effects are visualized in a sample of a Ctrl vs a miR-200c induced cell, as shown in the supplemental movie 1 (SM1). On single cell level, a broad distribution of run velocities and a huge variance in the fraction of time spent in the run state was observed (Figure 15g). With increasing miR-200c expression, the distribution narrowed, and the average velocity was decreasing as well as the time cells spent in run states. Furthermore, the fraction of cells that remained in the rest states for the time of the whole experiment increased by almost a factor of three.

Taken together, our data show that the induced miR-200c expression resulted in a reduced motility in all five migratory parameters and, hence, an overall decreased migratory potential. The observed process must be independent of the well

investigated miR-200c and ZEB1/2 induced EMT mechanisms [99]; due to the fact that MDA-MB-231 cells are not expressing E-cadherin [101,142,143].Our findings therefore suggest a novel mode of miR-200c acting on migration.

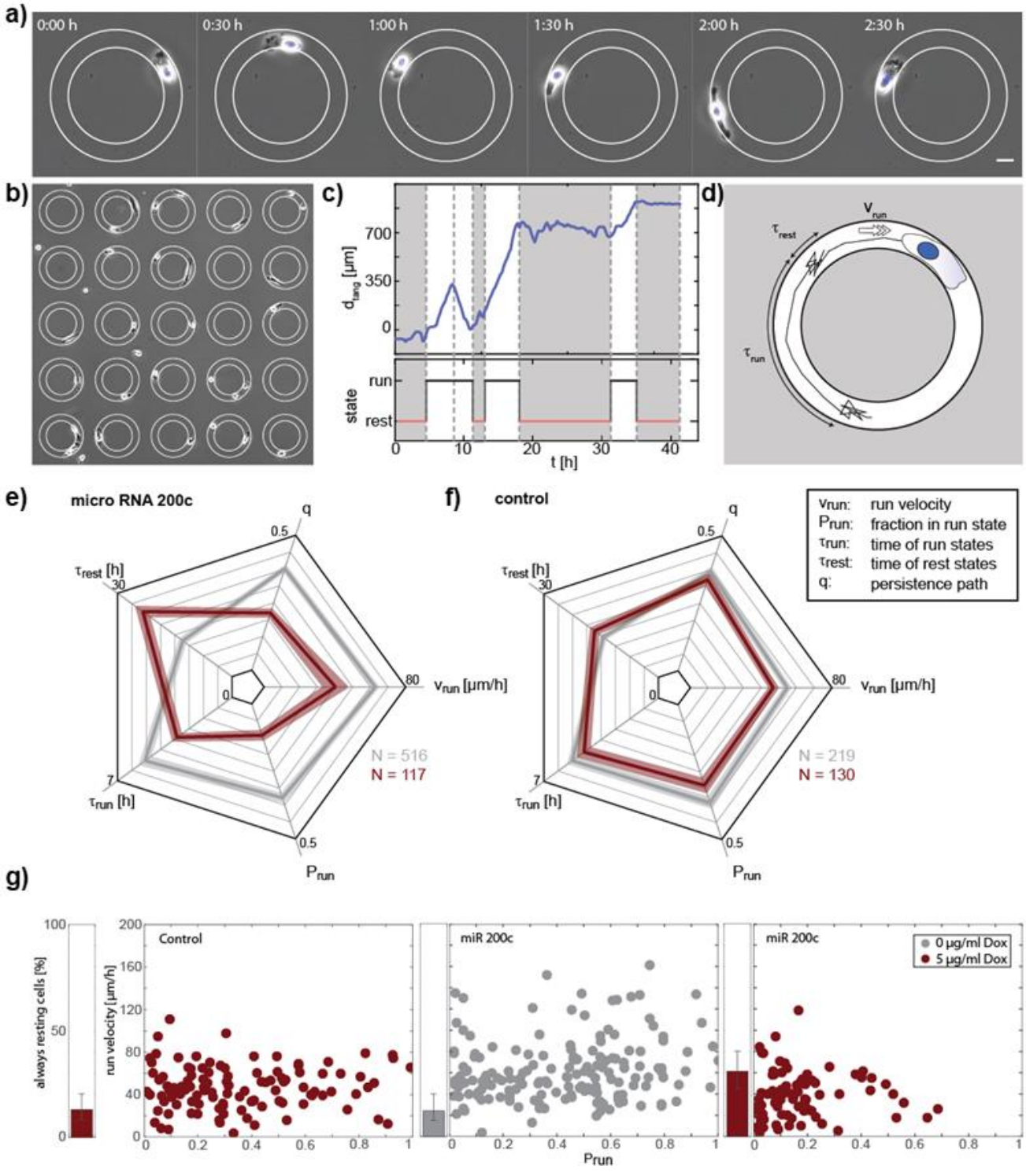

Figure 15 - miR-200c induction decreases migration of MDA-MB-231 cells as shown in the 1D migration assay (description next page)

(a) Phase contrast images of a MDA-MB 231 cell migrating on a ring shaped micro-lane. The ring is coated with fibronectin (edges marked in white) the surrounding is passivated with PEG. The scale bar is 20 µm. (b) Array of ring shaped micro lanes. Only rings that are occupied by one single cell are evaluated. (ring diameter 150 µm) (c) Angular position of one exemplary cell over time with classification into run and rest states. (d) Drawing of a cell track. Cell motion can be separated in run states with ballistic motion and rest states with random motion. The characteristic duration of run and rest states τ_{run} ,τ_{rest} as well as the velocity in the run state v_{run} are evaluated. (e, f) Multi-parameter analysis of cell motility of cell populations. Motility of cells is measured 48h after induction with 5 µg / ml doxycycline (red). For MDA-MB-231 TRPZ-200c cells (f) a clear reduction of cell motility can be seen in all of the 5 parameters compared to no induction (grey). For MDA-MB-231 TRPZ-Ctrl cells (h) no big effects on motility are observed with adding doxycycline. N is the number of cells analyzed. (g) Single cell analysis of P_{run} and v_{run} for the data shown in e, f) where each dot represents a single cell. One cell population is spread over a large range of velocities and fraction of time in the run state. Induction of miR 200c is causing a shift to slower velocities and less time spent in the rest state. (error bars in g and h indicate standard errors exept for τ_{run} ,τ_{rest} where it's CI of 99% of the fit)

4.3.2. MiRNA-200c induction changes the 3D morphology

As a decrease in migration often correlates with changes of the cytoskeleton, we investigated how miR-200c affects the cellular morphology. Hence, immunofluorescence imaging and analysis of the cellular shape was performed. Figure 16a shows a comparison of the actin-structure of MDA-MB-231 with either the Ctrl or the miR-200c construct stimulated with doxycycline for 72 h. While the TRIPZ-Ctrl cells maintained their mesenchymal, spindle-like shape, the miR-200c induction changed the cellular profile towards rounder, uniformly dilated cells as seen in the significant difference of the ratio of widest vs. longest spread of the cell. The three-dimensional shape of the cells was investigated by taking z stacks of confocal images of actin and filamin. Figure 16b and c show the 3D images with color coding for hight. In line with the previous results, the TRIPZ-Ctrl cells retained their spindle-like structure, after 72h and 168h of doxycycline stimulation. The miR-200c induction caused a gradual transition towards rounder and morphologically flatter cells over time, eventually resulting in evenly flat “pancake” like shape. For better visualization, these effects are presented in a 3D rendering animation of the stacks, shown in the supplemental movies (SM2 Ctrl and SM3 miR-200c). These results together show a strong effect of miR-200c induction on the cellular shape.

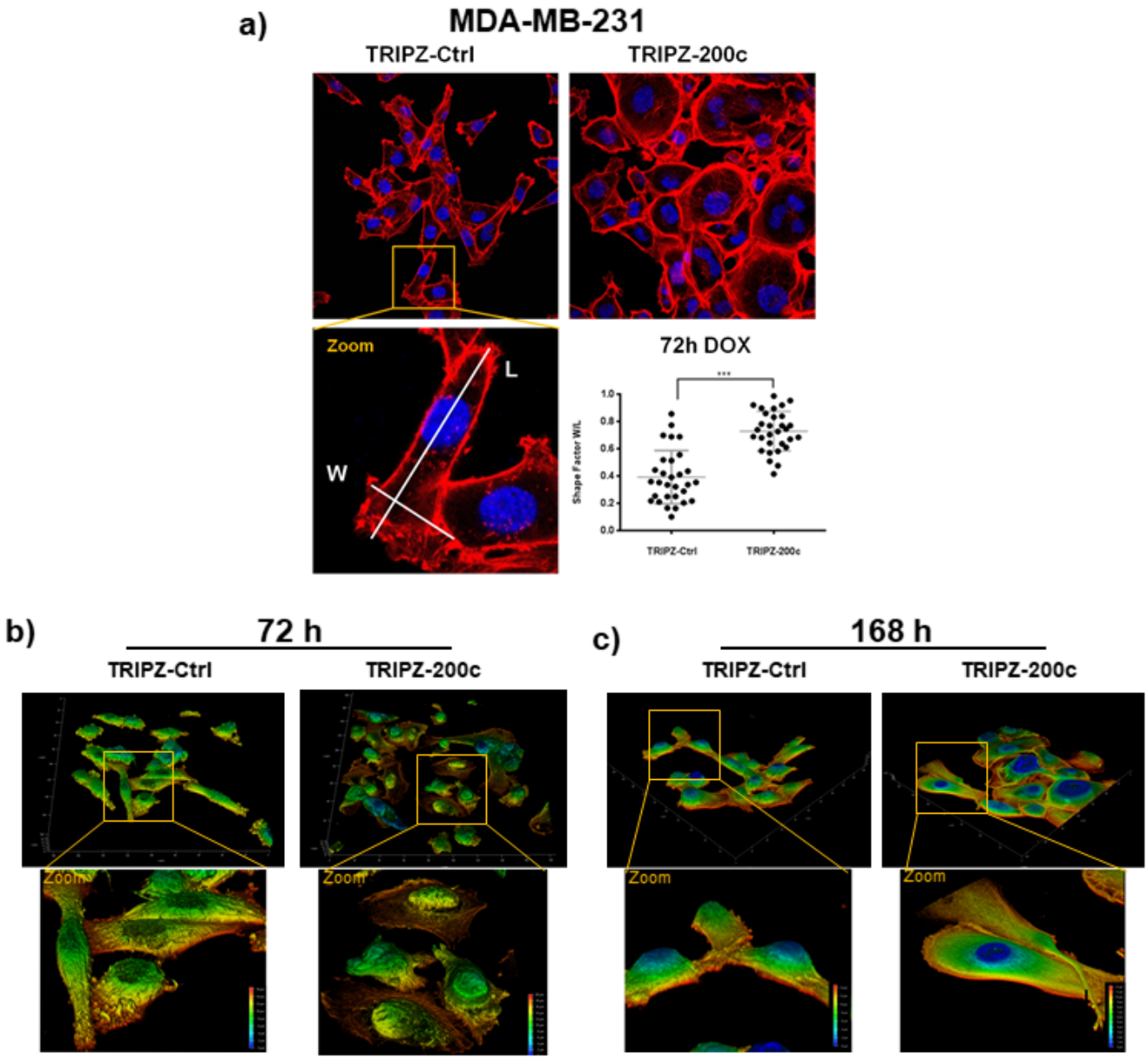

Figure 16 - Overexpression of miR-200c induced fast morphological changes in MDA-MB-231 cells

(a) Fluorescence staining of the cytoskeleton by Phalloidin (red) and nuclei (blue) in MDA-MB-231 decreased spindle-like phenotype after induction miR-200c, as shown by significant changes in the shape factors (N= 30; error bars are SD; *** $p > 0.001$). (b,c) Renderings of stacked immunofluorescence images of MDA-MB-231 showed decreased mesenchymal shape in 3D after induction of miR-200c for (b) 72 h as well as (c) further increased effects after 168 h compared to included controls. (d) Distribution of filamin A in a central cross section after induction with miR-200c for 72 h and 168 h as compared to induced control

4.3.3. Changed expression of FLNA is observed after a miRNA-200c knock-out and overexpression

A proteomic analysis of a genomic knock out (KO) of miR-200c in MCF7 breast cancer cells was previously reported by our group [136]. There, we showed that more than 50% of all differentially expressed proteins were affiliated to migratory processes (Figure 17a). Out of these proteins, filamin A was one of the prominent and promising targets and therefore chosen for further analysis in this study. To study the biological effect of miR-200c on FLNA the inducible MDA-MB-231 TRIPZ-200c or TRIPZ-Ctrl cells were utilized. In line with studies of the MCF7-200c-KO cells the inverse effects regarding filamin A expression were observed after induction of miR-200c. Here, the mRNA levels of FLNA decreased to 30% and protein expression to 40% compared to doxycycline stimulated TRIPZ-Ctrl cells (Figure 17b, c). Additionally, an immunofluorescence staining of filamin A was performed in both cell line models. i.e the MCF7-200c-KO and the MDA-MB-231 TRIPZ-200c. The KO of miR-200c in MCF7 resulted in increased cellular expression of filamin A (Figure 17d), while induction of miR-200c in MDA-MB-231 TRIPZ-200c cells resulted in decreased filamin A protein expression (Figure 17e). Taken together, miR-200c expression showed an indirect proportional relation to filamin A protein as well as mRNA in two complementary breast cancer cell line models.

Figure 17 miR-200c regulates migration associated genes such as filamin A (next page)

(a) A proteomic analysis of a TALENs knock-out (KO) of miR-200c in MCF7 cells revealed a set of proteins with differential expression, of which 50% are involved in migratory processes and are shown in the table. (RT qPCR showed that after adding 5 µg / ml doxycycline for 48 h the expression of FLNA mRNA (b) as well as filamin A protein(c)(normalized to tubulin) decreased significantly in MDA-MB 231 TRIPZ 200c cells. (d) Immunofluorescence staining of filamin A (green) and DAPI (blue) in MCF7 Ctrl and KO 200c showed significantly increased relative intensity of filamin A, in contrast to (e) the MDA-MB-231 cells which showed a strong decrease in filamin A intensity after induction of miR-200c (all N=3; error bars indicate standard deviation SD; * $p \leq 0.05$, ** $p \leq 0.01$, *** $p \leq 0.001$, **** $p \geq 0.0001$)

a)

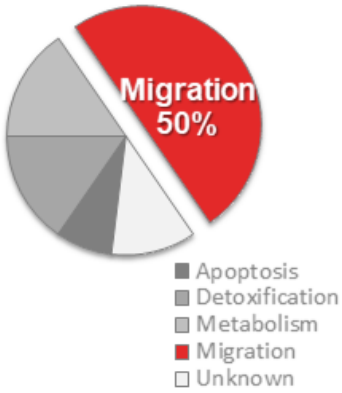

Protein names	Gene names	Expression up / down
Anterior gradient protein 2 homolog	AGR2	down
Src substrate cortactin	CTTN	down
Filamin-A	FLNA	up
Filamin-B	FLNB	up
Ras-related protein Rab-14	RAB14	down
Regulator of microtubule dynamics protein 1	RMDN1	up
Adseverin	SCIN	up
SH3 domain-binding glutamic acid-rich-like protein	SH3BGRL	up
Spectrin alpha chain, non-erythrocytic 1	SPTAN1	down
Tropomyosin alpha-1 chain	TPM1	up
UDP-glucose 6-dehydrogenase	UGDH	down

b)

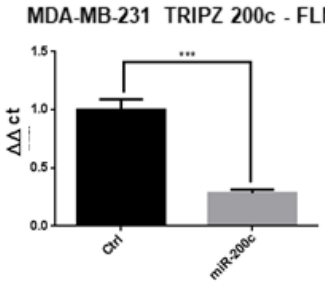

c)

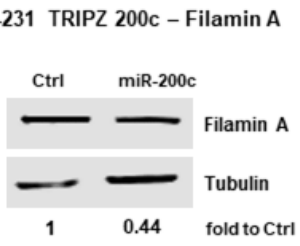

d)

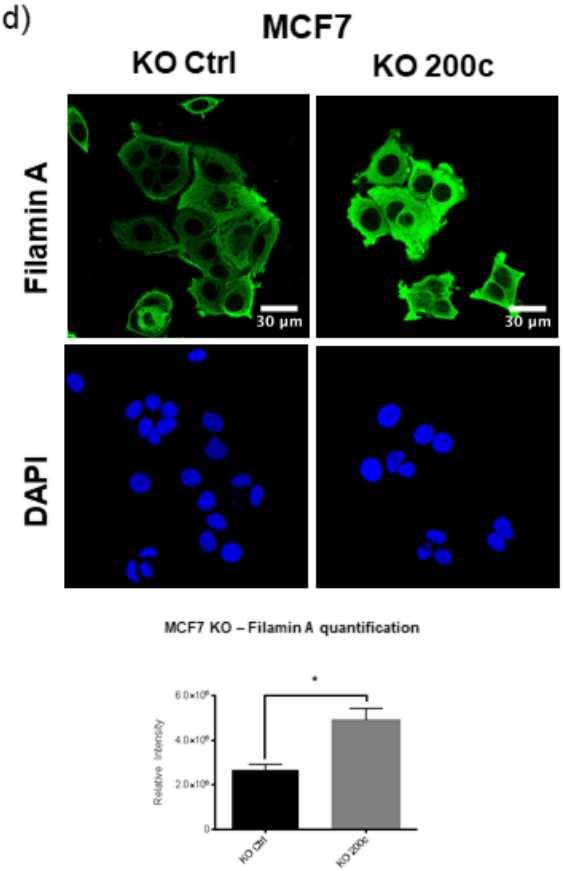

e)

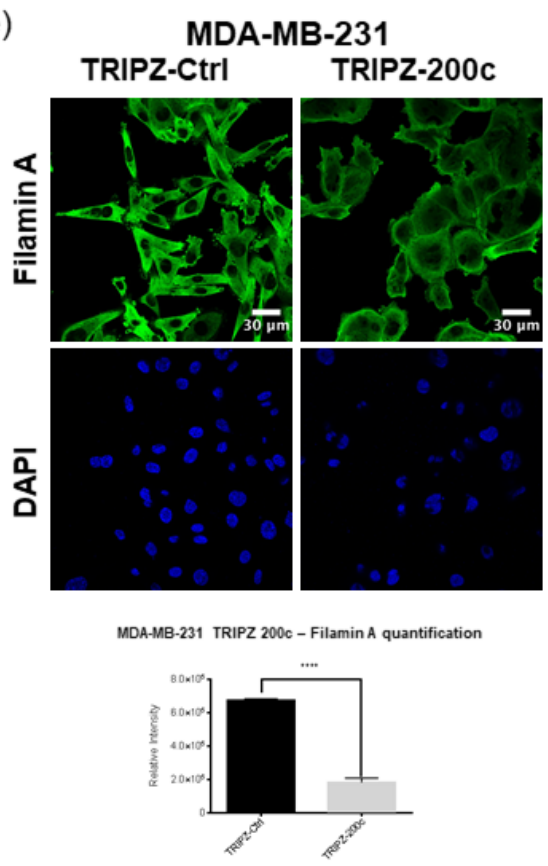

4.3.4. MiRNA-200c is regulating FLNA expression via JUN and MRTF-SRF

To further investigate the mechanism of miR-200c dependent regulation of FLNA, a rescue of miR-200c expression in the MCF7-200c-KO cells was performed, by stably introducing the inducible TRIPZ-200c plasmid. As expected, the induction successfully re-expressed miR-200c and consequently decreased FLNA mRNA (Figure 18a, b).

As no miR-200c binding site was predicted *in silico* in the FLNA 3'UTR, other regulatory mechanisms were investigated. First, a promotor analysis was performed, in order to determine transcription factors (TFs) which are potentially regulating FLNA expression and contain an *in silico* predicted miR-200c binding-site (Figure 18c). Four of those TFs were identified by RT-qPCR screening after miR-200c induction in MDA-MB-231 cells (Supplement S 9), but a reproducible decrease in expression of these TF was solely detected for JUN (Figure 18d). This result was confirmed in the miR-200c inducible MCF7 KO cells (Figure 18e).

To investigate the effect of JUN on FLNA expression, a siRNA knockdown of JUN was performed in wild type MDA-MB-231 as well as in MCF7 cells and compared to scrambled control siRNA. In both cases, the reduction of JUN mRNA also decreased FLNA mRNA expression (Figure 18f, g), with stronger relative effects in MCF7 cells than in MDA-MB-231.

Thus, we suggest JUN as a direct target of miR-200c and as putative regulator of FLNA expression.

Another possibility of miR-200c regulating FLNA is via SRF and MRTF. It was shown previously that miR-200c regulates SRF and MRTF[103], and also a regulation of FLNA by SRF was predicted in previous studies [144]. Thus, we tested the hypothesis that miR-200c is able to regulate FLNA via the MRTF/SRF axis by transiently introducing pgl4.34, a luciferase reporter for MRTF-dependent SRF activation, into both miR-200c inducible cellular systems. Here, a decrease in luciferase signal upon miR-200c expression was observed in both, MDA-MB-231 and MCF7 cells, compared to their respective doxycycline treated controls (Figure 18h, i). These results suggest a regulatory relation between miR-200c and FLNA based on the two different mechanisms, i.e. via transcriptional repression of filamin A through reduced JUN and the regulation by MRTF/SRF (Figure 18j).

Figure 18 - Filamin A is regulated by miR-200c by repression of JUN as well as SRF-MRTF (next page)

(a) After introduction of the TRIPZ-200c construct into MCF7 200c KO cells, miR-200c was re-expressed by 48 h of DOX induction and showed (b) significantly decreased FLNA expression. (c) *In silico* analysis of the FLNA promotor revealed 6 transcription factors which have a potential miR-200c binding site. (d) The expression of JUN was significantly decreased 48 h after induction of miR-200c in MDA-MB-231 as well as (e) re-expression in MCF7 compared to the respective TRIPZ-Ctrl cell line. (f, g) Decreased expression of FLNA was verified in MDA-MB-231 and MCF7 after transient transfection with siRNA against JUN (siJUN), compared to scrambled siRNA control (h, i) Induction of miR-200c for 48 h decreased the luciferase signal of a MRT-SRF reporter construct in MDA-MB-231 TRIPZ-200c as well as MCF7 TRIPZ-200c compared to their respective TRIPZ-Ctrl. (j) An alternative mechanism of miR-200c regulation of FLNA is based on reducing the MRT dependent SRF activation as well as the transcription factor jun. (all N=3; error bars are SD; * $p \leq 0.05$, ** $p \leq 0.01$, *** $p \leq 0.001$, **** $p \geq 0.0001$)

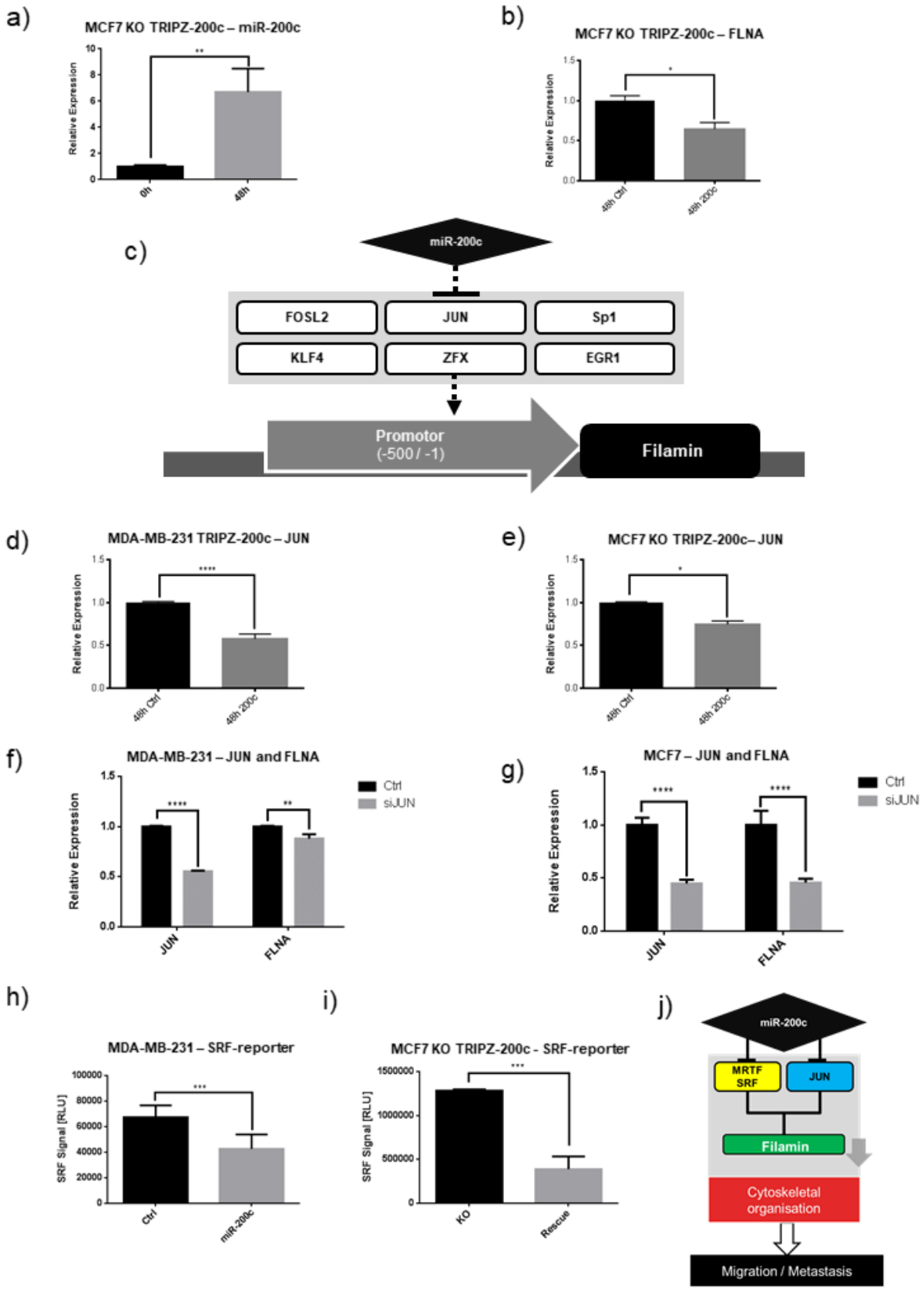
a)
MCF7 KO TRIPZ-200c – miR-200c
Relative Expression
0h
48h
b)
MCF7 KO TRIPZ-200c – FLNA
Relative Expression
48h Ctrl
48h 200c
c)
miR-200c
FOSL2
JUN
Sp1
KLF4
ZFX
EGR1
Promotor
(-500 / -1)
Filamin
d)
MDA-MB-231 TRIPZ-200c – JUN
Relative Expression
48h Ctrl
48h 200c
e)
MCF7 KO TRIPZ-200c– JUN
Relative Expression
48h Ctrl
48h 200c
f)
MDA-MB-231 – JUN and FLNA
Relative Expression
Ctrl
siJUN
JUN
FLNA
g)
MCF7 – JUN and FLNA
Relative Expression
Ctrl
siJUN
JUN
FLNA
h)
MDA-MB-231 – SRF-reporter
SRF Signal [RLU]
Ctrl
miR-200c
i)
MCF7 KO TRIPZ-200c - SRF-reporter
SRF Signal [RLU]
KO
Rescue
j)
miR-200c
MRTF
SRF
JUN
Filamin
Cytoskeletal
organisation
Migration / Metastasis

4.4. Discussion

miR-200c is a well-established player in different types of cancer, often described as guardian over multiple cancer promoting pathways like metabolic activity and proliferation[28,67,72], resistance to chemotherapeutics [27,134,135] , and inhibition of migration and EMT [26,72,74,92,99].

In different clinical studies the miR-200c expression correlated with decreasing spread of tumors and better treatability of some cancers, as shown in different studies for patients with breast cancer[26,77,82]. In the current literature, miR-200c's effect on metastasis is mainly attributed to the process of EMT, based on preventing ZEB1/2 mediated inhibition of E-cadherin expression and thereby inhibiting the transition of epithelial cells to the mesenchymal phenotype[74,99,104]. Still, miRNA-200c has shown effects on migration of cell lines, which do not express the genetic axis of ZEB-mediated E-cadherin regulation. One issue in the investigation of additional migratory effects of miR-200c lies in distinguishing novel functions from effects based on the prominent ZEB/E-cadherin axis. Therefore, our approach has based on the utilization of two different breast cancer cell lines (MCF7 and MDA-MB-231) which, due to epigenetic predispositions[101,142,143], ensure absence of ZEB/E-cadherin based effects. Proteomic analysis of a genomic miR-200c KO in MCF7, a high miR-200c expressing epithelial cell line[28] emphasized the importance of miR-200c in migratory processes [136].

In this study, we show the influence of miR-200c on migration based on two "gain of function" cell line models. First, mesenchymal and migratory MDA-MB-231 cells, which lack expression of miR-200c as well as E-cadherin, were transduced with a doxycycline inducible miR-200c expression construct (TRIPZ-200c). This approach ensured to minimize negative effects of transfections on the one hand, and on the other hand allowed for the efficient expression of miR-200c on a long-term scale, rendering the observation of slower processes in cellular remodeling possible. Furthermore, with the same construct, an inducible rescue of the miR-200c expression was performed in the MCF7 miR-200c KO cells.

The induction of miR-200c caused evident changes in the morphology of MDA-MB-231 cells, resulting in extensive remodeling of the cellular architecture as observed already after three days and even further increased after seven days. The resulting flat "pancake" shaped cells appeared to have highly decreased cellular stiffness as well as a lack of distinctive polarization that is commonly seen in spindle-like cells. Similar

observations of morphological or “spreading defects” were reported after a FLNA knock-down and were attributed to a deficiency in actin-crosslinking [139,145].

In contrast to the rather slow full EMT, the effects on speed and run-times of the cells were observed already 48 h hours after miR-200c induction, indicating a direct connection of this axis to the cellular motility. The long-term stimulation showed a change in modality which may be similar to EMT, but a complete transition to an epithelial “cobblestone” phenotype was not observed, possibly due to the lack of development of cellular adhesions by E-cadherin.

Furthermore, the 1D migration assay revealed decreased motility after miR-200c expression by showing changes of all measured parameters the decreased migratory capabilities of miR-200c high expressing cells show to be not based mainly on the absolute velocity, but more on the cells’ inability of polarizing and retaining polarization, as seen by the higher number of cells in temporary rest states or being completely immobile.

Our previously published proteomic analysis of a genomic miR-200c KO in MCF7 disclosed multiple changes in the expression of regulators of migratory processes, of which the effect on filamins A was most prominent [136]. Filamin A is supposed to affect cell motility based on multiple pathways, like the induction of changes in the structure and stiffness of the cell as direct building block in the system[145] or shifts in intracellular signaling[146] and resulting in alteration of different mechanisms important for migration, like the actin-treadmill and formation of focal adhesions[147,148 38]. This important role of filamin A as a capable regulator of cellular migration makes it interesting to investigate how miR-200c regulates filamin A. Especially as we found that induced miR-200c expression resulted in decreased expression of FLNA in both cell systems.

The investigation of the underlying mechanism of FLNA suppression was performed with two *in silico* analyses: The first was not yielding any predicted binding site of miR-200c in the FLNA 3’ UTR, while the other resulted in six potential miR-200c controlled transcription factors. Of the transcription factors, only JUN showed constant repression to miR-200c expression, which is in line with previous studies that identified JUN as potential miR-200c target [149]. JUN expression is necessary for the formation of the AP-1 complex together with c-Fos. Previously, the AP-1 complex was shown to promote tumorigenesis, cancer progression and also regulating cell morphology and migration [150-152]. Our experiments verified JUN promoting FLNA transcription as well as inhibition of JUN by miR-200c’s, resulting in decreased FLNA expression.

A recent study by Jurmeister et al. indicated one further possible regulatory mechanism. They found that miR-200c was inhibiting the MRTF dependent activation of SRF[103]. SRF is a known transcription factor of multiple immediate early genes, including c-fos[153], and therefore an important regulator of cell growth, differentiation and also migration[154,155] FLNA was previously[144] identified as a target of SRF. Consistently a decreased MRTF-dependent SRF activation was observed after miR-200c induction, indicating an additional axis of miR-200c based regulation of FLNA expression. Furthermore, increased c-Fos expression due to SRF stimulation may also promote the additionally observed JUN-based axis, by providing additional partners for the assembly of the AP-1 complex. Further, FLNA was shown to promote the activity of SRF [156] which may further increase the investigated effects due to this positive feedback loop.

Our data reveal a potential novel route of miR-200c regulating migration, independent of ZEB1/2. The inhibition of cytoskeletal components via miR-200c, like filamin A as shown here, support the role of miR-200c in maintaining the epithelial state and inhibiting metastasis as possibly important in a wider variety of cancer cells.

4.5. Materials and methods

Puromycin dihydrochloride and doxorubicin hydrochloride were obtained from Sigma (cat. P8833, D1515).

The MCF7 miR-200c KO cells were grown at 37 °C and 5 % CO_2 in high glucose DMEM (Sigma) supplemented with 10 % fetal calf serum (FCS / Gibco). MDA-MB-231 cells were cultured at 37 °C and 0 % CO_2 in L15 (Sigma) containing supplemented with 10 % fetal calf serum (FCS / Gibco). All derived cells, i.e. MDA-MB-231 TRIPZ200c and Ctrl, as well as MDA-MB-231 GFP were cultured same as the parental cells. All cells were routinely tested and confirmed as mycoplasm free.

The miR-200c KO via TALENs was performed as described previously[136].

As backbone for the TRIPZ-200c construct, the TRIPZ lentiviral inducible shRNA control plasmid (TRIPZ-Ctrl, Thermo Fisher Scientific, #RHS4743) was used. MiR-200c plus 125 bp upstream and downstream flanking genomic sequences, including XhoI and MluI restriction sites was amplified by PCR with the following primers:
Fwd: CTCGAGGCTCACCAGGAAGTGTCCCC
Rev: ACGCGTCCTTGTGCAACGCTCTCAGC.
After the construct was verified by sequencing (GATC Biotech AG), MDA-MB-231 and MCF7 200c KO cells were transducted with the TRIPZ-200c and TRIPZ-Ctrl utilizing a 2nd generation lentiviral system generated with the plasmids pCMV-dR8.2 dvpr and pCMV-VSV-G, which were a gift from Bob Weinberg (Addgene plasmid # 8454 and #8455). After transduction and 48 h selection with 5 µg/ml puromycin, a single cell dilution was performed to generate the monoclonal TRIPZ cell lines MDA-MB-231 TRIPZ-Ctrl, MDA-MB-231 TRIPZ-200c and MCF7 200c KO TRIPZ-200c.
Stimulation of the cells with doxycycline was performed in a concentration of 5 µg/ml in the respective medium for 48 h for mRNA analysis or 72 h for protein analysis. Medium was replaced with fresh, doxycycline containing medium every 48h to compensate for doxycycline degradation.

qPCR of miRNA was performed as described previously[136], in short: 600,000 cells were harvested and total RNA isolated from cells using miRCURY RNA Isolation Kit (Exiqon). cDNA synthesis was carried out by a miRNA specific reverse transcription

and detection with the qScript microRNA cDNA Synthesis Kit and PerfeCta SYBR Green SuperMix (Quanta Biosciences) with RT-PCR detection on a LightCycler 480 (Roche). The expression of miR-200c was normalized to miR-191[121], using the $2^{-\Delta CT}$ or $2^{-\Delta\Delta CT}$ method.
The following list contains the primers used for analysis of miRNAs:
miR200c: *GCGTAATACTGCCGGGTAAT*; miR-191: GCGCAACGGAATCCCAAAAG;

Cells were cultured in a 6 well plate for 72h after stimulation with doxycycline. Lysis, gel and blotting were performed as described previously[27]. For the detection, the primary antibodies for filamin A (Thermo Fisher, MA5-11705) and tubulin (Sigma, T 9026) were used and diluted by manufacturer's instructions. For secondary antibody detection, ALEXA FLUOR PLUS 800 (Thermo Fisher, A32730) were used, imaged with the Odyssey Fa and analyzed and quantified by Image Studio Software (LiCor).

The transcription factor binding sites were published previously[136]

RNA extraction was performed via the Total RNA Kit, peqGOLD (VWR) as by manufacturer's instructions. The cDNA synthesis was performed using the qScript cDNA synthesis kit (Quanta Bioscience) as by manufacturer's protocol.
Analysis of expression was performed with the Lightcycler 480 (Roche) and the Universal Probe Library (Roche) with following probe and primer (forward/reverse) combinations, all results were normalized to GAPDH as housekeeper:
FLNA, Probe 32, TCGCTCTCAGGAACAGCA / TTAATTAAAGTCGCAGGCACCTA
JUN, Probe 19, CCAAAGGATAGTGCGATGTTT / CTGTCCCTCTCCACTGCAAC
GAPDH, Probe 45, TCCACTGGCGTCTTCACC / GGCAGAGATGATGACCCTTTT
KLF4, Probe 83, TGACTTTGGGGTTCAGGTG / GTGGAGAAAGATGGGAGCAG
EGR1, Probe 22, AGCCCTACGAGCACCTGAC / GGTTTGGCTGGGGTAACTG
FOSL2, Probe 70, ACGCCGAGTCCTACTCCA / TGAGCCAGGCATATCTACC

Confocal images and 3D stacks were acquired using a Leica TCS SP8 SMD microscope equipped with a 40x HC PL APO oil objective. Pinhole size was adjusted

to 1.0 airy units and sequential scanning was performed at 400 Hz. 405nm, 488nm and 561nm laser lines were used for excitation.

For immunofluorescence staining, cells were fixed for 10 min with 4% EM grade formaldehyde. After 5 min washing with PBS, samples were permeabilized for 10 min with 0.5% TX-100 in PBS. Unspecific binding was blocked by 30 min incubation with 5% BSA (Sigma) at RT. Cells were then incubated overnight (4 °C) with the primary antibody for filamin A diluted according to the manufacturer's instructions (1:400, Thermo Fisher, MA5-11705). After 3 x 10 min washing with PBS, samples were incubated with secondary antibodies (1:500, AF488 goat-anti-mouse AB_2534069), rhodamine phalloidin (1:300, Sigma-Aldrich) and DAPI (0.5 µg/ml, Sigma-Aldrich) for 1 hour at RT, washed again 3 x 10 min with PBS. All stainings were performed in ibiTreat 8 well µ-slides (ibidi GmbH) coated with fibronectin (Corning). Total fluorescence intensities and nuclear shape factors were quantified using ImageJ v1.52. Z-plane scaled 3D stacks were rendered using the Leica LAS X software platform.

For the knockdown of JUN, a siRNA was used and compared to a negative control (Silencer Select, Thermo Fisher, assay s7659 and control 4390843). Cells were transfected with the K2 transfection reagent (Biontex) according to the manufacturer's recommendations.

For analysis of SRF/MRTF signaling, the pgl4.34 Plasmid (Promega, 9PIE135) was used. Transfection was performed in 6-well with cells grown to 80% confluence with K2 transfection reagent (Biontex, Germany) according to the manufacturer's instructions, into cells stimulated with 5µg/ml doxycycline for 24h. Luciferase measurement was performed 24h after transfection, as described previously[28].

Detailed description of production of the stamps and measurements are published in Schreiber et al. [140] and further described in the supplemental methods.
The motility parameters are defined as:
$\boldsymbol{v_{\mathbf{run}}}$: The run velocity is defined as the mean over the tangential velocity for time points when cells are in the run state $v_{run} = \langle |v_{tang}| \rangle$.

$\boldsymbol{\tau_{run}}$, $\boldsymbol{\tau_{rest}}$: To evaluate the persistence times of run and rest states τ_{run} and τ_{rest}, the survival function $S(t) = \mathrm{P}(T > t)$ is calculated. τ_{run} and τ_{rest} are determined by fitting $\log(S(t))$ by the function $f(t) = -\frac{1}{\tau}\, t + c$ evaluated at $t \in\ [2; 16\ ]h$. Very small times are excluded because defiations from an exponential behavior are observed here. To reduce the effects of the limited time window, only states that start at least 16 h before the end of the corresponding cell track are evaluated, while the fitting range for $S(t)$ ends at 16 h. The error range given is the 99% confidence interval for the fit.

$\boldsymbol{P_{run}}$: The fraction of time cells spend in the run state is defined as the time cells are in the run state divided by the total time of the trajectories.

$\boldsymbol{q}$: The persistence parameter q is defined as the maximum distance between two points of a cell trajectory divided by the total path length of the trajectory. This is averaged over all cells $q = \langle \frac{\max(\varphi) - \min(\varphi)}{\sum_i |\varphi_i|} \rangle$

Results are expressed as the mean ± SD of at least three biological replicas and analyzed using a two-sided student's t-test, if not stated otherwise. Software GraphPad Prism v6 and SigmaPlot 11 were utilized for the analysis of the data.

The data that support the findings of this study are available from the corresponding author upon reasonable request.

The authors thank the German Research Foundation (DFG) for financial support of SFB 1032 projects B01 (JOR), B04 (EW) and B08 (SZ), and Cluster of Excellence NIM (JOR, EW). JGR thanks the Mexican government for receiving a scholarship (CONACyT number 207973). The authors declare no competing financial interests.

The authors declare that they have no conflict of interest.

BL performed the experiments and wrote the paper. CS performed the 1D migration assays and wrote the paper. FAG performed the imaging experiments and wrote the paper. JGR generated the TRIPZ-constructs and performed the transcription factor

analysis. SZ, JOR and EW provided conceptual advice. AR conceived the study and wrote the manuscript. All authors commented on the manuscript and conclusions of this work.

4.6. Supplements

4.6.1. Supplemental methods

Micropatterning / 1D Migration

Production of stamps:

To a master for stamp preparation, silicon wafers were coated with TI Prime adhesion promoter and AZ40XT (MicroChemicals) photo-resist. Desired areas were exposed to UV light using laser direct imaging (Protolaser LDI, LPKF). The photoresist was then developed (AZ 826 MIF, MicroChemicals) and silanized (Trichloro(1H,1H,2H,2H-perfluoro-octyl)silane, Sigma-Aldrich). To create the stamp, polydimethylsiloxane (PDMS) monomer and crosslinker (DC 184 elastomer kit, Dow Corning) were mixed in a 10:1 ratio, poured onto the stamp master, degassed in a desiccator, and cured overnight at 50°C.

Microcontact printing:

Microcontact printing was used to produce fibronectin-coated ring-shaped lanes. PDMS stamps were treated with UV light (PSD-UV, novascan) for 5 min. Then the stamps were incubated for 45 min in a solution containing 40 µg/ml fibronectin (Yo proteins) and 10 µg/ml fibronectin labeled with Alexa Fluor 647 (Alexa Fluor NHS Ester, Thermo Fisher Scientific) dissolved in ultrapure water. Next, stamps were washed with ultrapure water, dried and placed on a petri dish (µ-Dish, Ibidi) which had been activated with UV light for 15 min. A droplet of a 2 mg/ml poly-L-lysine-grafted polyethylene glycol (PLL-PEG) (2 kDa PEG chains, SuSoS) solution (dissolved in a solution of 10 mM HEPES and 150 mM NaCl was placed at the edge of the stamps and drawn into the spaces between surface and stamp by capillary action. Stamps were removed and a glass coverslip was placed on the dish surface to ensure complete coverage of the surface with PEG solution. After a 30-min incubation, the coverslip was removed, and the surface was washed three times with phosphate-buffered saline (PBS) and stored in PBS until cells were seeded.

Cell Culture

MDA-MB-231 breast cancer cells were cultured in L15 medium (sigma aldrich) containing 10% TET system approved fetal calf serum (FCS) (Clontech). Cells were incubated at 37°C in a humidified atmosphere. For cell motility measurements, cells were cultured in medium containing 0 or 5 µg/ml Doxycycline for 44h. Then, about 10,000 cells were seeded per dish (µ-Dish, Ibidi). After 3 h, cell medium was replaced

with fresh medium containing 25 nM Hoechst 33342 dye (Invitrogen) and measurements were started within 1 hour.

Time-Lapse Microscopy

Scanning time-lapse measurements were performed using an automated inverted microscope (Nikon Ti) equipped with a 10x objective, a LED lamp (Spectra X, lumencor) and a sCMOS camera (pco.edge 4.2, pco). Cells were maintained at 37°C and a humidified atmosphere using a heating chamber (okolab). Phase-contrast and fluorescent images were automatically acquired every 10 min.

Cell Tracking

Cell tracking was performed using the image-processing software ImageJ. Isolated cells confined in the ring-shaped lanes were identified by eye. Fluorescence images of the nuclei were preprocessed by applying a bandpass filter and a threshold for fluorescence intensity, and the centers of mass of the stained nuclei were identified. Cell tracking was stopped in the case of cell division or when cells spanned over the middle part of the ring pattern. Cell tracks shorter than 20 h, as well as tracks of dying or non-moving cells were excluded from further analysis.

Data Analysis

Two-state analysis of tracks:

Track analysis was performed in MATLAB (Mathworks). A circle was fitted to cell position data to find the center of the ring-shaped lane. Switching to polar coordinates, the tangential component of the cell velocity was evaluated as), where indicates the azimuthal cell position at time *i* and *R* indicates the mean radius of the micropattern (*R* = 65 µm). To distinguish run from rest states, a iterative change-point analysis in combination with a classification of cell dynamics in the time intervals between change-points was applied. Change-points were identified when they exceeded a confidence level for the existence of change-points that was calculated via bootstrap analysis of the cumulative sum of the angular velocity. For all intervals between change points this was repeated until no more change-points were found. The resulting intervals were classified into run and rest states by analyzing the mean square displacement. Details are published in Schreiber et al.[cite]

The run velocity is defined as the mean over the tangential velocity for time points when cells are in the run state .

To evaluate the persistence times of run and rest states and the survival function is calculated. and are determined by fitting by the function evaluated at . Very small

times are excluded because deviations from an exponential behavior are observed here. To reduce the effects of the limited time window, only states that start at least 16 h before the end of the corresponding cell track are evaluated, while the fitting range for ends at 16 h. The error range given is the 99% confidence interval for the fit.

The fraction of time cells spend in the run state is defined as the time cells are in the run state divided by the total time of the trajectories.

q: The persistence parameter q is defined as the maximum distance between two points of a cell trajectory divided by the total path length of the trajectory. This is averaged over all cells

4.6.2. Supplemental figures

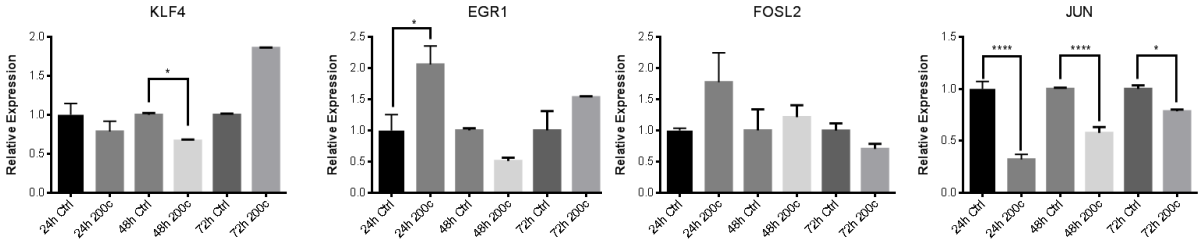

Supplement S 9

Analysis of different potential transcription factors for FLNA was performed after miR-200c induction. The graphs show the RT-qPCR results at different time points, with no consistent effect for any factor but JUN

4.6.3. Supplemental movies

The supplemental movies be viewed at in the online version of the publication or on https://www.cup.lmu.de/pb/aks/ewagner/projects/

5. Summary

In this work, novel functions of the two prominent miRNAs, miR-200c and miR-27a were unraveled.

In the first part, our findings in *chapter 2* revealed a novel role of the oncomir miR-27a in breast cancer. In the current literature, a high expression of miR-27a indicated more aggressive and metastatic tumors[157]. This is inline with the retrospective analysis shown in *chapter 2.3.4*. Still, in our analysis, by taking clinical settings into account, as well as molecular properties of the tumor cells (e.g. the receptor status), we uncovered a novel and ambivalent role of miR-27a as prognostic tumor marker.

The high expression of this oncomiR showed to be beneficial for a certain, miR-27a high expressing subgroup of estrogen receptor positive patients – but only if they underwent endocrine treatments. Or, conversely stated, patients with estrogen receptor positive phenotypes but low tumoral miR-27a levels, may not receive an optimal treatment with regular endocrine therapies. Although a therapeutic use of miR-27a would most likely not meet a favorable risk-benefit profile, the analysis of the miR-27a expression status could support the treating physician in the selection of a better and thus personalized therapies.

The second part of this work is focusing on miR-200c in breast cancer, which is one of the most important tumor suppressing miRNAs. Most previous studies were based on the artificial overexpression of the miRNA or on *in vivo* correlations. Therefore, it is possible that the unnatural surplus of this miRNA, acting as inhibitor, could lead to observations that are not relevant in the regular biological setting, as also discussed in *chapter 3.4*. Thus, a removal of miR-200c of an otherwise unmodified cellular breast cancer cell system, was chosen to illuminate another perspective, revealing novel roles and validating previous findings. For this reason, genomic knock-outs of miR-200c were conducted in the miR-200c high expressing MCF7 breast cancer cell line and were followed by a comprehensive proteomic screen, as described in *chapter 3*. With this means, a group of novel putative miR-200c targets were found. Interestingly, a major proportion of these potential target proteins did not contain any miR-200c binding sites, indicating that the effects were based on indirect mechanisms, like subtle changes in pathways upstream of the found proteins.

Consequently, the role of miR-200c in the regulation of one of these targets, the important cytoskeletal protein filamin A, was investigated in *chapter 4*. MiR-200c is known to inhibit progression of EMT by targeting ZEB1/2, resulting in an increase of

E-cadherin expression and therefore impede the transition. By our choice of appropriate cell models for these experiments, this particular mode of influence was excluded due to genetic predisposition of the cell lines, each respectively not expressing one of those key proteins. Thus, additionally to the “loss of function” knock-out model, an inducible overexpression of miR-200c was generated in an elsewise miR-200c-null cell line. Experiments conducted with these cell line models showed a strong effect of miR-200c induction on the migration of the cell lines, as well as a distinctive cellular remodeling after long-term induction of the miRNA. Filamin A was regarded as a potential key protein in those processes and a regulatory pathway of miR-200c on filamin A was indicated, based on targeting the transcriptional regulators JUN and SRF.

These novel regulatory networks that are indicated, may indicate the potential impact of miR-200c in a broad variety of breast cancer cells. All in all, contrary to miR-27a, miR-200c could have the potential to act as tumor suppressing agent.

Our studies altogether showed the potential of miRNAs as therapeutics and biomarkers, enabling physicians to better determine the characteristics of the tumor.

MiRNA signatures of breast cancer patients could be routinely measured in clinical practice, and miR-27a could be one important indicator in helping to choose the most promising therapeutic regimes.

For tumor suppressing miRNAs like miR-200c, one promising route of miRNA (or siRNA) delivery may lay in mimicking this intrinsic trafficking, by packaging miRNAs in artificial exosomes, in poly- or lipoplex formulations [158] or in future applications “reprogramming” of patient-derived exosomes[159,160].

Therefore, even more than 25 years after the discovery [1], miRNA research remains a field of high interest and ever rising clinical relevance. Due to standardized, fast and cheap genomic screening technologies, the utilization of clinical miRNA screenings for tumor classification and thus improved and personalized treatments are as close as never before, and miR-27a and miR-200c may hold an important role in the future.

6. Appendix

6.1. Abbreviations

AGO	Argonaute
ATCC	American Type Culture Collection
CDNA	Complementary DNA
CT	Cycle of threshold
DAPI	4',6-diamidino-2-phenylindole
DAVID	Database for Annotation, Visualization and Integrated Discovery
DMSO	Dimethyl sulfoxide
DNA	Deoxyribonucleic acid
DOX	Doxycycline
DXR	Doxorubicin
EDTA	Ethylenediamine tetraacetic acid
ELISA	Enzyme linked immunosorbent assay
EMT	Epithelial-mesenchymal transition
ENDO	Endoxifen
ER +/-	Estrogen receptor positive / negative
FCS	Fetal calf serum
FDR	False discovery rate
FUL	Fulvestrant
HSA	Homo sapiens
HR +/-	Hormone receptor positive / negative
IF	Immunofluorescence
IHC	Immunohistochemistry
KEGG	Kyoto Encyclopedia of Genes and Genomes
KO	Knock-out
LNA	Locked nucleic acid
LSM	Laser scanning microscopy
MET	Mesenchymal-epithelial transition

MIRNA	MicroRNA
MMU	Mus musculus
MRNA	MessengerRNA
MTT	3-(4,5-dimethylthiazol-2-yl)-2,5-diphenyltetrazolium bromide
NET	Buffer containing NaCl, EDTA and Tris-HCl
PBS	Phosphate buffered saline
POLYA	Polyadenylation
RISC	RNA-induced silencing complex
RLUC	Renilla luciferase reporter plasmid
RNA	Ribonucleic acid
RNAI	RNA interference
RT-PCR	Reverse transcription - polymerase chain reaction
SD	Standard deviation
SDS	Sodium dodecyl sulfate
SDS-PAGE	Sodium dodecyl sulfate - polyacrylamide gel
SEM	Standard error of the mean
SIRNA	Small interfering RNA
SLP	Stem loop primer
TAM	Tamoxifen
TOR	Toremifen
TRISHCL	Tris(hydroxymethyl)aminomethane hydrochloride
UTR	Untranslated region
W:W	Weight to weight ratio
WB	Western blot

6.2. Genes and proteins

AGR2	Anterior gradient protein 2 homolog
AKT	Protein kinase B (PKB)
ALDH7A1	Alpha-aminoadipic semialdehyde dehydrogenase
BCL2	B-cell lymphoma 2
BMI1	Polycomb ring finger oncogene
CA2	Carbonic anhydrase 2
CDK4/6	Cyclin-dependent kinase 4/6
CTTN;EMS1	Src substrate cortactin
DGCR8	Di George syndrome critical region 8 (= Pasha in *D. melanogaster*)
E2F1	Transcription factor E2F1
EGFP	Enhanced green fluorescent protein
EGFR	Epidermal growth factor receptor
ERBB	Epidermal growth factor receptor family
ESR1	Estrogen receptor alpha
FN1	Fibronectin
GAPDH	Glyceraldehyde 3-phosphate dehydrogenase
GOT2	Aspartate aminotransferase
GSTM3	Glutathione S-transferase Mu 3
HER2	Human epidermal growth factor receptor 2
HSP90AA1	Heat shock protein HSP 90-alpha
JUN	Jun proto-oncogene
KRAS	Kirsten rat sarcoma viral oncogene homolog
KYNU	Kynureninase
LIN-14	Protein lin-14 (*C. elegans*)
LIN-4	MicroRNA lin-4 (*C. elegans*)
MAPK	Mitogen-activated protein kinases
MCM4	DNA replication licensing factor MCM4
MEKK1	Mitogen-activated protein kinase kinase kinase 1
MSN	Moesin

MYC	V-myc avian myelocytomatosis viral oncogene homolog
NFKB	Protein complex, nuclear factor kappa-light-chain-enhancer
P53	Tumor protein p53
PHGDH	D-3-phosphoglycerate dehydrogenase
PI3K	Phosphatidylinositide 3-kinases
PKC	Protein kinase C
POL II	RNA polymerase II
PPM1F	Protein phosphatase 1F
PTEN	Phosphatase and tensin homolog
RAB14	Ras-related protein Rab-14
SH3BGRL	SH3 domain-binding glutamic acid-rich-like protein
SLC3A2	4F2 cell-surface antigen heavy chain
SRF	Serum response factor (c-fos serum response element-binding
TNFA	Tumor necrosis factor alpha
TPI1	Triosephosphate isomerase
TRBP	Transactivation response element RNA-binding protein
TPM1	Tropomyosin alpha-1 chain
TRKB	Neurotrophic tyrosine kinase, receptor, type 2 (NTRK2)
TUBB3	Tubulin, beta 3 class III
UGDH	UDP-glucose 6-dehydrogenase
WARS	Tryptophan-tRNA ligase
WNT	Wingless-type MMTV integration site family
ZEB1/2	Zinc finger E-box binding homeobox 1/2 (TCF8/SIP1)

7. References and indices

7.1. Literature

1 Lee, R. C., Feinbaum, R. L. & Ambros, V. The C. elegans heterochronic gene lin-4 encodes small RNAs with antisense complementarity to lin-14. *Cell* **75**, 843-854 (1993).

2 Lee, R. C. & Ambros, V. An extensive class of small RNAs in Caenorhabditis elegans. *Science* **294**, 862-864, doi:10.1126/science.1065329 (2001).

3 Bartel, D. P. MicroRNAs: genomics, biogenesis, mechanism, and function. *Cell* **116**, 281-297 (2004).

4 Gebert, L. F. R. & MacRae, I. J. Regulation of microRNA function in animals. *Nature reviews. Molecular cell biology* **20**, 21-37, doi:10.1038/s41580-018-0045-7 (2019).

5 Lodish, H. F., Zhou, B., Liu, G. & Chen, C. Z. Micromanagement of the immune system by microRNAs. *Nat Rev Immunol* **8**, 120-130, doi:10.1038/nri2252 (2008).

6 Peter, M. E. Targeting of mRNAs by multiple miRNAs: the next step. *Oncogene* **29**, 2161-2164, doi:10.1038/onc.2010.59 (2010).

7 Elefant, N., Altuvia, Y. & Margalit, H. A wide repertoire of miRNA binding sites: prediction and functional implications. *Bioinformatics* **27**, 3093-3101, doi:10.1093/bioinformatics/btr534 (2011).

8 Ferlay, J. *et al.* Cancer incidence and mortality worldwide: sources, methods and major patterns in GLOBOCAN 2012. *Int J Cancer* **136**, E359-386, doi:10.1002/ijc.29210 (2015).

9 American Cancer Society. v. (The Society, Atlanta, Ga.).

10 O'Bryan, S., Dong, S., Mathis, J. M. & Alahari, S. K. The roles of oncogenic miRNAs and their therapeutic importance in breast cancer. *European journal of cancer* **72**, 1-11, doi:10.1016/j.ejca.2016.11.004 (2017).

11 Teoh, S. L. & Das, S. The Role of MicroRNAs in Diagnosis, Prognosis, Metastasis and Resistant Cases in Breast Cancer. *Curr Pharm Des* **23**, 1845-1859, doi:10.2174/1381612822666161027120043 (2017).

12 Blows, F. M. *et al.* Subtyping of breast cancer by immunohistochemistry to investigate a relationship between subtype and short and long term survival: a collaborative analysis of data for 10,159 cases from 12 studies. *PLoS Med* **7**, e1000279, doi:10.1371/journal.pmed.1000279 (2010).

13 Senkus, E. *et al.* Primary breast cancer: ESMO Clinical Practice Guidelines for diagnosis, treatment and follow-up. *Annals of oncology : official journal of the European Society for Medical Oncology / ESMO* **26 Suppl 5**, v8-30, doi:10.1093/annonc/mdv298 (2015).

14 Svoronos, A. A., Engelman, D. M. & Slack, F. J. OncomiR or Tumor Suppressor? The Duplicity of MicroRNAs in Cancer. *Cancer research* **76**, 3666-3670, doi:10.1158/0008-5472.CAN-16-0359 (2016).

15 Lin, S. & Gregory, R. I. MicroRNA biogenesis pathways in cancer. *Nat Rev Cancer* **15**, 321-333, doi:10.1038/nrc3932 (2015).

16 Kim, S. Y. *et al.* miR-27a is a negative regulator of adipocyte differentiation via suppressing PPARgamma expression. *Biochemical and biophysical research communications* **392**, 323-328, doi:10.1016/j.bbrc.2010.01.012 (2010).

17 Alvarez, M. L., Khosroheidari, M., Eddy, E. & Done, S. C. MicroRNA-27a decreases the level and efficiency of the LDL receptor and contributes to the dysregulation of cholesterol homeostasis. *Atherosclerosis* **242**, 595-604, doi:10.1016/j.atherosclerosis.2015.08.023 (2015).

18 Sala Frigerio, C. *et al.* Reduced expression of hsa-miR-27a-3p in CSF of patients with Alzheimer disease. *Neurology* **81**, 2103-2106, doi:10.1212/01.wnl.0000437306.37850.22 (2013).

19 Chen, X., Huang, Z., Chen, D., Yang, T. & Liu, G. Role of microRNA-27a in myoblast differentiation. *Cell biology international* **38**, 266-271, doi:10.1002/cbin.10192 (2014).

20 Tang, W. *et al.* miR-27a regulates endothelial differentiation of breast cancer stem like cells. *Oncogene* **33**, 2629-2638, doi:10.1038/onc.2013.214 (2014).

21 Vimalraj, S., Miranda, P. J., Ramyakrishna, B. & Selvamurugan, N. Regulation of breast cancer and bone metastasis by microRNAs. *Disease markers* **35**, 369-387, doi:10.1155/2013/451248 (2013).

22 Pan, W., Wang, H., Jianwei, R. & Ye, Z. MicroRNA-27a promotes proliferation, migration and invasion by targeting MAP2K4 in human osteosarcoma cells. *Cellular physiology and biochemistry : international journal of experimental cellular physiology, biochemistry, and pharmacology* **33**, 402-412, doi:10.1159/000356679 (2014).

23 Ba, S., Xuan, Y., Long, Z. W., Chen, H. Y. & Zheng, S. S. MicroRNA-27a Promotes the Proliferation and Invasiveness of Colon Cancer Cells by Targeting SFRP1 through the Wnt/beta-Catenin Signaling Pathway. *Cellular physiology and biochemistry : international journal of experimental cellular physiology, biochemistry, and pharmacology* **42**, 1920-1933, doi:10.1159/000479610 (2017).

24 Chae, D. K. *et al.* MIR-27a regulates the TGF-beta signaling pathway by targeting SMAD2 and SMAD4 in lung cancer. *Mol Carcinog* **56**, 1992-1998, doi:10.1002/mc.22655 (2017).

25 Ljepoja, B., Garcia-Roman, J., Sommer, A. K., Wagner, E. & Roidl, A. MiRNA-27a sensitizes breast cancer cells to treatment with Selective Estrogen Receptor Modulators. *Breast* **43**, 31-38, doi:10.1016/j.breast.2018.10.007 (2019).

26 Mutlu, M. *et al.* miR-200c: a versatile watchdog in cancer progression, EMT, and drug resistance. *J Mol Med (Berl)*, doi:10.1007/s00109-016-1420-5 (2016).

27 Kopp, F., Oak, P. S., Wagner, E. & Roidl, A. miR-200c sensitizes breast cancer cells to doxorubicin treatment by decreasing TrkB and Bmi1 expression. *PloS one* **7**, e50469, doi:10.1371/journal.pone.0050469 (2012).

28 Kopp, F., Wagner, E. & Roidl, A. The proto-oncogene KRAS is targeted by miR-200c. *Oncotarget* **5**, 185-195 (2014).

29 Boettcher, M. & McManus, M. T. Choosing the Right Tool for the Job: RNAi, TALEN, or CRISPR. *Mol Cell* **58**, 575-585, doi:10.1016/j.molcel.2015.04.028 (2015).

30 Joung, J. K. & Sander, J. D. TALENs: a widely applicable technology for targeted genome editing. *Nature reviews. Molecular cell biology* **14**, 49-55, doi:10.1038/nrm3486 (2013).

31 Davies, C. *et al.* Long-term effects of continuing adjuvant tamoxifen to 10 years versus stopping at 5 years after diagnosis of oestrogen receptor-positive breast cancer: ATLAS, a randomised trial. *Lancet* **381**, 805-816, doi:10.1016/S0140-6736(12)61963-1 (2013).

32 Ring, A. & Dowsett, M. Mechanisms of tamoxifen resistance. *Endocr Relat Cancer* **11**, 643-658, doi:10.1677/erc.1.00776 (2004).

33 Burstein, H. J. *et al.* Adjuvant endocrine therapy for women with hormone receptor-positive breast cancer: american society of clinical oncology clinical practice guideline focused update. *J Clin Oncol* **32**, 2255-2269, doi:10.1200/JCO.2013.54.2258 (2014).

34 Guo, Y. *et al.* Prognostic and clinicopathological value of GATA binding protein 3 in breast cancer: A systematic review and meta-analysis. *PloS one* **12**, e0174843, doi:10.1371/journal.pone.0174843 (2017).

35 Curtis, C. *et al.* The genomic and transcriptomic architecture of 2,000 breast tumours reveals novel subgroups. *Nature* **486**, 346-352, doi:10.1038/nature10983 (2012).

36 Takaku, M. *et al.* GATA3 zinc finger 2 mutations reprogram the breast cancer transcriptional network. *Nat Commun* **9**, 1059, doi:10.1038/s41467-018-03478-4 (2018).

37 Oualla, K. *et al.* Novel therapeutic strategies in the treatment of triple-negative breast cancer. *Ther Adv Med Oncol* **9**, 493-511, doi:10.1177/1758834017711380 (2017).

38 Early Breast Cancer Trialists' Collaborative, G. *et al.* Relevance of breast cancer hormone receptors and other factors to the efficacy of adjuvant tamoxifen: patient-level meta-analysis of randomised trials. *Lancet* **378**, 771-784, doi:10.1016/S0140-6736(11)60993-8 (2011).

39 Hamam, R. *et al.* Circulating microRNAs in breast cancer: novel diagnostic and prognostic biomarkers. *Cell Death Dis* **8**, e3045, doi:10.1038/cddis.2017.440 (2017).

40 Tang, W. *et al.* MiR-27 as a prognostic marker for breast cancer progression and patient survival. *PloS one* **7**, e51702, doi:10.1371/journal.pone.0051702 (2012).

41 Quan, J. *et al.* MicroRNA-23a/24-2/27a as a potential diagnostic biomarker for cancer: A systematic review and meta-analysis. *Mol Clin Oncol* **8**, 159-169, doi:10.3892/mco.2017.1492 (2018).

42 Li, X. *et al.* MicroRNA-27a Indirectly Regulates Estrogen Receptor {alpha} Expression and Hormone Responsiveness in MCF-7 Breast Cancer Cells. *Endocrinology* **151**, 2462-2473, doi:10.1210/en.2009-1150 (2010).

43 Sommer, A. K. *et al.* Salinomycin co-treatment enhances tamoxifen cytotoxicity in luminal A breast tumor cells by facilitating lysosomal degradation of receptor tyrosine kinases. *Oncotarget* **7**, 50461-50476, doi:10.18632/oncotarget.10459 (2016).

44 Flach, K. D. & Zwart, W. The first decade of estrogen receptor cistromics in breast cancer. *J Endocrinol* **229**, R43-56, doi:10.1530/JOE-16-0003 (2016).

45 Welboren, W. J., Sweep, F. C., Span, P. N. & Stunnenberg, H. G. Genomic actions of estrogen receptor alpha: what are the targets and how are they regulated? *Endocr Relat Cancer* **16**, 1073-1089, doi:10.1677/ERC-09-0086 (2009).

46 Lanczky, A. *et al.* miRpower: a web-tool to validate survival-associated miRNAs utilizing expression data from 2178 breast cancer patients. *Breast Cancer Res Treat* **160**, 439-446, doi:10.1007/s10549-016-4013-7 (2016).

47 Antonov, A. V., Knight, R. A., Melino, G., Barlev, N. A. & Tsvetkov, P. O. MIRUMIR: an online tool to test microRNAs as biomarkers to predict survival in cancer using multiple clinical data sets. *Cell death and differentiation* **20**, 367, doi:10.1038/cdd.2012.137 (2013).

48 Dowsett, M. *et al.* Meta-analysis of breast cancer outcomes in adjuvant trials of aromatase inhibitors versus tamoxifen. *J Clin Oncol* **28**, 509-518, doi:10.1200/JCO.2009.23.1274 (2010).

49 Katase, K., Sugiyama, Y., Hasumi, K., Yoshimoto, M. & Kasumi, F. The incidence of subsequent endometrial carcinoma with tamoxifen use in patients with primary breast carcinoma. *Cancer* **82**, 1698-1703 (1998).

50 Zhou, S. *et al.* miR-27a regulates the sensitivity of breast cancer cells to cisplatin treatment via BAK-SMAC/DIABLO-XIAP axis. *Tumour Biol* **37**, 6837-6845, doi:10.1007/s13277-015-4500-1 (2016).

51 Bekele, R. T. *et al.* Oxidative stress contributes to the tamoxifen-induced killing of breast cancer cells: implications for tamoxifen therapy and resistance. *Sci Rep* **6**, 21164, doi:10.1038/srep21164 (2016).

52 Liu, Z., Shi, H. Y., Nawaz, Z. & Zhang, M. Tamoxifen induces the expression of maspin through estrogen receptor-alpha. *Cancer Lett* **209**, 55-65, doi:10.1016/j.canlet.2003.11.018 (2004).

53 Klinge, C. M. Estrogen Regulation of MicroRNA Expression. *Curr Genomics* **10**, 169-183, doi:10.2174/138920209788185289 (2009).

54 Frasor, J. *et al.* Profiling of estrogen up- and down-regulated gene expression in human breast cancer cells: insights into gene networks and pathways underlying estrogenic control of proliferation and cell phenotype. *Endocrinology* **144**, 4562-4574, doi:10.1210/en.2003-0567 (2003).

55 Ye, P. *et al.* Differential microRNA expression profiles in tamoxifen-resistant human breast cancer cell lines induced by two methods. *Oncol Lett* **15**, 3532-3539, doi:10.3892/ol.2018.7768 (2018).

56 Viedma-Rodriguez, R. *et al.* Mechanisms associated with resistance to tamoxifen in estrogen receptor-positive breast cancer (review). *Oncol Rep* **32**, 3-15, doi:10.3892/or.2014.3190 (2014).

57 Parl, F. F. Multiple mechanisms of estrogen receptor gene repression contribute to ER-negative breast cancer. *Pharmacogenomics J* **3**, 251-253, doi:10.1038/sj.tpj.6500201 (2003).

58 Mahfoudi, A., Roulet, E., Dauvois, S., Parker, M. G. & Wahli, W. Specific mutations in the estrogen receptor change the properties of antiestrogens to full agonists. *Proc Natl Acad Sci U S A* **92**, 4206-4210 (1995).

59 Jurkovicova, D. *et al.* Down-regulation of traditional oncomiRs in plasma of breast cancer patients. *Oncotarget* **8**, 77369-77384, doi:10.18632/oncotarget.20484 (2017).

60 Kopp, F. *et al.* Salinomycin treatment reduces metastatic tumor burden by hampering cancer cell migration. *Mol Cancer* **13**, 16, doi:10.1186/1476-4598-13-16 (2014).

61 Broos, S. *et al.* PhysBinder: Improving the prediction of transcription factor binding sites by flexible inclusion of biophysical properties. *Nucleic Acids Res* **41**, W531-534, doi:10.1093/nar/gkt288 (2013).

62 Gruber, C. J., Gruber, D. M., Gruber, I. M., Wieser, F. & Huber, J. C. Anatomy of the estrogen response element. *Trends Endocrinol Metab* **15**, 73-78, doi:10.1016/j.tem.2004.01.008 (2004).

63 Brodersen, P. & Voinnet, O. Revisiting the principles of microRNA target recognition and mode of action. *Nature reviews. Molecular cell biology* **10**, 141-148, doi:10.1038/nrm2619 (2009).

64 Wightman, B., Ha, I. & Ruvkun, G. Posttranscriptional regulation of the heterochronic gene lin-14 by lin-4 mediates temporal pattern formation in C. elegans. *Cell* **75**, 855-862 (1993).

65 Baumjohann, D. & Ansel, K. M. MicroRNA-mediated regulation of T helper cell differentiation and plasticity. *Nature reviews. Immunology* **13**, 666-678, doi:10.1038/nri3494 (2013).

66 Gangaraju, V. K. & Lin, H. MicroRNAs: key regulators of stem cells. *Nature reviews. Molecular cell biology* **10**, 116-125, doi:10.1038/nrm2621 (2009).

67 Rottiers, V. & Naar, A. M. MicroRNAs in metabolism and metabolic disorders. *Nature reviews. Molecular cell biology* **13**, 239-250, doi:10.1038/nrm3313 (2012).

68 Small, E. M. & Olson, E. N. Pervasive roles of microRNAs in cardiovascular biology. *Nature* **469**, 336-342, doi:10.1038/nature09783 (2011).

69 Ameres, S. L. & Zamore, P. D. Diversifying microRNA sequence and function. *Nature reviews. Molecular cell biology* **14**, 475-488, doi:10.1038/nrm3611 (2013).

70 Filios, S. R. & Shalev, A. beta-Cell MicroRNAs: Small but Powerful. *Diabetes* **64**, 3631-3644, doi:10.2337/db15-0831 (2015).

71 Cortez, M. A. *et al.* MicroRNAs in body fluids--the mix of hormones and biomarkers. *Nature reviews. Clinical oncology* **8**, 467-477, doi:10.1038/nrclinonc.2011.76 (2011).

72 Humphries, B. & Yang, C. The microRNA-200 family: small molecules with novel roles in cancer development, progression and therapy. *Oncotarget* **6**, 6472-6498, doi:10.18632/oncotarget.3052 (2015).

73 Muralidhar, G. G. & Barbolina, M. V. The miR-200 Family: Versatile Players in Epithelial Ovarian Cancer. *International journal of molecular sciences* **16**, 16833-16847, doi:10.3390/ijms160816833 (2015).

74 Perdigao-Henriques, R. *et al.* miR-200 promotes the mesenchymal to epithelial transition by suppressing multiple members of the Zeb2 and Snail1 transcriptional repressor complexes. *Oncogene* **35**, 158-172, doi:10.1038/onc.2015.69 (2016).

75 Dykxhoorn, D. M. *et al.* miR-200 enhances mouse breast cancer cell colonization to form distant metastases. *PloS one* **4**, e7181, doi:10.1371/journal.pone.0007181 (2009).

76 Le, M. T. *et al.* miR-200-containing extracellular vesicles promote breast cancer cell metastasis. *The Journal of clinical investigation* **124**, 5109-5128, doi:10.1172/JCI75695 (2014).

77 Kumar, S., Nag, A. & Mandal, C. C. A Comprehensive Review on miR-200c, A Promising Cancer Biomarker with Therapeutic Potential. *Current drug targets* **16**, 1381-1403 (2015).

78 Hamano, R. *et al.* Overexpression of miR-200c induces chemoresistance in esophageal cancers mediated through activation of the Akt signaling pathway. *Clinical cancer research : an official journal of the American Association for Cancer Research* **17**, 3029-3038, doi:10.1158/1078-0432.CCR-10-2532 (2011).

79 Huang, H. N. *et al.* miR-200c and GATA binding protein 4 regulate human embryonic stem cell renewal and differentiation. *Stem cell research* **12**, 338-353, doi:10.1016/j.scr.2013.11.009 (2014).

80 Liu, S. *et al.* miR-200c/Bmi1 axis and epithelial-mesenchymal transition contribute to acquired resistance to BRAF inhibitor treatment. *Pigment cell & melanoma research* **28**, 431-441, doi:10.1111/pcmr.12379 (2015).

81 Chang, I. *et al.* Loss of miR-200c up-regulates CYP1B1 and confers docetaxel resistance in renal cell carcinoma. *Oncotarget* **6**, 7774-7787, doi:10.18632/oncotarget.3484 (2015).

82 Chang, J. T., Wang, F., Chapin, W. & Huang, R. S. Identification of MicroRNAs as Breast Cancer Prognosis Markers through the Cancer Genome Atlas. *PloS one* **11**, e0168284, doi:10.1371/journal.pone.0168284 (2016).

83 Markou, A. *et al.* Direct Comparison of Metastasis-Related miRNAs Expression Levels in Circulating Tumor Cells, Corresponding Plasma, and Primary Tumors of Breast Cancer Patients. *Clin Chem* **62**, 1002-1011, doi:10.1373/clinchem.2015.253716 (2016).

84 Zhang, F., Wen, Y. & Guo, X. CRISPR/Cas9 for genome editing: progress, implications and challenges. *Hum Mol Genet* **23**, R40-46, doi:10.1093/hmg/ddu125 (2014).

85 Zu, Y. *et al.* TALEN-mediated precise genome modification by homologous recombination in zebrafish. *Nat Methods* **10**, 329-331, doi:10.1038/nmeth.2374 (2013).

86 Hsu, P. D., Lander, E. S. & Zhang, F. Development and applications of CRISPR-Cas9 for genome engineering. *Cell* **157**, 1262-1278, doi:10.1016/j.cell.2014.05.010 (2014).

87 Ran, F. A. *et al.* Double nicking by RNA-guided CRISPR Cas9 for enhanced genome editing specificity. *Cell* **154**, 1380-1389, doi:10.1016/j.cell.2013.08.021 (2013).

88 Kim, Y. K. *et al.* TALEN-based knockout library for human microRNAs. *Nature structural & molecular biology* **20**, 1458-1464, doi:10.1038/nsmb.2701 (2013).

89 UniProt, C. UniProt: a hub for protein information. *Nucleic Acids Res* **43**, D204-212, doi:10.1093/nar/gku989 (2015).

90 Huang da, W., Sherman, B. T. & Lempicki, R. A. Systematic and integrative analysis of large gene lists using DAVID bioinformatics resources. *Nat Protoc* **4**, 44-57, doi:10.1038/nprot.2008.211 (2009).

91 Huang da, W., Sherman, B. T. & Lempicki, R. A. Bioinformatics enrichment tools: paths toward the comprehensive functional analysis of large gene lists. *Nucleic Acids Res* **37**, 1-13, doi:10.1093/nar/gkn923 (2009).

92 Senfter, D., Madlener, S., Krupitza, G. & Mader, R. M. The microRNA-200 family: still much to discover. *Biomol Concepts* **7**, 311-319, doi:10.1515/bmc-2016-0020 (2016).

93 Pecot, C. V. *et al.* Tumour angiogenesis regulation by the miR-200 family. *Nat Commun* **4**, 2427, doi:10.1038/ncomms3427 (2013).

94 Slaymaker, I. M. *et al.* Rationally engineered Cas9 nucleases with improved specificity. *Science* **351**, 84-88, doi:10.1126/science.aad5227 (2016).

95 Reardon, S. Leukaemia success heralds wave of gene-editing therapies. *Nature* **527**, 146-147, doi:10.1038/nature.2015.18737 (2015).

96 Rossi, A. *et al.* Genetic compensation induced by deleterious mutations but not gene knockdowns. *Nature* **524**, 230-233, doi:10.1038/nature14580 (2015).

97 Chen, B. *et al.* Disruption of microRNA-21 by TALEN leads to diminished cell transformation and increased expression of cell-environment interaction genes. *Cancer Lett* **356**, 506-516, doi:10.1016/j.canlet.2014.09.034 (2015).

98 Jeong, G., Lim, Y. H., Kim, N. J., Wee, G. & Kim, Y. K. Knockout of miR-221 and miR-222 reveals common and specific targets for paralogous miRNAs. *RNA Biol*, 1-9, doi:10.1080/15476286.2016.1269994 (2016).

99 Gregory, P. A. *et al.* The miR-200 family and miR-205 regulate epithelial to mesenchymal transition by targeting ZEB1 and SIP1. *Nature cell biology* **10**, 593-601, doi:10.1038/ncb1722 (2008).

100 Howe, E. N., Cochrane, D. R. & Richer, J. K. Targets of miR-200c mediate suppression of cell motility and anoikis resistance. *Breast Cancer Res* **13**, R45, doi:10.1186/bcr2867 (2011).

101 Sinh, N. D., Endo, K., Miyazawa, K. & Saitoh, M. Ets1 and ESE1 reciprocally regulate expression of ZEB1/ZEB2, dependent on ERK1/2 activity, in breast cancer cells. *Cancer Sci* **108**, 952-960, doi:10.1111/cas.13214 (2017).

102 Chaffer, C. L. *et al.* Poised chromatin at the ZEB1 promoter enables breast cancer cell plasticity and enhances tumorigenicity. *Cell* **154**, 61-74, doi:10.1016/j.cell.2013.06.005 (2013).

103 Jurmeister, S. *et al.* MicroRNA-200c represses migration and invasion of breast cancer cells by targeting actin-regulatory proteins FHOD1 and PPM1F. *Mol Cell Biol* **32**, 633-651, doi:10.1128/MCB.06212-11 (2012).

104 Damiano, V. *et al.* Epigenetic silencing of miR-200c in breast cancer is associated with aggressiveness and is modulated by ZEB1. *Genes Chromosomes Cancer* **56**, 147-158, doi:10.1002/gcc.22422 (2017).

105 Zhou, A. X. *et al.* Filamin a mediates HGF/c-MET signaling in tumor cell migration. *Int J Cancer* **128**, 839-846, doi:10.1002/ijc.25417 (2011).

106 Zhong, Z. *et al.* Cyclin D1/cyclin-dependent kinase 4 interacts with filamin A and affects the migration and invasion potential of breast cancer cells. *Cancer Res* **70**, 2105-2114, doi:10.1158/0008-5472.CAN-08-1108 (2010).

107 Zhao, P. *et al.* Filamin A (FLNA) modulates chemosensitivity to docetaxel in triple-negative breast cancer through the MAPK/ERK pathway. *Tumour Biol* **37**, 5107-5115, doi:10.1007/s13277-015-4357-3 (2016).

108 Brychtova, V., Mohtar, A., Vojtesek, B. & Hupp, T. R. Mechanisms of anterior gradient-2 regulation and function in cancer. *Semin Cancer Biol* **33**, 16-24, doi:10.1016/j.semcancer.2015.04.005 (2015).

109 Hrstka, R. *et al.* The pro-metastatic protein anterior gradient-2 predicts poor prognosis in tamoxifen-treated breast cancers. *Oncogene* **29**, 4838-4847, doi:10.1038/onc.2010.228 (2010).

110 Gray, T. A., Alsamman, K., Murray, E., Sims, A. H. & Hupp, T. R. Engineering a synthetic cell panel to identify signalling components reprogrammed by the cell growth regulator anterior gradient-2. *Mol Biosyst* **10**, 1409-1425, doi:10.1039/c4mb00113c (2014).

111 Vitello, E. A. *et al.* Cancer-secreted AGR2 induces programmed cell death in normal cells. *Oncotarget* **7**, 49425-49434, doi:10.18632/oncotarget.9921 (2016).

112 Hayes, J. D., Flanagan, J. U. & Jowsey, I. R. Glutathione transferases. *Annu Rev Pharmacol Toxicol* **45**, 51-88, doi:10.1146/annurev.pharmtox.45.120403.095857 (2005).

113 Li, S. *et al.* Overcoming resistance to cisplatin by inhibition of glutathione S-transferases (GSTs) with ethacraplatin micelles in vitro and in vivo. *Biomaterials* **144**, 119-129, doi:10.1016/j.biomaterials.2017.08.021 (2017).

114 Liu, H., Shi, D., Liu, T., Yu, Z. & Zhou, C. Lentivirus-mediated silencing of SCIN inhibits proliferation of human lung carcinoma cells. *Gene* **554**, 32-39, doi:10.1016/j.gene.2014.10.013 (2015).

115 Wang, X. *et al.* Screening miRNAs for early diagnosis of colorectal cancer by small RNA deep sequencing and evaluation in a Chinese patient population. *OncoTargets and therapy* **9**, 1159-1166, doi:10.2147/OTT.S100427 (2016).

116 Miura, N. *et al.* Adseverin: a novel cisplatin-resistant marker in the human bladder cancer cell line HT1376 identified by quantitative proteomic analysis. *Mol Oncol* **6**, 311-322, doi:10.1016/j.molonc.2011.12.002 (2012).

117 Brocker, C., Cantore, M., Failli, P. & Vasiliou, V. Aldehyde dehydrogenase 7A1 (ALDH7A1) attenuates reactive aldehyde and oxidative stress induced cytotoxicity. *Chem Biol Interact* **191**, 269-277, doi:10.1016/j.cbi.2011.02.016 (2011).

118 Benchekroun, M. N., Sinha, B. K. & Robert, J. Doxorubicin-induced oxygen free radical formation in sensitive and doxorubicin-resistant variants of rat glioblastoma cell lines [corrected and republished erratum originally printed in FEBS Lett 1993 May 17;322(3):295-8]. *FEBS Lett* **326**, 302-305 (1993).

119 Rivankar, S. An overview of doxorubicin formulations in cancer therapy. *Journal of cancer research and therapeutics* **10**, 853-858, doi:10.4103/0973-1482.139267 (2014).

120 Hsu, P. D. *et al.* DNA targeting specificity of RNA-guided Cas9 nucleases. *Nat Biotechnol* **31**, 827-832, doi:10.1038/nbt.2647 (2013).

121 Peltier, H. J. & Latham, G. J. Normalization of microRNA expression levels in quantitative RT-PCR assays: identification of suitable reference RNA targets in normal and cancerous human solid tissues. *RNA* **14**, 844-852, doi:10.1261/rna.939908 (2008).

122 Tyanova, S. *et al.* Visualization of LC-MS/MS proteomics data in MaxQuant. *Proteomics* **15**, 1453-1456, doi:10.1002/pmic.201400449 (2015).

123 Cox, J. & Mann, M. MaxQuant enables high peptide identification rates, individualized p.p.b.-range mass accuracies and proteome-wide protein quantification. *Nat Biotechnol* **26**, 1367-1372, doi:10.1038/nbt.1511 (2008).

124 Tyanova, S. *et al.* The Perseus computational platform for comprehensive analysis of (prote)omics data. *Nature methods* **13**, 731-740, doi:10.1038/nmeth.3901 (2016).

125 Agarwal, V., Bell, G. W., Nam, J. W. & Bartel, D. P. Predicting effective microRNA target sites in mammalian mRNAs. *Elife* **4**, doi:10.7554/eLife.05005 (2015).

126 Riggi, N., Aguet, M. & Stamenkovic, I. Cancer Metastasis: A Reappraisal of Its Underlying Mechanisms and Their Relevance to Treatment. *Annu Rev Pathol* **13**, 117-140, doi:10.1146/annurev-pathol-020117-044127 (2018).

127 DeSantis, C. E. *et al.* International Variation in Female Breast Cancer Incidence and Mortality Rates. *Cancer Epidemiol Biomarkers Prev* **24**, 1495-1506, doi:10.1158/1055-9965.EPI-15-0535 (2015).

128 DeSantis, C. E., Ma, J., Goding Sauer, A., Newman, L. A. & Jemal, A. Breast cancer statistics, 2017, racial disparity in mortality by state. *CA Cancer J Clin* **67**, 439-448, doi:10.3322/caac.21412 (2017).

129 Soni, A. *et al.* Breast cancer subtypes predispose the site of distant metastases. *Am J Clin Pathol* **143**, 471-478, doi:10.1309/AJCPYO5FSV3UPEXS (2015).

130 Mariotto, A. B., Etzioni, R., Hurlbert, M., Penberthy, L. & Mayer, M. Estimation of the Number of Women Living with Metastatic Breast Cancer in the United States. *Cancer Epidemiol Biomarkers Prev* **26**, 809-815, doi:10.1158/1055-9965.EPI-16-0889 (2017).

131 Campbell, K. & Casanova, J. A common framework for EMT and collective cell migration. *Development* **143**, 4291-4300, doi:10.1242/dev.139071 (2016).

132 Schaeffer, D., Somarelli, J. A., Hanna, G., Palmer, G. M. & Garcia-Blanco, M. A. Cellular migration and invasion uncoupled: increased migration is not an inexorable consequence of epithelial-to-mesenchymal transition. *Mol Cell Biol* **34**, 3486-3499, doi:10.1128/MCB.00694-14 (2014).

133 Son, H. & Moon, A. Epithelial-mesenchymal Transition and Cell Invasion. *Toxicol Res* **26**, 245-252, doi:10.5487/TR.2010.26.4.245 (2010).

134 Ma, J., Dong, C. & Ji, C. MicroRNA and drug resistance. *Cancer gene therapy* **17**, 523-531, doi:10.1038/cgt.2010.18 (2010).

135 Pogribny, I. P. *et al.* Alterations of microRNAs and their targets are associated with acquired resistance of MCF-7 breast cancer cells to cisplatin. *Int J Cancer* **127**, 1785-1794, doi:10.1002/ijc.25191 (2010).

136 Ljepoja, B. *et al.* A proteomic analysis of an in vitro knock-out of miR-200c. *Sci Rep* **8**, 6927, doi:10.1038/s41598-018-25240-y (2018).

137 Nakamura, F., Stossel, T. P. & Hartwig, J. H. The filamins: organizers of cell structure and function. *Cell Adh Migr* **5**, 160-169 (2011).

138 Stossel, T. P. *et al.* Filamins as integrators of cell mechanics and signalling. *Nature reviews. Molecular cell biology* **2**, 138-145, doi:10.1038/35052082 (2001).

139 Baldassarre, M. *et al.* Filamins regulate cell spreading and initiation of cell migration. *PloS one* **4**, e7830, doi:10.1371/journal.pone.0007830 (2009).

140 Schreiber, C., Segerer, F. J., Wagner, E., Roidl, A. & Radler, J. O. Ring-Shaped Microlanes and Chemical Barriers as a Platform for Probing Single-Cell Migration. *Sci Rep* **6**, 26858, doi:10.1038/srep26858 (2016).

141 Maiuri, P. *et al.* The first World Cell Race. *Curr. Biol.* **22**, R673-R675, doi:http://dx.doi.org/10.1016/j.cub.2012.07.052 (2012).

142 Lombaerts, M. *et al.* E-cadherin transcriptional downregulation by promoter methylation but not mutation is related to epithelial-to-mesenchymal transition in breast cancer cell lines. *Br J Cancer* **94**, 661-671, doi:10.1038/sj.bjc.6602996 (2006).
143 Chao, Y. L., Shepard, C. R. & Wells, A. Breast carcinoma cells re-express E-cadherin during mesenchymal to epithelial reverting transition. *Mol Cancer* **9**, 179, doi:10.1186/1476-4598-9-179 (2010).
144 Sun, Q. *et al.* Defining the mammalian CArGome. *Genome Res* **16**, 197-207, doi:10.1101/gr.4108706 (2006).
145 Kasza, K. E. *et al.* Filamin A is essential for active cell stiffening but not passive stiffening under external force. *Biophys J* **96**, 4326-4335, doi:10.1016/j.bpj.2009.02.035 (2009).
146 Savoy, R. M. & Ghosh, P. M. The dual role of filamin A in cancer: can't live with (too much of) it, can't live without it. *Endocr Relat Cancer* **20**, R341-356, doi:10.1530/ERC-13-0364 (2013).
147 Flanagan, L. A. *et al.* Filamin A, the Arp2/3 complex, and the morphology and function of cortical actin filaments in human melanoma cells. *J Cell Biol* **155**, 511-517, doi:10.1083/jcb.200105148 (2001).
148 Truong, T., Shams, H. & Mofrad, M. R. Mechanisms of integrin and filamin binding and their interplay with talin during early focal adhesion formation. *Integr Biol (Camb)* **7**, 1285-1296, doi:10.1039/c5ib00133a (2015).
149 Guo, J. *et al.* Reduced miR-200b and miR-200c expression contributes to abnormal hepatic lipid accumulation by stimulating JUN expression and activating the transcription of srebp1. *Oncotarget* **7**, 36207-36219, doi:10.18632/oncotarget.9183 (2016).
150 Verde, P., Casalino, L., Talotta, F., Yaniv, M. & Weitzman, J. B. Deciphering AP-1 function in tumorigenesis: fra-ternizing on target promoters. *Cell Cycle* **6**, 2633-2639, doi:10.4161/cc.6.21.4850 (2007).
151 Shaulian, E. AP-1--The Jun proteins: Oncogenes or tumor suppressors in disguise? *Cell Signal* **22**, 894-899, doi:10.1016/j.cellsig.2009.12.008 (2010).
152 Xia, Y. & Karin, M. The control of cell motility and epithelial morphogenesis by Jun kinases. *Trends Cell Biol* **14**, 94-101, doi:10.1016/j.tcb.2003.12.005 (2004).
153 Norman, C., Runswick, M., Pollock, R. & Treisman, R. Isolation and properties of cDNA clones encoding SRF, a transcription factor that binds to the c-fos serum response element. *Cell* **55**, 989-1003 (1988).
154 Schwartz, B. *et al.* SRF is essential for mesodermal cell migration during elongation of the embryonic body axis. *Mech Dev* **133**, 23-35, doi:10.1016/j.mod.2014.07.001 (2014).
155 Hermann, M. R. *et al.* Integrins synergise to induce expression of the MRTF-A-SRF target gene ISG15 for promoting cancer cell invasion. *J Cell Sci* **129**, 1391-1403, doi:10.1242/jcs.177592 (2016).
156 Kircher, P. *et al.* Filamin A interacts with the coactivator MKL1 to promote the activity of the transcription factor SRF and cell migration. *Sci Signal* **8**, ra112, doi:10.1126/scisignal.aad2959 (2015).
157 Ljepoja, B. MiRNA-27a as a novel biomarker for tamoxifen treatment in luminal A breast cancer. *Master Thesis* (2014).
158 Muller, K., Klein, P. M., Heissig, P., Roidl, A. & Wagner, E. EGF receptor targeted lipo-oligocation polyplexes for antitumoral siRNA and miRNA delivery. *Nanotechnology* **27**, 464001, doi:10.1088/0957-4484/27/46/464001 (2016).
159 Alvarez-Erviti, L. *et al.* Delivery of siRNA to the mouse brain by systemic injection of targeted exosomes. *Nature biotechnology* **29**, 341-345, doi:10.1038/nbt.1807 (2011).
160 Lachelt, U. & Wagner, E. Nucleic Acid Therapeutics Using Polyplexes: A Journey of 50 Years (and Beyond). *Chem Rev* **115**, 11043-11078, doi:10.1021/cr5006793 (2015).

7.2. Index of figures

7.3. Index of tables

8. Publications

8.1. Original articles

- **Ljepoja, B.,** Schreiber, C., Gegenfurtner F., García-Roman, J, Zahler, S., Rädler, J., Wagner, E., Roidl, A. (2019) Inducible microRNA-200c decreases motility of breast cancer cells and reduces filamin A (in revision)
- Sommer, A.K**,** Falkenberg, M**., Ljepoja, B.,** Fröhlich, T., Arnold, G.J, Wagner, E., Roidl, A. (2019) Downregulation of GRK5 hampers the migration of breast cancer cells (submitted)
- **Ljepoja, B**., García-Roman, J., Sommer, A.K., Wagner, E., Roidl, A. (2018) MiRNA-27a sensitizes breast cancer cells to treatment with Selective Estrogen Receptor Modulators, Breast. 2019 Feb;43:31-38
- Sommer, A.K., Hermawan, A., **Ljepoja, B**., Fröhlich, T., Arnold, G.J., Wagner, E., Roidl, A. (2018) A proteomic analysis of chemoresistance development via sequential treatment with doxorubicin reveals novel players in MCF-7 breast cancer cells, Int J Mol Med. 2018 Oct;42(4):1987-1997
- **Ljepoja B**, García-Roman J, Sommer AK, Fröhlich T, Arnold GJ, Wagner E, Roidl A. (2018) A proteomic analysis of an in vitro knock-out of miR-200c, Sci Rep. 2018 May 2;8(1):6927
- Sommer, A.-K., Hermawan, A., Mickler, F.M., **Ljepoja, B**., Knyazev, P., Bräuchle, C., Ullrich, A., Wagner, E., Roidl, A. (2016) Salinomycin co-treatment enhances tamoxifen cytotoxicity in luminal A breast tumor cells by facilitating lysosomal degradation of receptor tyrosine kinases, Oncotarget. 2016 Aug 2;7(31):50461-5047

8.2. Posters

Ljepoja, B.*, García-Roman, J., Kopp, F., Wagner, E., Roidl, A (2014) miR-27a is a functional biomarker for tamoxifen treatment of luminal A/B breast tumors, EACR 2014 Munich

* Presenting author

.

9. Acknowledgements

Zuerst möchte ich mich bei Professor Dr. Ernst Wagner bedanken, für die Unterstützung, Ratschläge und Freiheiten, sowie das damit entgegengebrachte Vertrauen während meiner gesamten Arbeit. Und natürlich für die Skifahrten und Rodelrennen, die ich mehrmals erfolgreich überlebt habe.

Genau so möchte ich mich auch bei Dr. Andreas Roidl herzlichst bedanken, für die langjährige Betreuung, Inspiration, Ideen, Diskussionen und nicht zuletzt wegen der hervorragenden Arbeitsatmosphäre, in der wir zusammen eine enorme Bandbreite an biochemischen Methoden etabliert konnten. Und das hat sehr viel Spaß gemacht!

An dieser Stelle geht auch ein großer Dank an Ann-Katrin Sommer, die vor allem durch unser gemeinsames Büro, den Laboralltag mit mir durchstehen durfte (musste).

Dank gebührt auch Dr. Adam Hermawan und Dr. Jonathan García-Roman, die mir eine Unterstützung im Erlernen von neuen Methoden im Labor waren und dabei durchgehend für eine lockere, heitere Stimmung gesorgt haben.

Bei PD Dr. Martin Anton möchte ich mich ganz besonders bedanken, ohne die exzellente Einführung in die Arbeit mit viralen Vektoren, wären die hier dargestellten Experimente nicht durchführbar gewesen.

Auch möchte ich mich bei Dr. Thomas Fröhlich für seine maßgebliche Unterstützung bei der Durchführung, Auswertung und Darstellung der Proteom-Analysen bedanken.

Dank gebührt vor allem auch den fleißigen Helfern im Labor, die uns durchgehend mit neuen Materialien oder Puffern versorgt haben und auch mal ein defektes Großgerät nur mit einem Schraubenzieher und einem Stück Draht wieder reparieren konnten: Danke Wolfgang Rödel, Melinda Kiss, Miriam Höhn, Ursula Biebl und Markus Kovac!

Ein allgemeiner Dank gebührt natürlich dem gesamten Arbeitskreis, für exzellente Faschingsfeiern, angeregte Diskussionen in den Gruppenseminaren und unser hervorragendes Fußballteam, das fast immer gewonnen hat.

Auch möchte ich mich bei Dr. Jens-Peter Sölch dafür bedanken, dass er mir während den Jahren der Promotion die Möglichkeit gab, mich in spannende Projekte außerhalb der Universität einzubringen.

Und zu guter Letzt gebührt mein größter Dank meiner Familie, einen Eltern, die mich auf meinem langen Bildungsweg unterstützen „durften“. Die ersten Jahre mit Hausaufgaben-Hilfe und Frühstück, die letzten Jahre dann eher mit einem offenen Ohr, handwerklicher Unterstützung und aufmunternden Worten. Um euch zu beruhigen: Ja, jetzt habe ich *„endlich mal fertig studiert“.*